



University of
Stavanger

FACULTY OF SCIENCE AND TECHNOLOGY

MASTER'S THESIS

Study programme/specialization:

MSc. in Environmental Engineering
Specialization in Offshore Environmental
Technology

Spring Semester, 2021

Open Access

Author:

Rocio Ortega

Supervisor:

Dr. Mohamed Fawzy Mady

Title of master's thesis:

Antiscaling Evaluation of Novel Non-Polymeric Phosphonates for Oilfield Applications

Credits: 30 ECTS.

Keywords:

Calcite, Gypsum, Scale inhibitor, Static testing,
Squeeze treatment, Calcium compatibility,
Biodegradability, Hydroxybisphosphonate,
Sulfonate, Carboxylate

Number of pages: 92

+ supplemental material/other: 38

Stavanger, July 30th 2021.

ABSTRACT

Scale formation consists of an accumulation of mineral deposits, affecting fluids flow. It is a major flow assurance problem in the oilfield industry and can occur anywhere along water paths, from injectors through the reservoir to surface equipment. Areas such as the North Sea are highly prone to scale formation. Scale inhibitors (SIs) are commonly used to prevent the formation of these precipitates. Current commercially available SIs provide good inhibition efficiency but lack other important characteristics that must be considered before their application in the field, such as calcium tolerance, thermal stability, and biodegradability. Therefore, the principal aim of this research was to evaluate the antiscaling performance of novel non-polymeric phosphonated SIs derived from alendronic acid and fosfomycin as starting compounds.

A series of hydroxybisphosphonates-bearing phosphonate (**SI-2**), sulfonate (**SI-3** and **SI-5**) and carboxylate (**SI-4**, **SI-6**, and **SI-7**) groups were synthesized from the well-known non-toxic bone targeting drug, alendronic acid (**SI-1**). A second set of SIs with nitrogen-free phosphonate groups (**SI-9** and **SI-10**) were synthesized from the commercially available antibiotic fosfomycin (**SI-8**). Inhibition performance against calcite and gypsum scales was evaluated using static bottle tests based on the NACE Standard TM0374-2007. Compatibility with up to 50000 ppm Ca^{2+} ions was evaluated. Thermal stability was assessed at 130°C under anaerobic conditions over 7 days. Estimation of biodegradability was carried out by following the OECD 306 closed bottle method protocol.

Results showed that **SI-4**, **SI-7**, and **SI-10** exhibit good to excellent gypsum and calcite inhibition performance. **SI-3** and **SI-5** presented good calcite inhibition but are not efficient against the gypsum scale. After thermal aging at 130°C for 7 days, **SI-2** and **SI-7** performance remained stable against gypsum and calcite scales, while **SI-5** gave a stable performance only against the calcite scale. All proposed SIs from **SI-2** to **SI-7** exhibited an improvement in calcium compatibility in contrast to the parent compound **SI-1**. Furthermore, **SI-5**, **SI-8**, and **SI-9** remained as the tested SIs most tolerant to high calcium concentrations, followed by **SI-4** and **SI-7**. Biodegradability of all compounds resulted very low, not complying with our preliminary expectations.

This project serves as a contribution to the production chemistry field and highlights the success of synthesizing new non-polymeric gypsum and calcite scale inhibitors with good calcium compatibility and thermal stability. However, further studies and modifications are needed to improve biodegradability and evaluate the fate of these chemicals in the environment. The difficulty of developing production chemicals that can fulfill all the gaps for adequate performance in the field as well as complying with environmental regulations remains an ongoing challenge for researchers.

ACKNOWLEDGEMENTS

First and foremost, I would like to thank my parents, Irais and Oswaldo. You were, are, and will always be my source of energy and motivation to continue and give my best in all aspects of my life, including my journey throughout this thesis. Thank you for always being my greatest supporters, I hope life gives us the opportunity of being together again so that I can take care of you the same way you took care of me when I needed it the most.

Second, to my sister Paola and her husband, Gustavo. If it was not for you, I would not have had the chance of growing and transforming into who I am today, in both personal and professional aspects. Thank you for allowing me to be part of your home throughout this stage of my life. I would like to extend my gratitude to Gustavo, you helped me to see the light at the end of the tunnel at crucial times. Also, to Helen, Juan, and Anna, you fulfilled my days with joy and happiness.

Third, to my thesis supervisor, Dr. Mohamed F. Mady. Thank you for allowing me to delve into this research and all the experience I gained with it. You were always available with patience, knowledge, and dedication, and I am deeply grateful for that. We did our best, and I hope this work showcases it.

Fourth, to my boyfriend, Georgeio Semaan. Special thanks to you for bearing with me throughout this journey. Thank you for always pushing me beyond my limits and showing me that I can always do better; your endless motivation and support were vital for me to keep up with this work.

Fifth, I would like to thank associate professor Krista Kaster for her expertise, feedback, and encouragement during her courses. Special thanks for assisting me on the biodegradability section of this research.

Sixth, to my family and friends. I could not be more content with your presence in my life. You are all a fundamental part of me. To Maka and Julia, even from a distance you never failed to show me what real friendship is about. May God protect you and always keep your spirits alive.

Finally, thanks to my lab buddies, Eirik, Sumit, Radha and Alaa for all the chats and talks during our time there. You made this process more bearable to go through.

TABLE OF CONTENTS

ABSTRACT.....	I
ACKNOWLEDGEMENTS	II
TABLE OF CONTENTS	III
LIST OF ABBREVIATIONS.....	VI
LIST OF TABLES	VII
LIST OF FIGURES	VIII
1. INTRODUCTION.....	10
1.1. RESEARCH OBJECTIVES	11
1.1.1. GENERAL.....	11
1.1.2. SPECIFIC	11
2. THEORETICAL BACKGROUND	12
2.1. SCALE DEPOSITION	12
2.1.1. OVERVIEW.....	12
2.1.2. MECHANISMS OF SCALE FORMATION	12
2.1.3. TYPES OF SCALE	14
2.1.3.1. Calcite scale	14
2.1.3.2. Sulfate scale	15
2.1.4. DRIVING FORCES OF SCALE FORMATION: SUPERSATURATION, RATIO OF IONS, AND pH.....	15
2.2. SCALE REMEDIATION.....	16
2.3. SCALE INHIBITORS (SIs).....	17
2.3.1. MECHANISMS OF ACTION	17
2.3.1.1. Kinetic inhibition	18
2.3.1.2. Thermodynamic inhibition	18
2.3.2. CHARACTERISTICS OF ‘ <i>IDEAL</i> ’ SIs.....	18
2.3.3. INDUSTRIAL DEPLOYMENT OF SIs.....	19
2.3.3.1. Continuous injection and batch treatment	19
2.3.3.2. Squeeze treatment	19
2.3.4. COMMERCIAL SIs	20
2.3.5. PERFORMANCE EVALUATION OF SIs IN LABORATORY SETTINGS	21
2.4. ENVIRONMENTAL CHALLENGES	24
2.5. EARLIER STUDIES	26
2.6. NEW IDEA – PROJECT 1.....	27
2.7. NEW IDEA – PROJECT 2.....	29

3. MATERIALS AND METHODS	31
3.1. CHEMICALS AND EQUIPMENT	31
3.2. SYNTHESIS AND CHARACTERIZATION OF SIS	32
3.2.1. PROJECT 1.....	32
3.2.1.1. SI-1: <i>Alendronic acid</i>	32
3.2.1.2. SI-2: <i>((4-hydroxy-4,4-diphosphonobutyl)azanediyl)dimethanephosphonic acid</i>	33
3.2.1.3. SI-3: <i>((4-hydroxy-4,4-diphosphonobutyl)azanediyl)dimethanesulfonic acid</i>	33
3.2.1.4. SI-4: <i>3,3'-((4-hydroxy-4,4-diphosphonobutyl)azanediyl)dipropionic acid</i>	34
3.2.1.5. SI-5: <i>2,2'-((4-hydroxy-4,4-diphosphonobutyl)azanediyl)bis(ethane-1-sulfonic acid)</i>	35
3.2.1.6. SI-6: <i>(E)-4-((4-hydroxy-4,4-diphosphonobutyl)amino)-4-oxobut-2-enoic acid</i>	36
3.2.1.7. SI-7: <i>2,2'-((4-hydroxy-4,4-diphosphonobutyl)azanediyl)diacetic acid</i>	37
3.2.2. PROJECT 2.....	37
3.2.2.1. SI-8: <i>Fosfomycin disodium salt</i>	38
3.2.2.2. SI-9: <i>(2-(2-amino-3-hydroxy-2-(hydroxymethyl)propoxy)-1-hydroxypropyl)phosphonic acid</i>	38
3.2.2.3. SI-10: <i>(2-hydroxypropyl)phosphonic acid</i>	39
3.2.2.4. SI-11: <i>(2-(2-(bis(phosphonomethyl)amino)-3-hydroxy-2-(hydroxymethyl)propoxy)-1-hydroxypropyl)phosphonic acid</i>	39
3.2.2.5. SI-12: <i>(1-hydroxy-2-(3-hydroxy-2-(hydroxymethyl)-((phosphonomethyl)amino)propoxy)propyl)phosphonic acid</i>	40
3.3. LABORATORY TESTING OF SIS FOR OILFIELD APPLICATIONS.....	41
3.3.1. STOCK SOLUTIONS AND BRINES	41
3.3.1.1. Scale inhibitor solution, 1000 ppm	41
3.3.1.2. Brines composition	41
3.3.1.2.1. Gypsum scale	41
3.3.1.2.2. Calcite scale	42
3.3.1.2.3. Heidrun calcite scale	42
3.3.1.2.4. Heidrun barite scale.....	43
3.3.1.3. Ethylenediaminetetraacetic acid (EDTA) solution, 0.01 M	44
3.3.1.4. Ammonium purpurate indicator solution.....	44
3.3.2. STATIC JAR TESTS	44
3.3.3. HIGH-PRESSURE DYNAMIC TUBE BLOCKING TEST.....	46
3.3.4. THERMAL STABILITY TESTS	49
3.3.5. CALCIUM COMPATIBILITY TESTS.....	49
3.3.6. SEAWATER BIODEGRADABILITY TESTS	50
3.3.6.1. Seawater sampling	51
3.3.6.2. BOD analysis set up.....	51
4. RESULTS AND DISCUSSION	53
4.1. PROJECT 1	53
4.1.1. CHEMISTRY	53
4.1.2. STATIC BOTTLE TESTS.....	54
4.1.2.1. Gypsum scale.....	54
4.1.2.2. Calcite scale	56

4.1.2.3. Heidrun calcite scale	57
4.1.3. CALCIUM COMPATIBILITY	59
4.1.4. THERMAL STABILITY	62
4.1.4.1. Gypsum scale	62
4.1.4.2. Calcite scale	63
4.1.4.3. Heidrun calcite scale	65
4.2. PROJECT 2	67
4.2.1. CHEMISTRY	67
4.2.2. STATIC BOTTLE TESTS	68
4.2.2.1. Gypsum scale	68
4.2.2.2. Calcite scale	69
4.2.2.3. Heidrun calcite scale	71
4.2.3. CALCIUM COMPATIBILITY	72
4.2.4. THERMAL STABILITY	75
4.2.4.1. Gypsum scale	75
4.2.4.2. Calcite scale	76
4.2.4.3. Heidrun calcite scale	78
4.3. SEAWATER BIODEGRADABILITY	80
5. CONCLUSIONS	82
6. FUTURE RESEARCH	84
7. REFERENCES	85
8. APPENDIX A – NMR SPECTRA: PROJECT 1	93
9. APPENDIX B – FTIR SPECTRA: PROJECT 1	100
10. APPENDIX C – NUTRIENTS SOLUTIONS	103
11. APPENDIX D – STATIC BOTTLE TESTS RESULTS: PROJECT 1	104
12. APPENDIX E – CALCIUM COMPATIBILITY RESULTS – PROJECT 1	116
13. APPENDIX F – NMR SPECTRA: PROJECT 2	117
14. APPENDIX G – FTIR SPECTRA: PROJECT 2	120
15. APPENDIX H – STATIC BOTTLE TESTS RESULTS: PROJECT 2	121
16. APPENDIX I - SEAWATER BIODEGRADABILITY RESULTS	130

LIST OF ABBREVIATIONS

ATMP	-	Aminotris(methylenephosphonic) acid
BOD	-	Biological Oxygen Demand
CMI	-	Carboxymethylulin
DSR	-	Dynamic Scale Rig
DTPMP	-	Diethylenetriaminepenta(methylene-phosphonic acid)
EC	-	Half maximal effective concentration
EDTA	-	Ethylenediaminetetraacetic Acid
EOR	-	Enhanced Oil Recovery
FTIR	-	Fourier Transform Infrared spectroscopy
HPAA	-	2-Hydroxyphosphonoacetic Acid
HPDTBT	-	High-pressure Dynamic Tube Blocking Test
LC	-	Median Lethal dose
MIC	-	Minimum Inhibitor Concentration
NMR	-	Nuclear Magnetic Resonance
PPCA	-	Polyphosphinocarboxylic Acid
PVS	-	Polyvinyl Sulfonate
SEM	-	Scanning Electron Microscopy
SI	-	Scale Inhibitor
ThOD	-	Theoretical Oxygen Demand
XRD	-	X-Ray Diffraction

LIST OF TABLES

Table 1. Different types of scales ¹	14
Table 2. Classification of chemicals according to their environmental impact.	25
Table 3. Composition of gypsum brines used for static screening tests.	41
Table 4. Composition of calcite brines used for static screening tests.	42
Table 5. Composition of calcite brines according to the Heidrun Oilfield.	42
Table 6. Composition of barite brines according to the Heidrun Oilfield.	43
Table 7. Dosed solutions for static performance tests of SIs.	45
Table 8. Biodegradation tests: bottles distribution and set up.	52
Table 9. Gypsum inhibition performance of commercial SIs and SI-1 to SI-7.	54
Table 10. Calcite inhibition performance of commercial SIs and SI-1 to SI-7.	56
Table 11. Heidrun calcite inhibition performance of commercial SIs and SI-1 to SI-7.	58
Table 12. Ca ²⁺ tolerance tests at 30000 ppm (3 wt%) NaCl for SI-1, SI-4, SI-5 and SI-7.	60
Table 13. Ca ²⁺ tolerance tests. Appearance after 24 hours.	61
Table 14. Gypsum inhibition performance of SI-2, SI-5 and SI-7 after thermal aging.	62
Table 15. Calcite inhibition performance of SI-2, SI-5 and SI-7 after thermal aging.	63
Table 16. Heidrun calcite inhibition performance of SI-2, SI-5 and SI-7 after thermal aging.	65
Table 17. Gypsum inhibition performance of HPAA and SI-8 to SI-10.	68
Table 18. Calcite inhibition performance of HPAA and SI-8 to SI-10.	69
Table 19. Heidrun calcite inhibition performance of HPAA and SI-8 to SI-10.	71
Table 20. Ca ²⁺ tolerance tests at 30000 (3 wt%) NaCl for SI-8, SI-9, SI-10 and HPAA.	73
Table 21. Ca ²⁺ tolerance tests. Appearance after 24 hours.	74
Table 22. Gypsum inhibition performance of HPAA and SI-8 to SI-10 after thermal aging.	75
Table 23. Calcite inhibition performance of HPAA and SI-8 to SI-10 after thermal aging.	77
Table 24. Heidrun calcite inhibition performance of HPAA and SI-8 to SI-10 after thermal aging.	78
Table 25. Standard gypsum static tests results - Project 1	104
Table 26. Standard calcite static test results - Project 1	108
Table 27. Heidrun calcite static test results - Project 1	112
Table 28. Ca ²⁺ tolerance tests at 30000 ppm (3 wt%) NaCl for SI-2, SI-3 and SI-6.	116
Table 29. Standard gypsum static test results - Project 2.	121
Table 30. Standard calcite static test results - Project 2.	124
Table 31. Heidrun calcite static test results - Project 2.	127
Table 32. Seawater biodegradability results - Project 1 and Project 2.	130

LIST OF FIGURES

Figure 1. General scale formation mechanisms ⁵	13
Figure 2. Nucleation mechanisms: a) Homogeneous nucleation. b) Heterogeneous nucleation ⁷	14
Figure 3. In-house synthesized SIs using alendronic acid (SI-1) as starting compound.	28
Figure 4. In-house synthesized SIs using fosfomicin (SI-8) as starting compound.	30
Figure 5. Reflux set up (left) and solvent evaporation equipment (right).....	31
Figure 6. Chemical structure of SI-1.....	32
Figure 7. Synthesis route of SI-2.	33
Figure 8. Synthesis route of SI-3.	34
Figure 9. Synthesis route of SI-4.	34
Figure 10. Synthesis route of SI-5.	35
Figure 11. Synthesis route of SI-6.	36
Figure 12. Synthesis route of SI-7.	37
Figure 13. Chemical structure of SI-8.....	38
Figure 14. Synthesis route of SI-9.	38
Figure 15. Synthesis route of SI-10.	39
Figure 16. Synthesis route of SI-11.	40
Figure 17. Synthesis route of SI-12.	40
Figure 18. Color change at end point for Ca ²⁺ titration with murexide.	44
Figure 19. Duration test results for static bottle tests.....	45
Figure 20. Titration set up for Ca ²⁺ analysis by titration with EDTA (left). Dynamic scale rig used for high-pressure tube blocking testing of SIs (right).....	47
Figure 21. Stages of SI testing in a dynamic scale rig (pressure vs. time).	49
Figure 22. Gypsum inhibition performance of selected SIs.....	55
Figure 23. Calcite inhibition performance of selected SIs.....	57
Figure 24. Heidrun calcite inhibition performance of selected SIs.....	59
Figure 25. Gypsum inhibition performance of SI-2, SI-5 and SI-7 after thermal aging.....	63
Figure 26. Calcite inhibition performance of SI-2, SI-5 and SI-7 after thermal aging.	65
Figure 27. Heidrun calcite inhibition performance of SI-2, SI-5, and SI-7 after thermal aging.....	66
Figure 28. Gypsum inhibition performance of HPAA and SI-8 to SI-10.	69
Figure 29. Calcite inhibition performance of HPAA and SI-8 to SI-10.	70
Figure 30. Heidrun calcite inhibition performance of HPAA and SI-8 to SI-10.....	72
Figure 31. Gypsum inhibition performance of HPAA and SI-8 to SI-10 after thermal aging.....	76
Figure 32. Calcite inhibition performance of HPAA and SI-8 to SI-10 after thermal aging.....	78
Figure 33. Heidrun calcite inhibition performance of HPAA and SI-8 to SI-10 after thermal aging	79

Figure 34. Seawater biodegradability performance of SI-1 to SI-9.....	80
Figure 35. ¹ H NMR for SI-1.	93
Figure 36. ³¹ P NMR for SI-1.....	93
Figure 37. ¹ H NMR spectra for SI-2.....	94
Figure 38. ³¹ P NMR spectra for SI-2.	94
Figure 39. ¹ H NMR spectra for SI-3.....	95
Figure 40. ³¹ P NMR spectra for SI-3.	95
Figure 41. ¹ H NMR for SI-4.	96
Figure 42. ³¹ P NMR for SI-4.....	96
Figure 43. ¹ H NMR for SI-5.	97
Figure 44. ³¹ P NMR for SI-5.....	97
Figure 45. ¹ H NMR for SI-6.	98
Figure 46. ³¹ P NMR for SI-6.....	98
Figure 47. ¹ H NMR for SI-7.	99
Figure 48. ³¹ P NMR for SI-7.....	99
Figure 49. FTIR spectra for SI-1.....	100
Figure 50. FTIR spectra for SI-2.....	100
Figure 51. FTIR spectra for SI-3.....	100
Figure 52. FTIR spectra for SI-4.....	101
Figure 53. FTIR spectra for SI-5.....	101
Figure 54. FTIR spectra for SI-6.....	101
Figure 55. FTIR spectra for SI-7.....	102
Figure 56. ¹ H NMR spectra for SI-8.	117
Figure 57. ³¹ P NMR for SI-8.....	117
Figure 58. ¹ H NMR for SI-9.	118
Figure 59. ³¹ P NMR for SI-9.....	118
Figure 60. ¹ H NMR for SI-10.	119
Figure 61. ³¹ P NMR for SI-10.....	119
Figure 62. FTIR spectra for SI-8.....	120
Figure 63. FTIR spectra for SI-9.....	120
Figure 64. FTIR spectra for SI-10.....	120

1. INTRODUCTION

Scale formation is one of the main flow assurance problems faced in oil and gas production installations. It refers to the precipitation of inorganic minerals due to favored supersaturation conditions found in formation waters. This problem is more common in mature oilfields, where seawater is reinjected into the reservoir to enhance oil recovery (EOR). The difference in the ionic nature of seawater and formation water when mixed during this process leads to scale formation. If scale is not treated early, it will potentially hinder the production process, causing an increase in operational expenses, and even worse, the potential loss of the well.

One of the most used techniques to overcome scaling problems is the deployment of scale inhibitors (SIs)¹. SIs are water-soluble chemicals used to prevent nucleation and/or crystal growth of inorganic scales. Therefore, scale inhibitors are necessary to ensure a continuous flow of hydrocarbons through production pipelines. Polyphosphates, phosphate esters, non-polymeric phosphonates, aminophosphonates, polyphosphonates, polysulfonates, and polycarboxylates, are among the most common classes of SIs used in oilfield applications^{1,2}. Most of the current scale inhibitors have a good correlation between inhibition performance and costs, but their main drawback is their poor biodegradability and calcium compatibility. In some cases, it is required that SIs also present high thermal stability for applications such as squeeze treatments. Hence, as environmental regulations become more rigid, new production chemicals must adhere to certain criteria in order to qualify for use in the oil and gas industry. Therefore, there exists a constant need for developing suitable chemicals which allow a high scale inhibition efficiency together with an improved environmental footprint in order to fulfill the requirements set by various stakeholders.

The main objective of this project is to evaluate the performance of a series of scale inhibitors synthesized from alendronic acid and fosfomicin as starting compounds. These starting compounds are currently used in medical applications. Alendronic acid is a widely known aminobisphosphonate drug used for bone-targeting purposes, such as the treatment of osteoporosis and Paget's disease. On the other hand, fosfomicin contains an epoxide structure, and it is used as an antibiotic to treat urinary infections. The initiative of using these chemicals as starting compounds rises from their low toxicity and the presence of functional groups in their structures that are known to be favorable features in scale inhibitors, which together could give an improved biodegradation performance in contrast to commercial SIs.

A series of modified alendronic acid and fosfomycin compounds will be synthesized and characterized. The inhibition performance will be assessed against calcite and gypsum scales according to the NACE Standard TM0374-2007³. Thermal stability will be assessed for selected compounds. Additionally, calcium compatibility and biodegradation tests will also be performed in order to compare the overall performance of the obtained products with commercially available SIs.

1.1. Research objectives

1.1.1. General

To evaluate alendronic acid and fosfomycin as starting compounds to produce environmentally friendly scale inhibitors for oilfield applications.

1.1.2. Specific

- a. Synthesis and characterization of environmentally friendly scale inhibitors for oilfield applications using alendronic acid and fosfomycin disodium salt as starting materials.
- b. Evaluate the inhibition performance, thermal stability, compatibility with calcium ions, and biodegradation of the synthesized compounds.
- c. Compare the performance of the synthesized compounds with commercially available scale inhibitors.

2. THEORETICAL BACKGROUND

2.1. Scale deposition

2.1.1. Overview

Scale formation refers to the deposition of sparingly soluble salts due to the mixture of water currents with different ionic compositions. This is a problem that affects several industries. For this research, the oil industry will be the main focus. Scale formation is among the most common flow assurance problems in oil production, together with gas hydrates and corrosion¹. Scale forms at any location in production facilities as long as the conditions of precipitation are favorable. This is a matter of concern due to the fact that when scale formation initiates, its development is progressive, forming dense layers quickly unless treated early¹. If not controlled, scale formation in the long term will lead to obstruction of wells and will accumulate in different processing equipment, triggering a chain of problems, thereby decreasing oilfield productivity and causing economic losses. In spite of that, there exists a lot of interest in preventing the formation of these precipitates.

The life cycle of a reservoir plays an important role in the scale formation process. As the reservoir matures, oil levels start decreasing, and formation water levels tend to increase. Therefore, water is reinjected into the reservoir in order to overcome pressure losses by a method known as enhanced oil recovery (EOR)⁴. During this process, seawater and formation water get in contact. Their different water chemistries is the major contributing factor to scale formation. As more and more reservoirs mature, inorganic scale problems have steadily increased throughout the past years, implying high costs on operators.

2.1.2. Mechanisms of scale formation

The general mechanism of scale formation is shown in Figure 1. In the first stage, the solution becomes supersaturated with anions and cations, which collide, forming ion pairs, e.g., when seawater and formation water meet during EOR. Ionic collisions will then form micro-nuclei (nucleation), which will aggregate and act as formation sites for micro-crystals. Micro-crystals will consequently agglomerate and grow into larger crystals by the adsorption of more scaling ions. When further growth occurs, crystals grow heavier and deposit onto surfaces.

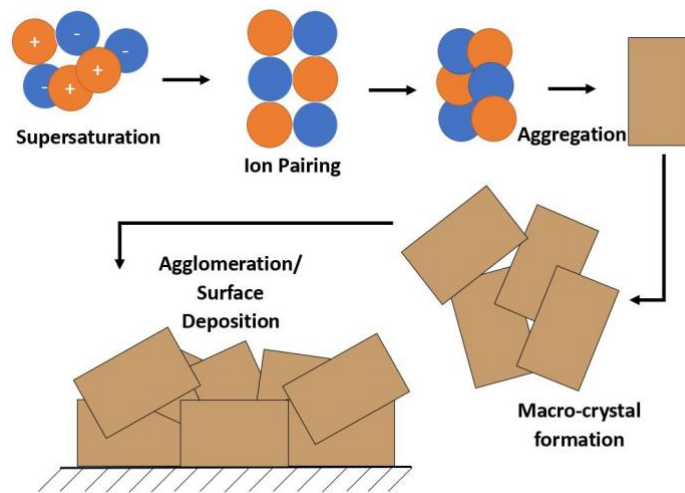


Figure 1. General scale formation mechanisms⁵.

In this order, crystallization is the following mechanism through which scales consequently grow. Two main paths of this mechanism have been reported, known as liquid-bulk and surface crystallization^{4,6,7}.

Liquid-bulk crystallization, as its name indicates, occurs in the bulk of the liquid phase, and it is also referred to as homogeneous nucleation. This mechanism consists of the formation of unstable clusters of atoms without the interference of external materials. Atoms clusters are formed by fluctuations in equilibrium ion concentration in supersaturated solutions. As shown in Figure 2a, seed crystals subsequently grow by adsorption of ions onto their surfaces, expanding the overall size of the crystal and forming cake-like layered structures.

Furthermore, surface crystallization, also known as heterogeneous nucleation, takes place on a preexisting fluid-surface boundary. It occurs in the presence of foreign substances (e.g., suspended solids, scale nuclei, metal joints and valves, and corrosion sites present on metal surfaces), which trigger the deposition of scales on the surface encountered. A representation of this mechanism is shown in Figure 2b. Nucleation sites include surface defects, such as pipe surface roughness, existing scale, or perforations in production lines.

It is highly relevant to understand the mechanisms of the scaling process in order to study and consider the optimal approach for remediation or inhibition.

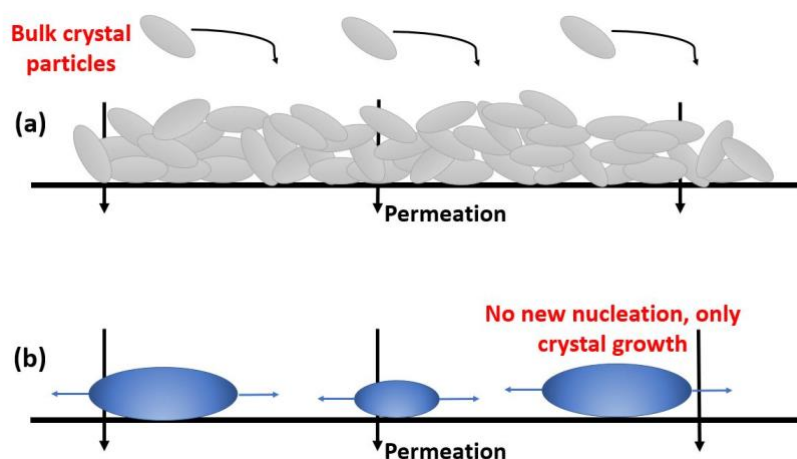


Figure 2. Nucleation mechanisms: a) Homogeneous nucleation. b) Heterogeneous nucleation⁷.

2.1.3. Types of scale

The most common scales encountered in the oil industry are presented in Table 1. Chemical reactions through which they are formed, and the name of the mineral they produce are also given.

Table 1. Different types of scales¹.

Oilfield scale	Chemical reaction	Mineral
Calcium Carbonate	$Ca^{2+} + 2HCO_3^- \rightleftharpoons CaCO_{3(s)} + H_2O + CO_2$	Calcite
Calcium Sulfate	$Ca^{2+} + SO_4^{2-} \rightleftharpoons CaSO_{4(s)}$	Gypsum
Strontium Sulfate	$Sr^{2+} + SO_4^{2-} \rightleftharpoons SrSO_{4(s)}$	Celestite
Barium Sulfate	$Ba^{2+} + SO_4^{2-} \rightarrow BaSO_{4(s)}$	Barite
Iron Sulfide	$Fe^{2+} + H_2S \rightarrow FeS_{(s)} + 2H^+$	Troilite
Zinc Sulfide	$Zn^{2+} + H_2S \rightarrow ZnS_{(s)} + 2H^+$	Sphalerite
Lead Sulfide	$Pb^{2+} + H_2S \rightarrow PbS_{(s)} + 2H^+$	Galena
Sodium Chloride	$Na^+ + Cl^- \rightarrow NaCl$	Halite

Among the presented scales, emphasis will be made on calcite, barite, and gypsum as they will be studied throughout this project.

2.1.3.1. Calcite scale

Calcite is one of the most commonly encountered scale deposits and the most thermodynamically stable polymorph of calcium carbonate⁸. Formation water is usually rich in bicarbonate and calcium ions. When equilibrium conditions are disturbed (e.g., pressure drop), the reaction showed in Table 1 moves towards the right, producing more CO₂ in order to increase the pressure. Therefore, calcite formation is enhanced. When CO₂ production is high, the pH will remain low enough, and calcium carbonate will not be able to form. However, further downstream, pressure will drop progressively, and here, calcite mainly forms¹.

Furthermore, water found within carbonate and calcite-cemented sandstone reservoirs usually contain high concentrations of divalent cations such as Ca^{2+} and Mg^{2+} . Such is the case of the Heidrun oilfield in the North Sea⁹.

2.1.3.2. Sulfate scale

Sulfate scales are more commonly formed when formation water and injected seawater are mixed (e.g., in EOR), or when two different fluids mix in topside flowlines. Seawater carries high concentrations of sulfate (SO_4^{2-}) ions. When it is in contact with divalent ions (Ca^{+2} , Ba^{+2} , Sr^{+2}) naturally found in formation water, sulfate scales begin to form^{1,6}. Usually, reservoirs with sandstone formation rock are rich in Ba^{2+} and Sr^{2+} ions¹⁰. Specifically, barite scale is among the major problems in offshore fields, and it is stated as the most difficult scale to deal with. It is pH-independent, and therefore exhibits enhanced stability, as well as insolubility in water. This will be further mentioned in Section 2.1.4. On the other side, calcium sulfate (gypsum) is also commonly encountered but it is slightly soluble in water and many chelate dissolvers¹. This type of scale is more commonly found on heat exchangers¹¹.

Furthermore, the solubility product constant (K_{sp}) indicates the ability of a specific solute to be dissolved in a particular solution. The higher the K_{sp} , the more soluble the solute is. K_{sp} values at different temperatures for barite and gypsum have been reported, showing that gypsum presents the highest K_{sp} at all temperatures whereas barite presents the lowest¹².

2.1.4. Driving forces of scale formation: supersaturation, ratio of ions, and pH

There are different driving forces that lead to scale formation. First, when equilibrium conditions in the production cycle are disturbed (e.g., pressure and/or temperature), supersaturation of the scale forming salt is enhanced. For example, if the temperature is increased, the water phase of the solution will tend to evaporate. With time, the solution will become saturated and eventually supersaturated, resulting in exceeding the solubility limit and therefore, causing the formation of scales⁴. Alternatively, the formation of carbonate scales serves as an example of pressure changes within the production system which lead to scale formation. This was explained previously in Section 2.1.3.1.

Equivalence in the ratio of cations and anions present in the aqueous solution is another requirement for scale formation: if the concentration of one of the species in the solution is low, scale will usually not form. For example, during EOR, seawater (rich in SO_4^{2-}) and formation water (rich in Ca^{2+} and Ba^{+2}) are mixed and reinjected into the reservoir. As they are incompatible waters, their mixing will cause sulfate scales deposition.

Another factor that influences the formation of certain scales is pH. Such is the case of gas flooded reservoirs, where CO₂ gas is injected as an approach for oil recovery⁴. There, as similarly discussed in Section 2.1.3.1, CO₂ is partially dissolved in water and further converted into carbonic acid, allowing the dissolution of scale, e.g., calcite. Eventually, after a pressure drop, CO₂ will be released from the solution, causing an increase in pH and subsequent precipitation of the calcium carbonate scale. Some scales, such as sulfates and halite are not formed depending on brine pH. This reason makes them the most difficult to deal with once they are formed, as they cannot be remediated by acid treatment. It is more economically feasible to prevent their formation with SIs. On the contrary, sulfide and carbonate scales are pH-dependent scales and therefore easier to deal with and dissolve^{1,6}.

2.2. Scale remediation

Several factors such as the nature, site, and severity of scale, determine the chemical or mechanical method that can be applied to counteract the presence of scale precipitation. However, many other factors influence the choice of the descaling method¹³. First, the accessibility of equipment and the possibility of dismantling has to be considered, although this may be an expensive alternative with significant losses of production. This method is mostly considered when no chemical method is suitable⁴. Second, metallurgical, temperature and disposal or discharge factors when choosing a particular chemical. Finally, one must consider the properties of the scale formed as some of them are only removed using specific chemicals (inhibitors or dissolvers) and effective removal might not be reached e.g., if tubing is mostly or completely obstructed. A brief description of the different methods to mitigate scale are discussed below.

First on the list is ‘smart water’ treatment. This method consists of the removal of sulfate ions from the injection water before reentering the production system. This process is done by membrane nanofiltration modules, requiring intensive maintenance and increased costs. However, it might be the best solution against scale in oilfields where it is predicted that sulfate and sulfide scales may occur. In addition, this method may also reduce reservoir souring and thus, inadvertently, affect the degree of microbial corrosion^{1,6}.

Mechanical removal of the existing scale can take place. Abrasive, abrasive/hydraulic, hydraulic, and thermal techniques are some of the techniques used for this purpose. The most common are abrasive/hydraulic techniques such as hydrojetting or milling¹. Drilling has also been used to remove scale. However, the process itself presents many limitations and complications, which renders this method non-feasible most of the time and a costly ineffective option for scale remediation⁶.

Lastly, chemical management involving scale dissolution and/or inhibition. As discussed in Section 2.1.4, certain types of scales are pH-dependent and hence soluble in acidic medium. Sometimes when scale is allowed to occur, the equipment is washed with an acidic solution or chelate solvers such as salts of EDTA (ethylenediaminetetraacetic acid) in order to dissolve the already formed scale¹. However, chelating procedures tend to be costly as stoichiometric relationships have to be carefully considered in order to achieve enough efficiency. Another drawback of this remediation method is that inorganic acids such as HCl are generally very corrosive, adding the need of corrosion inhibitors in the system⁶. In the scale inhibition scenario, SIs are deployed in order to prevent nucleation, crystal growth, and the overall deposition of scales in oilfield production. SI deployment is still the most preferred method to counteract the scaling problem, and this will be further detailed in the next section.

2.3. Scale inhibitors (SIs)

SIs are usually hydrophilic chemicals used for preventing or retarding crystal formation and growth of inorganic scales⁶. They are widely used due to their cheap and effective nature. However, the challenge of synthesizing an ideal SI that can provide a satisfactory overall performance as well as meeting environmental regulations criteria still remains ongoing. Depending on their chemical structure, SIs present different features which make them useful and unique for certain applications. SIs can be deployed into the production system by different means, such as continuous injection or squeeze treatment. The mechanisms of inhibition, characteristics, and deployment of SIs will be discussed throughout this section.

2.3.1. Mechanisms of action

The presence of certain functional groups in the chemical structures of SIs will help to increase inhibition as they can interact with divalent cations (Ca^{2+} and Mg^{2+}) on the crystal surface. Such is the case of phosphate ions ($-\text{OPO}_3\text{H}^-$), phosphonate ions ($-\text{PO}_3\text{H}^-$), phosphinate ions ($-\text{PO}_2\text{H}^-$), carboxylate ions ($-\text{COO}^-$), amides ($-\text{CONH}_2$), ester ($-\text{COOR}$), and sulfonate ions ($-\text{SO}_3^-$), as they are able to mimic the carbonate and sulfate dianions in the scales^{1,14}. Usually, SIs containing more than one of these molecules are highly effective for oilfield applications. However, the most effective SIs are those that can be prepared in their anionic dissociated form¹. In this sub-section, two main mechanisms of scale inhibition will be presented: kinetic and thermodynamic inhibition.

2.3.1.1. Kinetic inhibition

Inhibitors that act by this mechanism adsorb onto the crystal's surface, consequently preventing crystal growth. This mechanism could occur through two further sub-mechanisms. First, nucleation inhibition, where SIs occupy nucleation sites disrupting scale forming molecules. And second, crystal growth inhibition, where SIs are adsorbed to the active growth sites of the crystal, causing morphological changes preventing further scale growth^{4,15}.

Polymers such as polyvinyl sulfonate (PVS) and the common SI polyphosphinocarboxylic acid (PPCA), are recognized as good nucleation inhibitors, whereas non-polymeric SIs with small phosphonate groups such as diethylenetriamine penta(methylphosphoric acid) (DTPMP) are effective crystal growth inhibitors⁴. However, regardless of the mechanism of inhibition, it is desired that the SI has strong interaction with the produced water anions or cations in order to uphold its antiscaling potential.

2.3.1.2. Thermodynamic inhibition

This mechanism is based on decreasing the activity of supersaturated ions in the solution. This is made possible by adding complexing and chelating agents that react with cations in solution more favorably than the anions which produce a specific scale. Some common inhibitors used for this purpose are EDTA and nitrilo triacetic acid^{4,15}. Another way of accomplishing thermodynamic inhibition is by manipulating the conditions of the system, such as pH, temperature of pressure. For example, higher solubility of calcite is obtained at decreasing pH and increased partial pressure of CO₂.

2.3.2. Characteristics of 'ideal' SIs

Due to varying conditions between oilfields, there are several factors to consider when selecting a scale inhibitor^{1,16}. First, it is desired that SIs provide effective scale inhibition performance at low concentration and at the same time last for extended periods. As chemicals are expensive to produce, minimum doses imply lower operational costs. Also, compatibility with seawater, formation water and other production chemicals need to be evaluated to avoid any further downstream problems. In some cases, if the SI does not tolerate high concentrations of divalent cations (e.g., Ca²⁺ and Mg²⁺) precipitation of Ca²⁺-SI complexes are likely to occur, leading to a series of reduced flow problems. The impact of using SIs alongside other production chemicals must also be recognized and assessed beforehand, as side effects or other production issues may arise.

For squeeze treatments, a balance between adsorption-desorption properties of the SI is desired to release them into the production water at concentrations that provide good inhibition efficiency. Furthermore, stability properties are also important. SIs should remain stable during their intended lifetime, this means, from transport to storage until their application in the field. HPHT conditions are common in oil production and could unfavorably affect the stability of the SI.

Finally, environmental regulations must be followed before deploying any chemical as they will be discharged in the surrounding environment. Low toxicity and bioaccumulation, as well as high biodegradability are important criteria for green chemicals to meet, especially in areas with strict environmental requirements, such as the North Sea region¹⁷.

2.3.3. Industrial deployment of SIs

SIs are deployed in the field by three main methods: continuous injection, batch treatment, and squeeze treatment^{1,18}. Advantages and disadvantages of these methods have been discussed in detail¹⁸. However, they are briefly presented in the following two sections.

2.3.3.1. Continuous injection and batch treatment

The continuous injection method is usually carried out in fields where produced water injection is needed. As its name indicates, it consists of continuously injecting a SI solution at a point with enough turbulence to afford even mixing¹⁸. SIs can be introduced to the system in both topside and downhole via chemical injection lines¹. Alternatively, during batch treatment, a certain amount of SI is pumped periodically through the system and is allowed to act for an extended period of time¹⁸.

2.3.3.2. Squeeze treatment

The most widely and preferred mechanism for SI deployment in the oil and gas industry is squeeze treatment. For this approach, it is desired that the SI presents high thermal stability as it will be forced to operate at extremely high temperatures in the formation rock. Squeeze treatment consists of the injection of SI into the reservoir formation rock, proximal to the wellbore area. During this process, the production system is shut off, then, the SI is injected and given time to adsorb into the rocks pores. When the estimated time of adsorption has passed, the well is turned on back to normal operation. Then, the SI is slowly released as the produced water flows through the rock, preventing scale formation. With time, SI concentration in produced water will decrease, reaching a concentration where it no longer has an inhibitory effect. At this point, re-squeezing is needed¹.

The overall squeeze procedure is costly; therefore, the SI must be able to demonstrate good performance at ppm concentrations as well as good retention onto the rock in order to provide long squeeze lifetimes. There are other mechanisms of action apart from adsorption by which SIs are held into the rock matrix. SIs can also be retained into the rock by precipitation in the formation rock. However, this mechanism is not recommended as in the long term can cause clogging of pores and reduce hydrocarbon outflow^{4,19}.

Phosphonates and aminophosphonates have been widely studied as SIs for squeeze treatment¹⁹. They adsorb well onto the formation rock, providing a long squeeze lifetime and decreasing the need of frequent well management and re-squeeze. But a drawback is that classic SIs (DTPMP and ATMP) demonstrate low biodegradability implying that they cannot be used in offshore regions with strict environmental regulations. Also, many of them lack good compatibility with high calcium brines, leading to precipitation and deposition of a Ca²⁺-SI complex⁸.

2.3.4. Commercial SIs

Most common classes of scale inhibitors are polyphosphates, phosphate esters, non-polymeric phosphonates and aminophosphonates, polyphosphonates, polycarboxylates, polysulfonates, phosphino-polymers, and polyphosphonates¹. Polymeric scale inhibitors present a highly acceptable performance at low concentrations against calcite, barite, and gypsum scales as well as an environmentally acceptable nature^{4,20}. They have been shown to withstand high temperatures, which allows them as good candidates for squeeze applications. An overview of some common commercial SIs is given in this section.

Aminophosphonates are widely recognized commercial SIs, such is the case of ATMP (aminotris(methylenephosphonic) acid), DTPMP and EDTMP (ethylenediamine tetra(methylene phosphonic acid)). However, low calcium tolerance and low biodegradability for products of this nature have been reported. For example, DTPMP and ATMP have presented BOD₂₈ values of 15% and 34%, respectively²¹. Due to their chemical composition, aminophosphonates contribute to unwanted eutrophication in discharge water bodies. Therefore, researchers are working towards finding suitable replacements for aminophosphonates SIs with other classes of SIs.

Polyepoxysuccinic acid (PESA) and polyaspartic acid (PASP) form a class of biodegradable SIs due to their nitrogen and phosphorous-free nature. A biodegradation of 83-87% over 28 days has been reported previously for PASP⁶. Both PESA and PASP have been studied against calcite, gypsum and barium formation, showing good inhibition performance^{22,23}. However, their efficiency decreases when temperature or Ca²⁺ concentrations increase²³.

Furthermore, polycarboxylic acid (PCA) has also been tested for calcite and barite scales, showing adequate performance as well as good hydrothermal stability. A BOD₂₈ test resulted in 68.6% biodegradation according to the OECD 306 method. Toxicity studies were also carried out demonstrating that PCA can be considered as non-toxic. Its performance was evaluated through static and dynamic conditions and compared to that of PASP, obtaining a better performance for PCA²⁴.

Furthermore, relatively few derivatives of natural polymers that provide a more environmentally friendly fate have been developed as SIs¹⁷. Carboxymethylinulin (CMI) is a polysaccharide-based polycarboxylate. It has been proved to act as a green inhibitor, especially for calcite, due to the presence of carboxylic acid groups and the absence of phosphorous and nitrogen in its structure. BOD₂₈ values for this chemical have been reported to be superior to 20% together with evaluations of toxicity, making it a particularly good alternative for environmentally sensitive areas^{6,25}.

Polymers of vinyl sulfonate are also effective as SIs, especially against barite scales. Most environmental profiles of these compounds are still under review¹⁷. PVS is a sulfonated polymeric SI mainly used for squeeze applications due to its ability to withstand high temperatures and high calcium concentrations. It is also efficient at low pH values and temperatures up to 4°C^{1,17,26}. However, in general terms, polysulfonates do not absorb strongly to formation rock, requiring greater quantities to be used and negatively affecting their squeeze lifetime¹.

2.3.5. Performance evaluation of SIs in laboratory settings

There are two main tests used to evaluate the performance of SIs adapted to the oil industry in laboratory settings, the static jar test and dynamic tube blocking test^{3,27}. The first is commonly used due to its simplicity and low cost to examine SIs performance in the liquid bulk phase. The latter is a more sophisticated method that provides more precise and accurate results at certain pre-set conditions, mimicking conditions found in wells. Both of these methods can be carried out for different known water chemistries.

The initial approach of this thesis was meant to be based on the dynamic tube blocking test. Unfortunately, due to prolonged technical malfunctions, it had to be replaced for static bottle tests as an alternative method. Before arriving to this decision, additional approaches were considered as alternatives to the two main methods. A summary of these alternatives is given in this section. Additionally, other performance tests must be adjunctly included in the evaluation of SIs before considering their application in the field. Such is the case of thermal stability, compatibility with high Ca²⁺ concentrations, and their potential for biodegradation. All these aspects will allow for an overall

judgment of the performance of SIs and their potential use and effectiveness in the industry. These methods also evaluated throughout this research, will be described in more detail in Section 3.3.

First, static bottle tests according to the NACE TM0374-2007 standard provide uniformity in results due to their established brines composition and testing conditions. The protocol consists of mixing cationic and anionic brines according to field conditions with different dosages of SI at a given temperature for a specific length of time. Samples are then processed for ion analysis via titration with EDTA. This method is a low-cost alternative that allows for a simple comparison between different SIs. However, they are time-consuming and do not provide any deep-knowledge insight or simulation of field conditions. Several limitations such as restricted pressure and temperature (up to 100°C) affect the results if SIs are to be considered for field applications. Therefore, they should only be used as a pre-screening method in conjunction with others, such as the dynamic tube blocking test. Also, in cases where SIs are not compatible with a high concentration of Ca^{2+} , misleading results can be obtained due to the precipitation of SI^{23} .

The static bottle test method has been widely applied to evaluate and compare the performance of different SIs^{23,26,28-34}. For example, researchers have tested a copolymer of acrylic acid-diphenylamine sulfonic acid for calcite and gypsum scale inhibition at concentrations of 300 ppm CO_3^{2-} and 2000 ppm SO_4^{2-} ³². Their results show that the copolymer suits better for inhibiting gypsum scale at low temperatures and neutral pH. Once temperature and pH increase, the SI begins to lose efficiency rapidly. The SI presented an inhibition efficiency of 100% at 2 ppm, pH 7, and 50 °C, quickly falling to 86% at 2 ppm, pH 7, and 80 °C when assessed against calcite. At the same conditions, the efficiency only decreases by 2% when assessed against gypsum.

Recently, another approach for SI evaluation has been developed³⁵. The so-called Kinetic Turbidity Test (KTT) uses Ultraviolet-Visible spectrophotometry to monitor scale formation at different dosages of SI within a period of time. The spectrophotometer in question requires a multi-sample holder with magnetic stirring and temperature control in all cells. This allows for varying testing conditions where absorbance data can be obtained at different times and temperatures. This is a time efficient method that offers good reproducibility. Furthermore, the absorbance data obtained with this method also allows for studying the rate of the kinetics of scale formation under a variety of conditions. An approach to carry out this method has been proposed and compared to results obtained via static bottle tests, showing that KTT results comply with the pre-screening performance from static bottle tests³⁵. Additional studies about scale formation kinetics, SI efficiency, inhibition mechanisms, and SI-brine compatibility have been studied using this method³⁶. This approach has been preferred as SI evaluation in some studies^{37,38}.

Conductivity measurements have also been developed for the evaluation of SIs³⁹. The method determines the supersaturation level of a specific scale formed from a determined brine composition at desired conditions in the presence and absence of SI. The cationic and anionic brines usually consist of a chloride salt solution of the divalent cation (e.g., CaCl₂ or BaCl₂) and the sodium salt of the respective anion (e.g., Na₂SO₄ or Na₂CO₃), respectively. The cationic brine is set up with a conductivity sensor under stirring, and it is further titrated with the anionic brine. Conductivity and volumes of titrating solution are recorded until a sudden drop in conductivity occurs, indicating scale formation. The degree of supersaturation is then calculated as a ratio between the supersaturation obtained in the presence of SI and the obtained without SI. Usually, this method is supplemented with other approaches such as static bottle tests^{29,40,41}.

Additionally, high-pressure dynamic tube blocking test (HPDTBT) or dynamic scale rig (DSR) is a commonly used laboratory method that allows for testing the performance of SIs over brines with complex water chemistry^{24,42-45}. This system allows two incompatible brines to meet each other on a narrow capillary. As scale forms, the differential pressure across the coil increases, and this is measured to evaluate the performance of SIs. The main advantage of scale rigs is that they have a versatile design that can be manipulated up to 410 bar (6000 psi) and 200°C, depending on the system studied⁴⁶. For example, for oilfield applications, the oven temperature can be set to 100°C and a pressure of 80 bar^{43,47,48}. They have also been used for kidney stones inhibition studies where the system should be adjusted to body conditions, this is, approximately 37°C and a pressure of 1500-1600 psi⁴⁹.

The main purpose of conducting a HPDTBT is to determine the minimum inhibitor concentration (MIC) and fail inhibitor concentration (FIC). FIC is defined as the inhibitor concentration at which the chemical loses its potential to inhibit scale. This means that scale is formed, and the differential pressure increases abruptly. The MIC is the inhibitor concentration tested before the FIC, at which the SI was effective at inhibiting scale formation. A more detailed description of this methodology will be discussed in Section 3.3.3.

Core flood tests are another robust alternative to dynamic testing. They are carried out by fluid pumping onto a core sample at reservoir conditions. Flow rates and pressure drops across the core are measured, allowing for an evaluation of the rock's permeability and an estimation of the expected squeeze lifetime^{1,50,51}.

Scanning Electron Microscopy (SEM) and X-Ray Diffraction Spectroscopy (XRD) techniques have also been used for SI evaluation, providing information about morphology and structure deformation of precipitated crystals, as well as inhibition mechanisms^{32,45}. Usually, scale precipitates with and

without inhibitor are examined, allowing to study the effect of SI on crystal's shapes. The modification of regular and compact scale crystals by the presence of SIs has been reported to retard the scale formation process³³. A combined method of static bottle tests and SEM/XRD techniques has been reported for screening SIs in low scaling regimes⁵². Results were compared to those obtained using KTT, concluding that the proposed method serves as a rapid evaluation of SIs and as an alternative to dynamic tests.

Simulation methods such as Molecular Dynamics (MD) also provide information about the interaction between SIs and crystal surfaces of scales^{53,54}. For example, interactions between CMI and calcite scales have been investigated using MD at different temperatures and degrees of polymerization of CMI⁵⁵.

2.4. Environmental challenges

As actively mentioned throughout this literature review, the need for more environmentally friendly chemicals is a challenge for big industries, especially for the oilfield industry. The current high energy demand and ongoing exploitation of hydrocarbons go hand in hand with vast volumes of chemicals discharged into the environment. Discharge regulations have become more stringent due to the increased awareness of environmental hazards, forcing different industries at a worldwide level, to decrease and replace the release of toxic (or potentially toxic) compounds into more bioavailable and hence, biodegradable, chemicals. Biodegradability is an environmental factor that matters greatly in the logistics and operation of processes, as it indicates the ability of bacteria to break down (mineralization to CO₂) certain compounds.

OSPAR (named from the original Oslo and Paris conventions) is a legal agreement between 15 different countries leading international cooperation with the purpose of protecting the marine environment of the North-East Atlantic. OSPAR presents the required guidelines to follow for ecotoxicological examination of applied chemicals in offshore drilling in the North Sea⁵⁶. In order to determine the ecotoxicology of a product, OSPAR requires three fundamental classes of tests:

- a. Acute toxicity, which refers to the harmful impacts of a substance that appear in key indicator species of fish or crustaceans in order to detect the lethality level. This is carried out in different periods of time or in one single dose, depending on the test chosen.
- b. Bioaccumulation potential, associated with the relative solubility of a chemical in lipids and water. It refers to the accumulation of substances in the environment before they are taken in by the first organism in a food chain. Bioaccumulation can be determined based on relative solubility

in octanol (representing fatty tissue) and water, calculated as the logarithm of the octanol-water distribution coefficient ($\log P_{ow}$)⁵⁷. If this coefficient is larger than or equal to three, the substance is considered to be a bioaccumulation risk unless the experimental examination of a bioaccumulation factor (BCF) shows the opposite.

- c. Seawater biodegradation testing is specified in the OECD (Organisation for Economic Co-operation and Development) 306 protocol. Two methods have been proposed, the Shake Flask Method and the Closed Bottle Method²⁵. In this project, Closed Bottle Method will be performed over a 28-days period. Here, biodegradation is calculated as the ratio between the oxygen consumed (biological oxygen demand, BOD) during the degradation period and the calculated theoretical oxygen demand (ThOD).

In the Norwegian Sector, Harmonised Offshore Chemical Notification Format (HOCNF) is a document that ranks chemicals according to their environmental impact, as presented in Table 2. It applies to chemicals used in offshore activities and in the OSPAR maritime area. Moreover, OSPAR commission has created a list of chemicals considered to Pose Little or No Risk (PLONOR) to the environment. Chemicals that take part on this list, considered ‘green’ chemicals, are not strongly regulated. These are non-toxic, do not bioaccumulate and are readily biodegradable.

Table 2. Classification of chemicals according to their environmental impact.

Category	Discharge	Criteria
Black	Not allowed to discharge under any circumstance	Mutagenic or harmful to reproduction BOD ₂₈ < 20%
Red	Only discharged under special conditions. Chemicals to be phased out.	2 out of 3 criteria: BOD ₂₈ < 60% LogP _{ow} ≥ 3 LC ₅₀ or EC ₅₀ ≤ 10 mg/L
Yellow	Can generally be discharged by offshore industry.	Not in black, red or green categories 20% ≤ BOD ₂₈ < 60%
Green	None or minimal environmental impact. No specific conditions required for their discharge.	PLONOR list log P _{ow} < 3 LC ₅₀ or EC ₅₀ > 100 mg/L

Produced water from oil industry effluents carry a considerable amount of chemicals that are harmful to the environment, including SIs. Most current commercial SIs, provide good inhibition performance. However, these compounds are not obtained from natural sources, they are synthetically produced. Therefore, they may resist biodegradation as microorganisms are not able to assimilate and break them down. Furthermore, it is important to note that nitrogen and phosphorous are limiting nutrients for microorganisms. As SIs are usually nitrogenated or phosphonated compounds, they are contributors to water systems disturbances, like eutrophication^{58,59}. Therefore, it is important to study the ability of microorganisms to assimilate new chemicals in different ecosystems.

A general aim in the production chemistry research field is finding SIs with overall high scale inhibition efficiency whilst also having high biodegradation potential.

2.5. Earlier studies

A wide number of researchers are working on finding the optimal formula for synthesizing eco-friendly scale inhibitors. A brief review of the most recent accomplishments is given in this section.

Chitosan, a polysaccharide, has been evaluated and researched as a SI^{28,29,60}. Chitosan comes from the deacetylation of chitin which is usually found in the hard shells of crustacean organisms⁶¹. Studies have shown that chitosan considerably inhibits calcite scale formation but performs poorly when assessed against gypsum scale^{28,60}. A mixture of sodium alginate and chitosan has been proposed to inhibit both calcite and gypsum scales more efficiently than the commercial (hydroxyethylidene)bisphosphonic acid (HEDP)²⁸. Studies have reported the non-toxicity and biocompatibility of chitosan⁶². However, others have stated that in some cases chitosan may not be readily biodegradable due to its natural complex structures that form the exoskeletons of organisms¹⁷.

Furthermore, pteroyl-L glutamic acid (PGLU) otherwise known as folic acid, an essential vitamin for regular body functionality, has also been tested for calcite scale inhibition in static and dynamic tests showing excellent efficiency⁶³. Researchers have also tried to use plant-based extracts as natural, low cost biodegradable scale inhibitors^{64,65}. However, these were found to be thermally unstable at high temperatures, decreasing their suitability for oilfield applications such as squeeze treatment. Natural substances containing phosphorous such as brown sea algae have also been evaluated against calcite, gypsum, barite, and strontium carbonate scales, showing good to excellent performance compared to HEDP⁴¹. At around 15 ppm algae extract inhibition was calculated to be 100% at 70 °C against gypsum. Any further decrease in concentration led to a rapid decrease in efficiency. On top of that, the SI did not hold up against barite inhibition even at concentrations exceeding 200 ppm, meaning they are extremely inefficient at treating barite scale.

As mentioned in Section 2.3.4., most commercial non-polymeric SIs have incorporated into their structure the aminomethylenephosphonate functional group (e.g., ATMP, DTPMP, EDTMP). However, the presence of such group decreases their biodegradability substantially, as they are usually complexed with Ca^{2+} and Mg^{2+} . The formation of these complexes in natural waters limits their bioavailability¹⁷. Therefore, oil and gas companies are actively working with researchers to find suitable replacements as a great deal of importance is given towards environmentally friendly and biodegradable scale inhibitors with little to no toxicity.

An alternate commercial phosphonate SI is HEDP, a biodegradable bisphosphonate commonly used in oilfield scale treatment applications. From a general perspective, bisphosphonates are also a known set of compounds used to treat bone diseases for more than four decades⁶⁶. The low toxicity of bisphosphonates has previously served as an incentive for researchers to synthesize SIs. A set of bisphosphonates functionalized with amino groups were synthesized and examined against barite and calcite scales showing poor and moderate inhibition, respectively, as opposed to the commercially used DTPMP and ATMP²¹. More recently, aliphatic and aromatic hydroxybisphosphonates were also tested against calcite and barite formation but showed poor calcium compatibility⁶⁷. Conclusions withdrawn from these studies state that if the water chemistry suggests low calcium concentrations, using low toxicity bisphosphonates as SIs may be a potential way forward for topside and downhole applications.

The use of nanotechnology for scale management in oilfield production has also gained interest by researchers and companies. Development of nanotechnology for inhibition of inorganic scale and how this relatively new branch of technology has contributed to an improved oilfield SI squeeze applications and lifetimes has been reviewed⁶⁸. Although nanomaterials have been studied for the past two decades, they are still not fully developed for field use but is expected that it can be a more economic and efficient alternative than conventional methods of maintaining scale.

2.6. New idea – Project 1

The purpose of this project is to synthesize and evaluate new SIs from a non-toxic and commercially available hydroxybisphosphonate known as alendronic acid, which is widely used as a medication to treat osteoporosis. Alendronic acid will be tested for scale inhibition efficiency and will be referred to as **SI-1**. Different sulfonate, phosphonate, and carboxylate groups will be attached to the structure of alendronic acid to improve its performance as SI. As mentioned in Section 2.3.1, these functional groups are known to enhance the metal-binding capabilities of SIs with scaling cations and, therefore, limit scale formation. The proposed modified alendronic acid structures are presented in Figure 3.

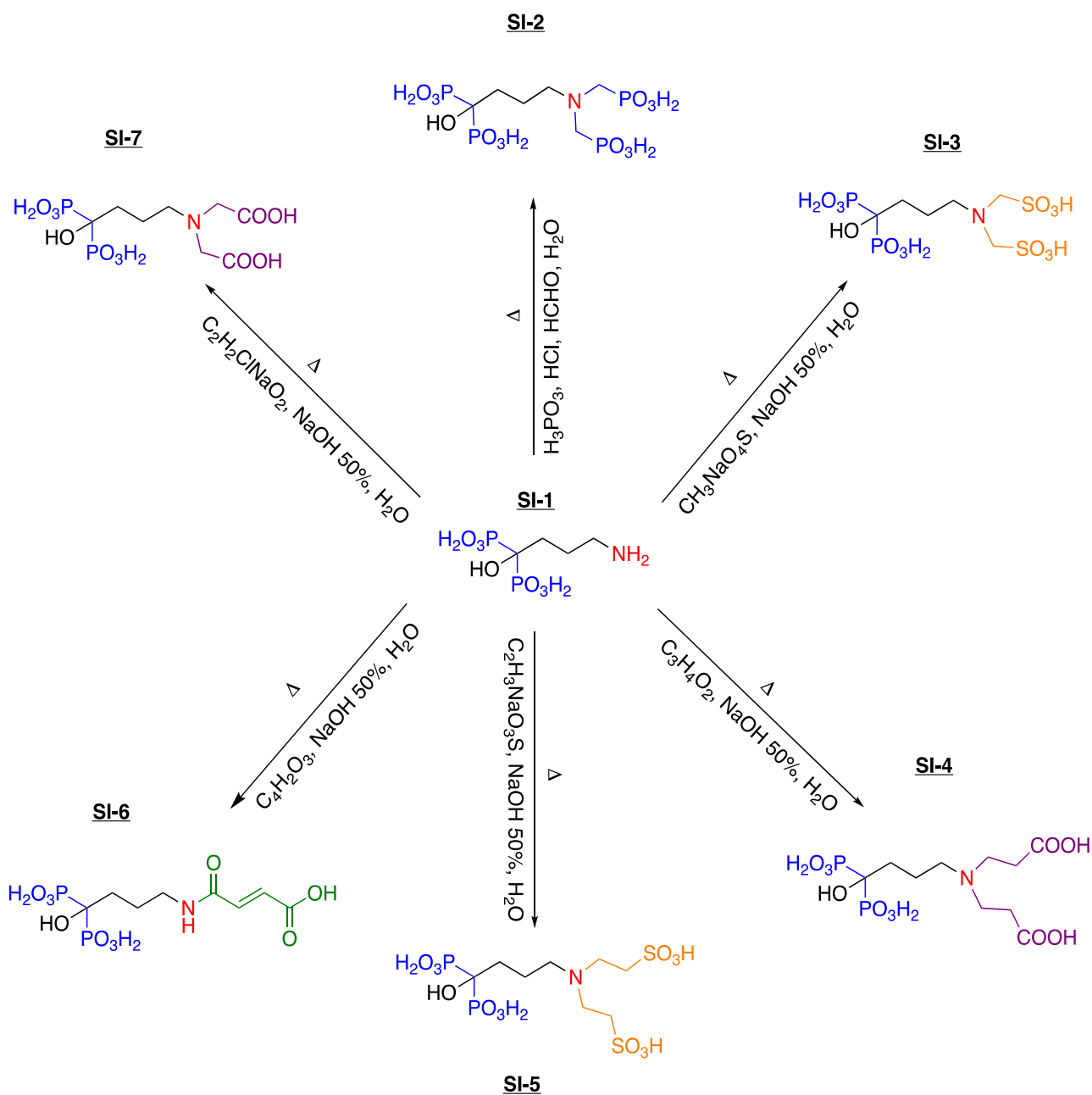


Figure 3. In-house synthesized SIs using alendronic acid (SI-1) as starting compound.

The synthesized products will be characterized, and the performance of the different functional groups against calcite and gypsum scales will be studied according to the NACE TM0374-2007 standard. The overall performance of the synthesized products will be compared to commercially available scale inhibitors, such as ATMP, PVS and CMI. As far as the author is concerned, the alendronic acid derivatives presented in this research have not been reported as SIs for oilfield applications. However, other bisphosphonates that serve as bone-targeting compounds have been evaluated as SIs^{67,69}. As previously mentioned, one of the main drawbacks of commercial SIs is their poor biodegradability. Therefore, the relatively small molecule size of alendronic acid and its low toxicity serve as motivation to design chemicals that could give good scale inhibition performance together with good calcium tolerance and biodegradation.

2.7. New idea – Project 2

Fosfomycin is a small molecule that belongs to the class of phosphonic antibiotics used for the treatment of urinary tract infections. However, similarly to alendronic acid, it is considered as starting compound to synthesize potential scale inhibitors that could provide good inhibition efficiency and improved biodegradation performance due to its small structure and low toxicity.

Herein, fosfomycin disodium salt (**SI-8**) will be evaluated as a scale inhibitor against oilfield scales. In addition, **SI-8** will be used as a starting material to synthesize a new series of non-polymeric phosphonate-based SIs. First, the bioavailable version of fosfomycin, commercially known as fosfomycin trometamol (**SI-9**), will be synthesized according to the European Patent 1 762 573 A1⁷⁰. This structure contains an ether linkage, and it has been shown that this functional group improves biodegradation performance⁷¹.

SI-9 will be further phosphonated via the Moedritzer-Irani reaction⁷². Two sets of reactions of this type will be carried out. First, 1 equivalent of **SI-9** to 2 equivalents of reactants (H_3PO_3 , HCl, HCHO) will be used to give **SI-11**. After that, 1:1 proportion of reactants will be used to obtain **SI-12**. Furthermore, a hydrolysis reaction of **SI-8** will be carried out under highly acidic conditions at 100°C to produce **SI-10**. This will allow the comparison of performance between the epoxide ring of **SI-8** and the linear structure derived from the same compound (**SI-10**). Target structures of SIs derived from fosfomycin are summarized in Figure 4.

As mentioned in the previous section, nearly all small phosphonate molecules used as commercial SIs, contain aminomethylenephosphonate groups (e.g., ATMP). However, their main disadvantage is poor biodegradability and low calcium compatibility. At the same time, they are significant contributors to eutrophication as nitrogen and phosphorus are limiting nutrients for microorganisms⁵⁹. This reason serves as motivation to synthesize and evaluate SIs with nitrogen-free phosphonate groups. The overall idea of this project is to synthesize aminomethylenephosphonates and nitrogen-free phosphonates derived from the same starting compound and evaluate their performance as SIs.

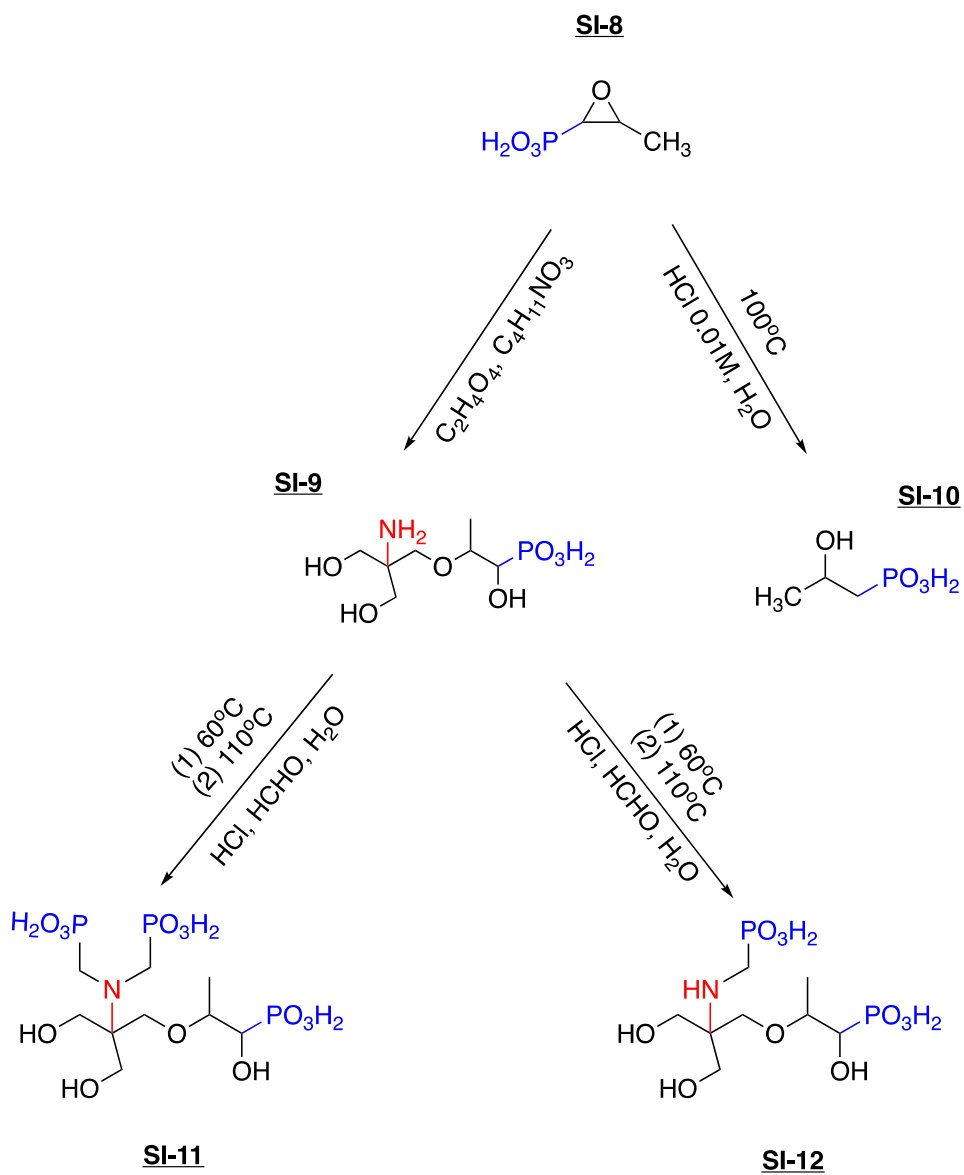


Figure 4. In-house synthesized SIs using fosfomicin (SI-8) as starting compound.

3. MATERIALS AND METHODS

3.1. Chemicals and equipment

Chemicals used in this project were purchased from Tokyo Chemical Industry CO., LTD., Sigma-Aldrich (Merck), VWR chemicals, and ACROS organics. All solvents were used as purchased without further purification. Commercial scale inhibitors ATMP, CMI, and PVS were obtained from Thermphos International, Italmach Chemicals, and Clariant Specialty Chemicals, respectively.

For all syntheses described below in Section 3.2, reflux set up equipped with a thermometer, hot plate magnetic stirrer C-MAG HS 7 (IKA®, Germany), an oil bath, and a reflux condenser were used, as shown in Figure 5. A rotary evaporator RV 10 digital (IKA®, Germany) equipped with a PC 3001 VARIOpro (Vacuubrand®, Germany) pumping unit was used to remove solvents under reduced pressure. For pH measurements and weighing chemicals, a Handylab 1 pHmeter (Schott®, Germany) and an Ohaus Adventurer AX523/E (USA) balance were used, respectively.

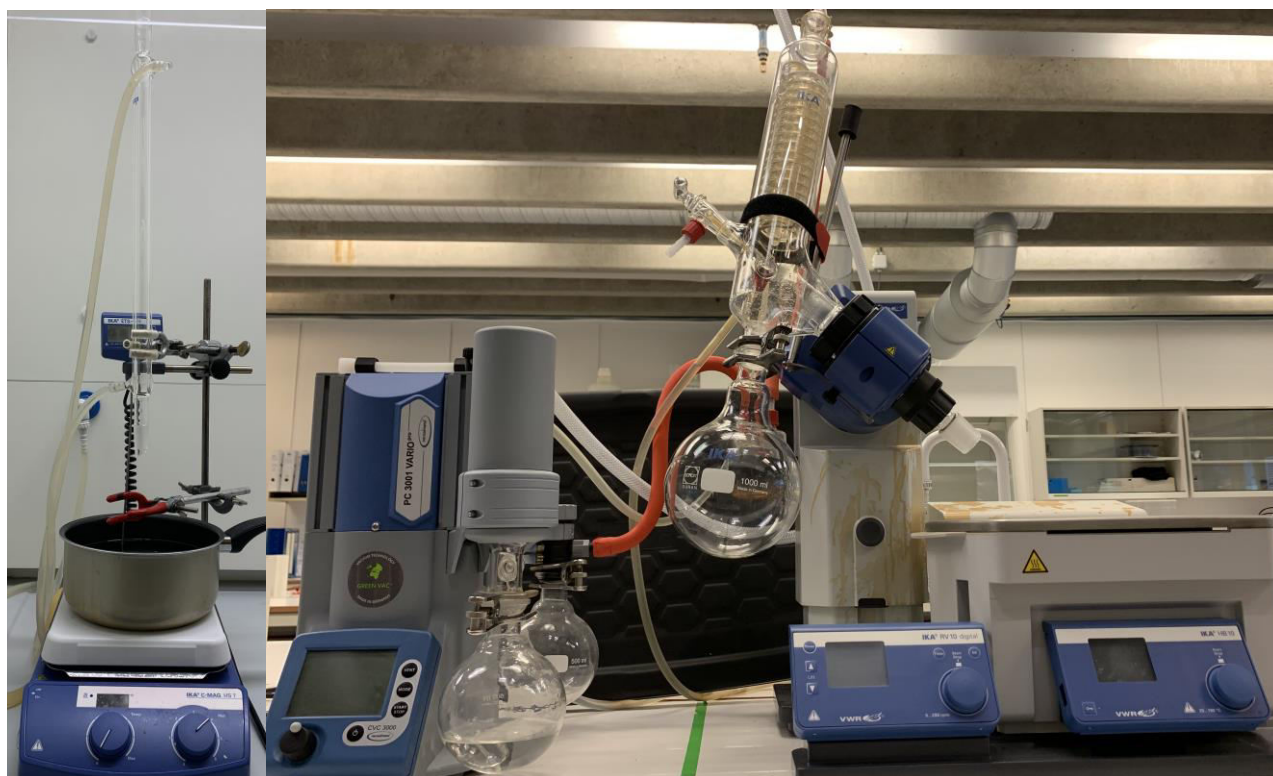


Figure 5. Reflux set up (left) and solvent evaporation equipment (right).

3.2. Synthesis and characterization of SIs

In this thesis, two research projects were performed. First, a series of non-toxic hydroxybisphosphonates derived from alendronic acid were synthesized. Second, fosfomycin, a natural product antibiotic, was modified to produce aminomethylenephosphonates as well as nitrogen-free phosphonated SIs. All products obtained were characterized and screened as SIs for calcite and gypsum oilfield scales.

The structures of the synthesized products were characterized using nuclear magnetic resonance (NMR) spectroscopy and Fourier-transform infrared (FTIR) spectroscopy. ^1H and ^{31}P NMR chemical shifts were obtained in deuterium oxide (D_2O), using a 400 MHz Bruker NMR Spectrometer (USA). The data was processed using TopSpinTM 3.2 software. Additionally, an Agilent Cary 630 FTIR spectrometer (USA) equipped with a diamond composite ATR (Attenuated Total Reflectance) crystal was used. FTIR data was processed using MicroLab PC software. All NMR and FTIR spectra are provided in Appendices A and B (Project 1) and F and G (Project 2), respectively.

3.2.1. Project 1

This section describes the syntheses of **SI-2** to **SI-7** using alendronic acid (**SI-1**) as the main reactant. The syntheses of these compounds were carried out during the spring of 2019⁷³. For clarification, the compounds were obtained after synthesis in their dried form and were purified further during this project. Details of synthesis and purification are mentioned in their respective subsections.

3.2.1.1. **SI-1**: Alendronic acid

SI-1 was purchased from Tokyo Chemical Industry CO., LTD. The chemical structure is shown in Figure 6.

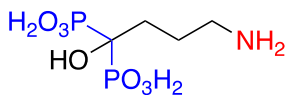


Figure 6. Chemical structure of SI-1.

(4-amino-1-hydroxybutane-1,1-diyl)bis(phosphonic acid) (**SI-1**): IR ν_{max} (cm^{-1}): 3196 (NH_2), 3086 (OH), 919, 824 (PO_3). ^1H NMR (D_2O , 400 MHz) δ ppm: 2.96 (t, 2H, $\text{NH}_2\text{-CH}_2\text{-CH}_2\text{-}$), 1.99 -1.89 (br, 4H, $\text{-CH}_2\text{-CH}_2\text{-C(OH)(PO}_3\text{H}_2)_2$). ^{31}P NMR (D_2O , 162 MHz) δ ppm: 18.49.

3.2.1.2. SI-2: ((4-hydroxy-4,4-diphosphonobutyl)azanediyl)dimethanephosphonic acid

A 100 mL two-neck round bottom flask equipped with a reflux condenser at 80°C and magnetic stirring was loaded with alendronic acid (2.50 g, 10.04 mmol) and phosphorous acid (1.68 g, 20.48 mmol) together with 20 mL of deionized water. HCl 37% (1.98 g, 54.24 mmol) was added dropwise to the solution. Then, formaldehyde 37% (1.63 g, 54.23 mmol) was injected dropwise with a syringe through a rubber cork over a 30-minutes window. The reactor was kept under the same conditions overnight and a balloon filled with N₂ gas. The crude solution was transferred to a 250 mL one-neck flask for solvent removal under reduced pressure using a rotary evaporator. An oily product was obtained and left under stirring with acetone overnight. Then, the suspension was filtered using a Büchner funnel, obtaining a white powder. The synthesis route of this reaction is shown in Figure 7.

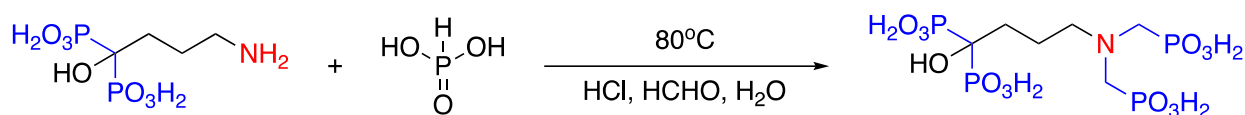


Figure 7. Synthesis route of SI-2.

For further purification, the product was dissolved in approximately 25 mL of deionized water on a one-neck round bottom flask. Then, the pH was adjusted to 4.38 using 0.01 M HCl. The solution was left under reflux at 110°C overnight. The next day, it was filtered using a Büchner funnel to remove solid impurities. The water phase in the filtrate was removed under pressure using a rotary evaporator, affording pale-yellow crystals as final product.

(4-hydroxy-4,4-diphosphonobutyl)azanediyl)dimethanephosphonic acid (SI-2): Yield: 56%. IR ν_{\max} (cm⁻¹): 3371 (OH), 1046, 898 (PO₃). ¹H NMR (D₂O, 400 MHz) δ ppm: 3.46 - 3.43 (d, 4H, 2×-CH₂-PO₃H₂), 3.11-2.95 (br, 2H, -N-CH₂-CH₂-), 2.04 - 1.93 (br, 4H, -CH₂-CH₂-C(OH)(PO₃H₂)₂). ³¹P NMR (D₂O, 162.00 MHz) δ ppm: 17.71, 7.08.

3.2.1.3. SI-3: ((4-hydroxy-4,4-diphosphonobutyl)azanediyl)dimethanesulfonic acid

A 100 mL two-neck flask equipped with a reflux condenser at 80°C and magnetic stirring was loaded with alendronic acid (2.50 g, 10.04 mmol) and formaldehyde-sodium bisulfite adduct (2.83 g, 21.13 mmol) along with 30 mL of deionized water. Sodium hydroxide (0.80 g, 20.08 mmol) was also added to the solution. The pH of the solution was further adjusted to 11.67 by adding NaOH 50% dropwise. The reaction was kept overnight under the same conditions and a balloon filled with N₂ gas. The next day, pH was measured to make sure it remained constant. Thereafter, the reaction was kept overnight whilst stirring at 80°C.

The crude solution was transferred to a 250 mL one-neck flask for solvent removal under reduced pressure using a rotary evaporator. A white solid product was obtained after water removal. The synthesis route of this reaction is shown in Figure 8.

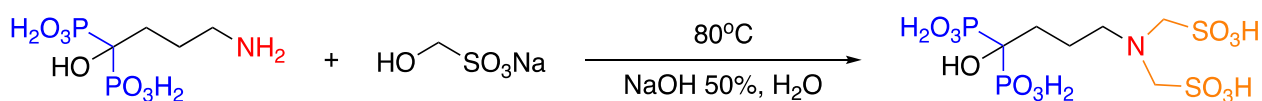


Figure 8. Synthesis route of SI-3.

For further purification, the product was dissolved in approximately 25 mL of deionized water on a one-neck round bottom flask. Then, the pH was adjusted to 5.87 using 0.01 M HCl. The solution was left under reflux at 110°C overnight. The next day, it was filtered using a Büchner funnel to remove any solid impurities. The water phase in the filtrate was removed under pressure using a rotary evaporator. A sticky powder was obtained and further washed with diethyl ether under strong stirring overnight. The solvent was left to evaporate at room temperature. The final product was dried at 60°C overnight in a TS 8056 oven (Termaks, Norway), affording a white powder sodium salt of **SI-3**.

((4-hydroxy-4,4-diphosphonobutyl)azanediyl)dimethanesulfonic acid (**SI-3**): Yield: 53%. IR ν_{\max} (cm⁻¹): 3373 (OH), 1162, 1027 (SO₃), 904, 776 (PO₃). ¹H NMR (D₂O, 400 MHz) δ ppm: 4.34 (s, 4H, 2× -CH₂-SO₃H), 2.99 (t, 2H, -N-CH₂-CH₂-), 1.96 – 1.91 (br, 4H, -CH₂-CH₂-C(OH)(PO₃H₂)₂). ³¹P NMR (D₂O, 162.00 MHz) δ ppm: 17.91.

3.2.1.4. SI-4: 3,3'-((4-hydroxy-4,4-diphosphonobutyl)azanediyl)dipropionic acid

A 100 mL two-neck flask equipped with a reflux condenser at 80°C and magnetic stirring was loaded with alendronic acid (2.50 g, 10.04 mmol) and acrylic acid (1.45 g, 20.07 mmol) along with 30 mL of deionized water. Sodium hydroxide (0.80 g, 20.08 mmol) was then added to the solution. The pH of the solution was adjusted to 11.36 by adding NaOH 50% dropwise. The reaction was kept overnight under the same conditions and a balloon filled with N₂ gas. The next day, pH was measured to make sure it remained constant. Thereafter, the reaction was kept overnight whilst stirring at 80°C. Moreover, the crude solution was transferred to a 250 mL one-neck flask for solvent removal under reduced pressure using a rotary evaporator. A white powder was obtained. The synthesis route of this reaction is shown in Figure 9.

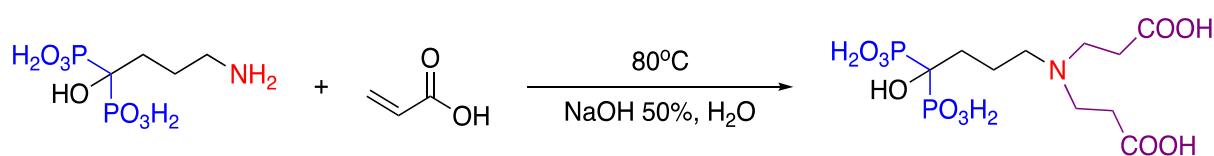


Figure 9. Synthesis route of SI-4.

For further purification, the product was dissolved in approximately 25 mL of deionized water on a one-neck round bottom flask. Then, the pH was adjusted to 4.98 using 0.01 M HCl. The solution was left under reflux at 110°C overnight. The next day, it was filtered using a Büchner funnel to remove any solid impurities. The water phase in the filtrate was removed under pressure using a rotary evaporator to afford a white sodium salt of **SI-4**.

3,3'-((4-hydroxy-4,4-diphosphonobutyl)azanediyl)dipropionic acid (SI-4), Yield: 81%. IR ν_{\max} (cm⁻¹): 3428, 3361 (OH), 1578 (CO), 1052, 880 (PO₃). ¹H NMR (D₂O, 400 MHz,) δ ppm: 3.32 (t, 4H, 2× -CH₂-CH₂-COOH), 3.15 (t, 2H, -N-CH₂-CH₂-), 2.59 (t, 4H, 2× -CH₂-CH₂-COOH), 2.01-1.94 (br, 4H, -CH₂-CH₂-C(OH)(PO₃H₂)₂). ³¹P NMR (D₂O, 162.00 MHz) δ ppm: 17.81.

3.2.1.5. **SI-5**: 2,2'-((4-hydroxy-4,4-diphosphonobutyl)azanediyl)bis(ethane-1-sulfonic acid)

A 100 mL two-neck flask equipped with a reflux condenser at 80°C and magnetic stirring was loaded with alendronic acid (2.50 g, 10.04 mmol) and vinyl sulfonic sodium salt (10.45 g, 80.29 mmol) along with 30 mL of deionized water. Sodium hydroxide (0.80 g, 20.08 mmol) was added to the solution. The pH of the solution was further adjusted to 11.24 by adding NaOH 50% dropwise. The reaction was kept overnight under the same conditions and a balloon filled with N₂ gas. The next day, pH was measured to make sure it remained constant. Thereafter, the reaction was kept overnight whilst stirring at 80°C. Moreover, the crude solution was transferred to a 250 mL one-neck flask for solvent removal under reduced pressure using a rotary evaporator. The product was washed with diethyl ether and filtered using a Büchner funnel to obtain a white powder. The synthesis route of this reaction is shown in Figure 10.

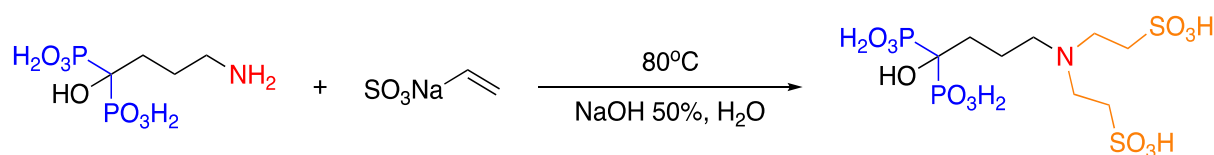


Figure 10. Synthesis route of SI-5.

For further purification, the product was dissolved in approximately 25 mL of deionized water on a one-neck round bottom flask. Then, the pH was adjusted to 5.89 using 0.01 M HCl. The solution was left under reflux at 110°C overnight. The next day, it was filtered using a Büchner funnel to remove any solid impurities. The water phase in the filtrate was removed under pressure using a rotary evaporator. A sticky powder was obtained and further washed with diethyl ether under strong stirring overnight. The solvent was left to evaporate at room temperature. As the final product was sticky, it was then washed with methanol overnight. Then, the solvent was removed under reduced pressure using a rotary evaporator affording a white solid sodium salt of **SI-5**.

2,2'-((4-hydroxy-4,4-diphosphonobutyl)azanediyl)bis(ethane-1-sulfonic acid) (**SI-5**): Yield: 83%. IR ν_{\max} (cm⁻¹): 3459 (OH), 1179, 1042 (SO₃), 911, 745 (PO₃). ¹H NMR (D₂O, 400 MHz) δ ppm: 3.33 (t, 4H, 2× -CH₂-CH₂-SO₃H), 3.27 (t, 2H, -N-CH₂-CH₂-), 3.15 (t, 4H, 2× -CH₂-CH₂-SO₃H), 2.05 - 1.91 (br, 4H, -CH₂-CH₂-C(OH)(PO₃H₂)₂). ³¹P NMR (D₂O, 162.00 MHz) δ ppm: 17.78.

3.2.1.6. **SI-6**: (*E*)-4-((4-hydroxy-4,4-diphosphonobutyl)amino)-4-oxobut-2-enoic acid

A 100 mL two-neck flask equipped with a reflux condenser at 80°C and magnetic stirring was loaded with alendronic acid (2.50 g, 10.04 mmol) and maleic anhydride (0.98 g, 10.04 mmol) along with 30 mL of deionized water. Sodium hydroxide (0.40 g, 10.04 mmol) was then added to the solution. The pH of the solution was further adjusted to 11.15 by adding NaOH 50% dropwise. The reaction was kept overnight under the same conditions and a balloon filled with N₂ gas. The next day, pH was measured to make sure it remained constant. Thereafter, the reaction was kept overnight whilst stirring at 80°C. Moreover, the crude solution was transferred to a 250 mL one-neck flask for solvent removal under reduced pressure using a rotary evaporator. The product was washed with acetone under stirring overnight. Finally, the product was filtered using a Büchner funnel, and a white powder was obtained. The synthesis route of this reaction is shown in Figure 11.

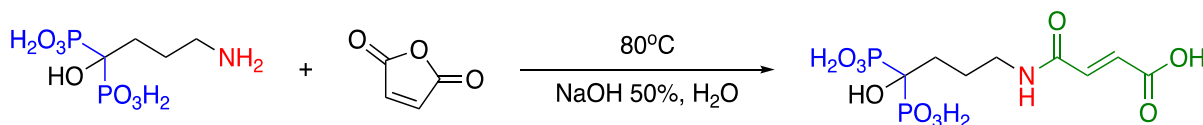


Figure 11. Synthesis route of **SI-6**.

For further purification, the product was dissolved in approximately 25 mL of deionized water on a one-neck round bottom flask. Then, the pH was adjusted to 4.58 using 0.01 M HCl. The solution was left under reflux at 110°C overnight. The next day, it was filtered using a Büchner funnel to remove any solid impurities. The water phase in the filtrate was removed under pressure using a rotary evaporator and a beige salt of **SI-6** was obtained.

(*E*)-4-((4-hydroxy-4,4-diphosphonobutyl)amino)-4-oxobut-2-enoic acid (**SI-6**): Yield: 86%. IR ν_{\max} (cm⁻¹): 3484, 3350 (OH), 1622, 1550 (CO), 1064, 860 (PO₃). ¹H NMR (D₂O, 400 MHz) δ ppm: 6.24 (s, 2H, -CH=CH-COOH), 2.98 (t, 2H, -N-CH₂-CH₂-), 1.99 - 1.92 (br, 4H, -CH₂-CH₂-C(OH)(PO₃H₂)₂). ³¹P NMR (D₂O, 162.00 MHz) δ ppm: 17.82.

3.2.1.7. SI-7: 2,2'-((4-hydroxy-4,4-diphosphonobutyl)azanediyl)diacetic acid

A 100 mL two-neck flask equipped with a reflux condenser at 80°C and magnetic stirring was loaded with alendronic acid (2.50 g, 10.04 mmol) and sodium chloroacetate (2.34 g, 20.07 mmol) along with 30 mL of deionized water. Sodium hydroxide (0.80 g, 20.08 mmol) was then added to the solution. The pH of the solution was adjusted to 11.47 by adding NaOH 50% dropwise. The reaction was kept overnight under the same conditions and a balloon filled with N₂ gas. The next day, pH was measured to make sure it remained constant. Thereafter, the reaction was kept overnight whilst stirring at 80°C. Moreover, the crude solution was transferred to a 250 mL one-neck flask for solvent removal under reduced pressure using a rotary evaporator. A white powder was retained in the flask after removing the solvent. The synthesis route of this reaction is shown in Figure 12.

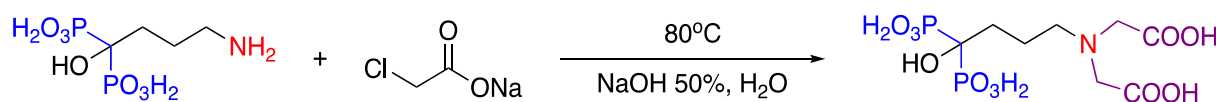


Figure 12. Synthesis route of SI-7.

For further purification, the product was dissolved in approximately 25 mL of deionized water on a one-neck round bottom flask. Then, the pH was adjusted to 4.63 using 0.01 M HCl. The solution was left under reflux at 110°C overnight. The next day, it was filtered using a Büchner funnel to remove any solid impurities. The water phase in the filtrate was removed under pressure using a rotary evaporator. A sticky product was obtained and further washed with diethyl ether under vigorous stirring overnight. The solvent was left to evaporate at room temperature. The final product was dried at 60°C overnight in a TS 8056 oven (Termaks, Norway). Finally, a white powder of sodium salt of **SI-7** was obtained.

2,2'-((4-hydroxy-4,4-diphosphonobutyl)azanediyl)diacetic acid (**SI-7**): Yield: 72%. IR ν_{\max} (cm⁻¹): 3418 (OH), 1617 (CO), 1062, 905 (PO₃). ¹H NMR (D₂O, 400 MHz) δ ppm: 3.75 (s, 4H, 2 × -N-CH₂-COOH), 3.22 (t, 2H, -N-CH₂-CH₂-), 1.99 – 1.89 (br, 4H, -CH₂-CH₂-C(OH)(PO₃H₂)₂). ³¹P NMR (D₂O, 162.00 MHz) δ ppm: 17.77.

3.2.2. Project 2

This section describes the synthesis of (2-(2-amino-3-hydroxy-2-(hydroxymethyl)propoxy)-1-hydroxypropyl)phosphonic acid, more commonly known as fosfomicin trometamol (**SI-9**), using fosfomicin disodium salt (**SI-8**) as starting compound. Moreover, the epoxide ring of **SI-8** was hydrolyzed under acidic conditions to produce **SI-10**. Then, further phosphonation of **SI-9** was carried out via the Moedritzer-Irani reaction^{22,72}.

3.2.2.1. SI-8: Fosfomycin disodium salt

SI-8 was purchased from Tokyo Chemical Industry CO., LTD. The chemical structure is shown in Figure 13.

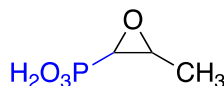


Figure 13. Chemical structure of SI-8.

(3-methyloxiran-2-yl)phosphonic acid (SI-8): IR ν_{\max} (cm^{-1}): 1409 (CH_3), 1089 (PO_3). ^1H NMR (D_2O , 400 MHz) δ ppm: 3.20-3.13 (m, 1H, $-\text{CH}-\text{CH}_3$), 2.75-2.69 (dd, 1H, $-\text{CH}-\text{PO}_3\text{H}_2$), 1.38-1.37 (d, 3H, $-\text{CH}-\text{CH}_3$). ^{31}P NMR (D_2O , 162.00 MHz) δ ppm: 9.99.

3.2.2.2. SI-9: (2-(2-amino-3-hydroxy-2-(hydroxymethyl)propoxy)-1-hydroxypropyl)phosphonic acid

This reaction was carried out according to the patent EP 1 762 573 A1⁷⁰. A 100 mL two-neck flask equipped with a reflux condenser at 65°C and magnetic stirring was loaded with fosfomycin disodium salt (2.00 g, 10.98 mmol) in 16 mL of methanol. Another 100 mL one-neck flask with the same arrangement was set up at 50°C and loaded with oxalic acid dihydrate (1.39 g, 10.99 mmol), tromethamine (1.33 g, 10.99 mmol), and 9 mL of methanol. After complete dissolution, the temperature of the second reaction was raised to 65°C. After that, this solution was gradually added to the first reaction at the same temperature, using a dropping funnel. After completion, the final solution was left to cool down to room temperature for 3 hours, and further cooled in a fridge at 4°C overnight. The following day, the milky suspension was filtered under vacuum using a Büchner funnel. The filtrate was concentrated using a rotary evaporator. The product was further washed with 15 mL of a 1:1 mixture of acetone-ethanol under strong stirring at room temperature for 3 hours. A suspension with white crystals was obtained and filtered under vacuum using a Büchner funnel, while washing with absolute ethanol. A white powder was obtained. The synthesis route of this reaction is shown in Figure 14.

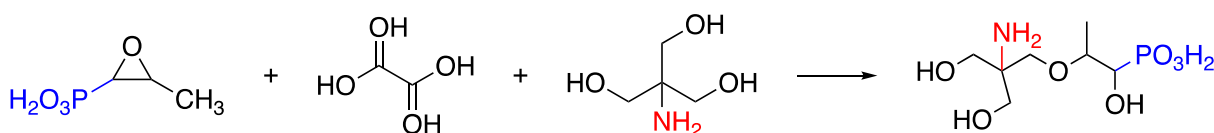


Figure 14. Synthesis route of SI-9.

(2-(2-amino-3-hydroxy-2-(hydroxymethyl)propoxy)-1-hydroxypropyl)phosphonic acid (**SI-9**): Yield: 86%. IR ν_{\max} (cm^{-1}): 3048 (NH_2), 2945, 2822 (OH), 1138 (CO), 1035 (PO_3). ^1H NMR (D_2O , 400 MHz) δ ppm: 3.60 (s, 6H, ($\text{CH}_2(\text{OH}))_2\text{-C}(\text{NH}_2)\text{-CH}_2$), 3.27-3.21 (m, 1H, $-\text{CH}-\text{CH}_3$), 2.87-2.80 (dd, 1H, $-\text{CH}(\text{OH})(\text{PO}_3\text{H}_2)$), 1.36-1.35 (d, 3H, $-\text{CH}-\text{CH}_3$). ^{31}P NMR (D_2O , 162.00 MHz) δ ppm: 12.29.

3.2.2.3. **SI-10**: (2-hydroxypropyl)phosphonic acid

A 50 mL one-neck flask equipped with a reflux condenser at 100°C and magnetic stirring was loaded with fosfomycin disodium salt (2.00 g, 10.98 mmol) in 6 mL of deionized water. The pH of the solution was adjusted to 2.89 using 0.1 M HCl and left to stir overnight. The following day, water was removed using a rotary evaporator. A hygroscopic product was obtained and washed with absolute ethanol under strong stirring for 4 hours at room temperature. After removing the solvent under vacuum using a rotary evaporator, a white powder was obtained. The synthesis route of this reaction is shown in Figure 15.

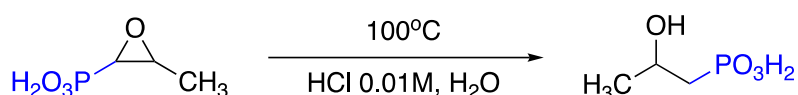


Figure 15. Synthesis route of SI-10.

(2-hydroxypropyl)phosphonic acid (**SI-10**): Yield: 76%. IR ν_{\max} (cm^{-1}): 3249 (OH), 1457 (CH_3), 1041 (PO_3). ^1H NMR (D_2O , 400 MHz) δ ppm: 3.99 - 3.92 (m, 1H, $-\text{CH}(\text{OH})-$), 3.46-3.42 (dd, 2H, $-\text{CH}_2\text{-PO}_3\text{H}_2$), 1.21-1.20 (d, 3H, $-\text{CH}-\text{CH}_3$). ^{31}P NMR (D_2O , 162.00 MHz) δ ppm: 17.33.

3.2.2.4. **SI-11**: (2-(2-(bis(phosphonomethyl)amino)-3-hydroxy-2-(hydroxymethyl)propoxy)-1-hydroxypropyl)phosphonic acid

A 100 mL two-neck flask equipped with a reflux condenser at 60°C and magnetic stirring was loaded with **SI-9** (1.00 g, 3.86 mmol). Phosphorous acid (0.65 g, 7.87 mmol) dissolved in 10 mL of deionized water was added dropwise. Next, HCl 37% (0.78 g, 21.43 mmol) was added dropwise. Then, formaldehyde 37% (0.63 g, 20.90 mmol) was added dropwise over 30 minutes. The temperature of the reaction was then raised to 110°C and left under stirring for 48 hours. After cooling down to room temperature, the liquid phase of the solution was removed using a rotary evaporator. An oily product was obtained and washed with methanol under strong stirring overnight. Thereafter, the solvent was removed under reduced pressure using a rotary evaporator and a white powder was obtained. The synthesis route of the reaction is shown in Figure 16.

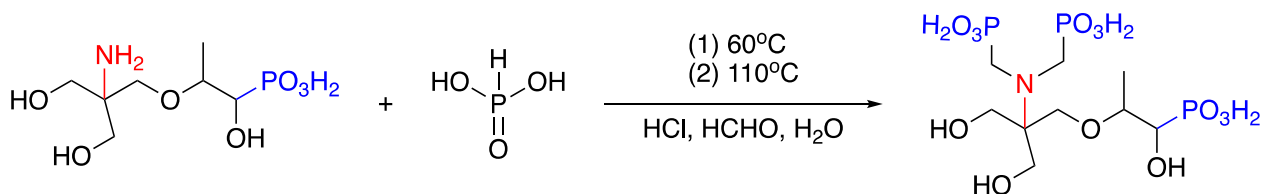


Figure 16. Synthesis route of SI-11.

3.2.2.5. SI-12: (1-hydroxy-2-(3-hydroxy-2-(hydroxymethyl)-((phosphonomethyl)amino)propoxy)propyl)phosphonic acid

A 100 mL two-neck flask equipped with a reflux condenser at 60°C and magnetic stirring was loaded with **SI-9** (1.00 g, 3.86 mmol). Phosphorous acid (0.32 g, 3.93 mmol) dissolved in 10 mL of deionized water was added dropwise. Next, HCl 37% (0.380 g, 10.425 mmol) was added dropwise. Then, formaldehyde 37% (0.31 g, 10.45 mmol) was added dropwise over 30 minutes. The temperature of the reaction was then raised to 110°C and left under stirring for 48 hours. After cooling down to room temperature, the liquid phase of the solution was removed using a rotary evaporator. An oily product was obtained and washed with ethanol under strong stirring overnight. After that, the solvent was removed under reduced pressure using a rotary evaporator, and a white powder was obtained. The synthesis route of this reaction is presented in Figure 17.

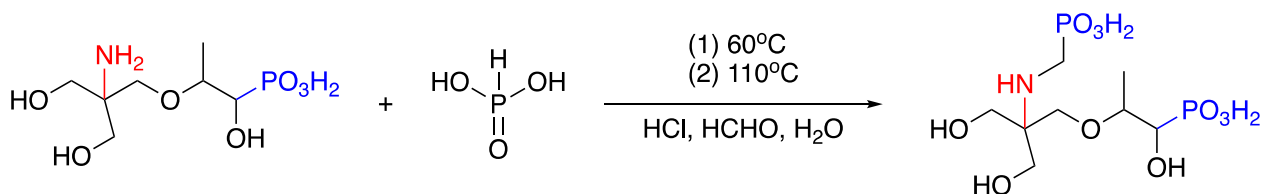


Figure 17. Synthesis route of SI-12.

The syntheses of **SI-11** and **SI-12** were not successful. Although the procedures were repeated several times, the desired products were not obtained when studying the NMR spectra. This could have happened due to the strongly acidic conditions of the Moedritzer-Irani reaction that caused hydrolysis on the fosfomicin backbone. Therefore, these products were not further investigated.

3.3. Laboratory testing of SIs for oilfield applications

In this project, the protocol described by the NACE Standard TM0374-2007 to determine the inhibition efficiency against calcium carbonate (calcite) and calcium sulfate (gypsum) was followed³. Initially, the scale inhibition performance was meant to be studied using a DSR, but this was not possible due to technical malfunctions in the apparatus. Therefore, we have decided to perform static tests as an alternative method. As it is the first time this method was used by our research group, a detailed methodology is provided. This section lists the solutions, apparatus, and procedures followed to study the scale inhibition efficiency of the different chemicals discussed in Section 3.2.

3.3.1. Stock solutions and brines

3.3.1.1. Scale inhibitor solution, 1000 ppm

A 1000 ppm stock solution of SIs was used. The pH was adjusted between 4.5 to 6 to resemble a typical oil and gas reservoir. Solutions were stored in glass vials or bottles, remaining stable for several weeks.

3.3.1.2. Brines composition

All brines described in this section were prepared using deionized water. Schott® bottles of 500 mL or 1 L capacity were used for storage, accordingly. The solutions were stirred with a MR Hei – Mix D (Heidolph, Germany) magnetic stirrer until completely dissolved.

3.3.1.2.1. Gypsum scale

For the calcium sulfate precipitation screening test, brines were prepared according to the NACE Standard TM0374-2007³ as described in Table 3.

Table 3. Composition of gypsum brines used for static screening tests.

Calcium-containing brine (B1)					
ion	ppm	chemical formula	g/250mL	g/500mL	g/L
Na ⁺	2950	NaCl	1.875	3.750	7.500
Ca ²⁺	3028	CaCl ₂ •2H ₂ O	2.775	5.550	11.100
Sulfate-containing brine (B2)					
ion	ppm	chemical formula	g/250mL	g/500mL	g/L
Na ⁺	2950	NaCl	1.875	3.750	7.500
SO ₄ ²⁻	7209	Na ₂ SO ₄ anhydrous	2.665	5.330	10.660
1:1 mixture					
ion	ppm				
Na ⁺	2950				
Ca ²⁺	1514				
SO ₄ ²⁻	3605				

3.3.1.2.2. Calcite scale

For the calcium carbonate precipitation screening test, brines were prepared according to the NACE Standard TM0374-2007³ as described in Table 4 below.

Table 4. Composition of calcite brines used for static screening tests.

Calcium-containing brine (B1)					
ion	ppm	chemical formula	g/250mL	g/500mL	g/L
Na ⁺	12982	NaCl	8.250	16.500	33.000
Ca ²⁺	3314	CaCl ₂ •2H ₂ O	3.038	6.075	12.150
Mg ²⁺	440	MgCl ₂ •6H ₂ O	0.920	1.840	3.680
Bicarbonate-containing brine (B2)					
ion	ppm	chemical formula	g/250mL	g/500mL	g/L
Na ⁺	12982	NaCl	8.250	16.500	33.000
HCO ₃ ⁻	5346	NaHCO ₃	1.840	3.680	7.360
1:1 mixture					
			ion	ppm	
			Na ⁺	12982	
			Ca ²⁺	1657	
			Mg ²⁺	220	
			HCO ₃ ⁻	2673	

3.3.1.2.3. Heidrun calcite scale

Additionally to the brines proposed by the NACE Standard TM0374-2007³, an alternative of calcite formation was also tested. The compositions of the brines are shown in Table 5. They are based on produced fluids from the Heidrun oilfield in the North Sea, and it has been used previously by our research group in dynamic tests^{22,74,75}. However, it has not been used for static laboratory screening. Due to this reason, it was decided to evaluate the inhibition performance of different SIs using this brine composition while following the standard protocol.

Table 5. Composition of calcite brines according to the Heidrun Oilfield.

Calcium-containing brine (B1)					
ion	ppm	chemical formula	g/250mL	g/500mL	g/L
Na ⁺	19 508	NaCl	12.398	24.795	49.590
Ca ²⁺	2 040	CaCl ₂ •2H ₂ O	1.870	3.740	7.480
Mg ²⁺	530	MgCl ₂ •6H ₂ O	1.108	2.215	4.430
K ⁺	1 090	KCl	0.520	1.039	2.078
Ba ²⁺	570	BaCl ₂ •2H ₂ O	0.253	0.507	1.014
Sr ²⁺	290	SrCl ₂ •6H ₂ O	0.221	0.441	0.882
Bicarbonate-containing brine (B2)					
ion	ppm	chemical formula	g/250mL	g/500mL	g/L
Na ⁺	19508	NaCl	12.398	24.795	49.590
HCO ₃ ⁻	2005	NaHCO ₃	0.690	1.380	2.760
1:1 mixture					
			ion	ppm	
			Na ⁺	19508	
			Ca ²⁺	1020	
			Mg ²⁺	265	
			K ⁺	545	
			Ba ²⁺	285	
			Sr ²⁺	145	
			HCO ₃ ⁻	1002	

3.3.1.2.4. Heidrun barite scale

As similarly discussed in the previous section, an alternative brine mixture for barite formation was also tested. The composition of the brines shown in Table 6, is based on data from the Heidrun oilfield in the North Sea. This brine composition has been used previously by our research group for studying the performance of SIs using the DSR^{22,47,75}. However, it has not been used for static laboratory screening. Due to this reason, it was decided to analyze the different SIs using this brine composition.

Table 6. Composition of barite brines according to the Heidrun Oilfield.

Barium-containing brine (B1)					
ion	ppm	chemical formula	g/250mL	g/500mL	g/L
Na ⁺	15 201	NaCl	9.660	19.320	38.640
Ca ²⁺	1 448	CaCl ₂ •2H ₂ O	1.328	2.655	5.310
Mg ²⁺	1633	MgCl ₂ •6H ₂ O	3.415	6.830	13.660
K ⁺	1 007	KCl	0.480	0.960	1.920
Ba ²⁺	287	BaCl ₂ •2H ₂ O	0.128	0.255	0.510
Sr ²⁺	145	SrCl ₂ •6H ₂ O	0.110	0.220	0.440
Sulfate-containing brine (B2)					
ion	ppm	chemical formula	g/250mL	g/500mL	g/L
Na ⁺	13 785	NaCl	8.760	17.520	35.040
SO ₄ ²⁻	2 962	Na ₂ SO ₄ anhydrous	1.095	2.190	4.380
1:1 mixture					
	ion			ppm	
	Na ⁺			14493	
	Ca ²⁺			724	
	Mg ²⁺			817	
	K ⁺			503	
	Ba ²⁺			143	
	Sr ²⁺			72	
	SO ₄ ²⁻			1480	

Barite inhibition tests via titration with EDTA were not successful during this research. Although two different Ba²⁺ indicators suggested in the literature were used (thymolphthalein and metalphthalein⁷⁶), it was not possible to obtain the expected ion concentrations in the blanks at room temperature. Immediately at mixing, the blank samples became turbid, showing that somehow the scaling process had already started. As discussed in Section 2.1.3.2, this is the worst scale to deal with as it presents the lowest K_{sp} among all sulfate scales and it does not take a high concentration of Ba²⁺ ions in the formation water for barite to deposit^{1,12}. Furthermore, the cationic brine used, also contains Sr²⁺ ions. Although in this case, Sr²⁺ is present in relatively low concentration, strontium and barium can cooperate in the presence of sulfate to form a mixed sulfate scale¹.

Due to the complexity of carrying out this test with the Heidrun oilfield water chemistry during the timeframe of this research, this was not further investigated. Other methods for studying the inhibition of the barite scale are found in the literature⁷⁷.

3.3.1.3. Ethylenediaminetetraacetic acid (EDTA) solution, 0.01 M

To prepare the EDTA titrant solution, 3.72 g of $\text{Na}_2\text{EDTA}\cdot 2\text{H}_2\text{O}$ were diluted to 1000 mL with deionized water in a volumetric flask⁷⁸. This solution was prepared weekly and stored in a 1 L Schott® bottle at room temperature.

3.3.1.4. Ammonium purpurate indicator solution

Many indicators are recommended for calcium titration^{78,79}. Ammonium purpurate, also known as murexide, was selected as it was immediately available for use in our laboratory. This indicator changes from pink to purple at the end point, as shown in Figure 18. The indicator was prepared weekly by dissolving 0.06 g of dye in 40 g of absolute ethylene glycol⁷⁹. It was stored in an amber glass dropper bottle at room temperature. Other ways of preparing this dye are found in the literature^{79,80}.



Figure 18. Color change at end point for Ca^{2+} titration with murexide.

3.3.2. Static jar tests

To evaluate the scale inhibition performance of the different SIs studied throughout this project, static laboratory screening tests were performed according to the NACE standard TM0374-2007³. Cationic and anionic brines (B1 and B2, respectively) were prepared accordingly, as described in Section 3.3.1.2. A total volume of 40 mL of 1:1 solution of cationic brine (B1) and anionic brine (B2) was used to produce the corresponding scale, e.g., calcite and gypsum. Consequently, in 50 mL Schott Duran® glass bottles, different concentrations of SI were dosed into known volumes of B1 and B2 by diluting a 1000 ppm stock solution of SI. Details are shown in Table 7. Automatic pipettes of 10 mL, 1000, and 100 μL (Thermo Fisher Scientific, USA) were used for this purpose. The tested concentrations of SI were chosen based on the concentrations used by our research group in the DSR test^{21,22,75}. Two blank samples were prepared.

Table 7. Dosed solutions for static performance tests of SIs.

SI concentration (ppm)	B1 (mL)	B2 (mL)	1000 ppm stock SI (mL)
100	20	16	4
50	20	18	2
20	20	19.2	0.8
10	20	19.6	0.4
5	20	19.8	0.2
2	20	19.92	0.08
1	20	19.96	0.04
0	20	20	0

Once all samples were prepared, they were capped tightly and mixed thoroughly. All samples except one of the blanks, were placed in a pre-heated oven at 80°C and kept for 5 hours. To determine the time that samples required to be spent in the oven, a series of tests with blank samples were performed prior to SI testing. The blank samples were placed in an oven at 80°C for 1, 2, 3, 4, 5, 6, and 24 hours, and further analyzed to determine the Ca²⁺ concentration in the solution via titration with EDTA. Results are shown in Figure 19. After 5 hours, no significant change in the Ca²⁺ retained in solution is detected. Therefore, it is chosen to perform the tests for 5 hours because at this time, the maximum amount of scale is formed.

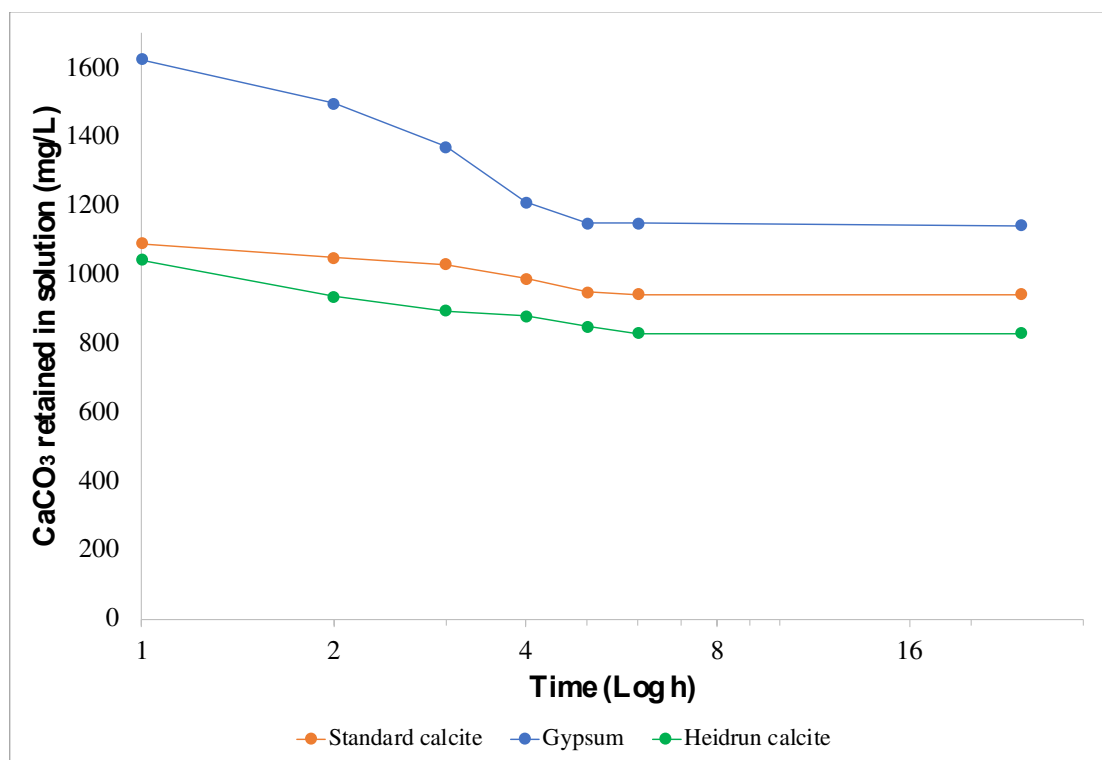


Figure 19. Duration test results for static bottle tests.

The Ca²⁺ concentration in each sample was determined following the procedure given by ASTM D-511⁷⁸. The analysis consisted of withdrawing 1 mL of aliquot (without prior filtration) and diluting it to 50 mL with deionized water in a conic flask. Consequently, pH was adjusted to 12-13 with 100 µL of NaOH 50% and 200 µL of murexide indicator were added. The titration setup consisted of a 25:0.05 mL glass burette (HirschmannTM, Germany) and a Lab Disc (VWR®, Germany) stirrer, as

shown in Figure 20 (left). The sample was then titrated with EDTA 0.01 M until a color change from pink to purple occurred (see Figure 18). The volume of EDTA consumed was recorded, and the Ca^{2+} concentration was estimated as shown in Equation 1.

$$Ca^{2+}(ppm) = \frac{A \times B}{D} \times 40100 \quad \text{Equation 1}$$

Where A is the EDTA volume required to titrate Ca^{2+} in the sample (mL), B is the concentration of EDTA (mol/L), D is the total volume of sample used (50 mL), and 40100 represents the molecular weight of Ca^{2+} in mg/mol.

The scale inhibition efficiency is calculated as the concentration of Ca^{2+} retained in solution in relation to the blank at room temperature, as this sample contains the maximum Ca^{2+} in solution before it precipitates as scale. This is interpreted as the higher the Ca^{2+} concentration retained in solution, the higher the inhibition efficiency will be, showing that the SI has the ability to keep the ions in solution, avoiding scale formation. Therefore, percent inhibition values were calculated as follows³:

$$\% \text{ inhibition} = \frac{C_a - C_b}{C_o - C_b} \times 100 \quad \text{Equation 2}$$

Where C_a refers to the Ca^{2+} in the sample after 5 hours, C_b is the Ca^{2+} concentration in the blank after 5 hours, and C_o the Ca^{2+} concentration in the blank before precipitation. Each sample was titrated in triplicates.

3.3.3. High-Pressure Dynamic Tube Blocking Test

Due to technical problems that could not be solved during the spring semester because of international border restrictions caused by COVID-19, the SIs synthesized throughout this project could not be tested in the DSR. Regardless, this section is discussed to reiterate the importance of dynamic tests in scale inhibition studies.

A DSR manufactured by Scaled Solutions Ltd. (UK) was meant to be used to evaluate the performance of the scale inhibitors presented in this project. The Scale Rig 5000TM consists of three pumps, as shown in Figure 20. Each one pumps fluids up to 10.00 mL/min through a test coil made of 316 steel, with 1.00 mm internal diameter and a length of 3.00 m. To mimic downhole conditions, the coil is placed inside an oven which is set to 100°C and the pressure in the tubing system is set to 80.00 bar. From bottom left to right, in Figure 20 (right), the following features can be observed:

1. Pump 1: contains brine 1 (B1) with scaling cations resembling formation water at a constant flow rate of 5.00 mL/min.
2. Pump 2: contains brine 2 (B2) with scaling anions. It simulates the injection seawater, where the SI is injected in the field. It also pumps a tetrasodium ethylenediaminetetraacetate solution (EDTA 5 wt%) and deionized water, which are necessary for cleaning the test coil after the scale has been formed.
3. Pump 3: contains the scale inhibitor (SI) solution. Preparation was discussed in Section 3.3.1.1.

Detailed water chemistry and preparation of B1 and B2 were discussed in Sections 3.3.1.2.3 and 3.3.1.2.4. However, for dynamic testing, these solutions must be degassed before use.



Figure 20. Titration set up for Ca^{2+} analysis by titration with EDTA (left). Dynamic scale rig used for high-pressure tube blocking testing of SIs (right).

The DSR is connected to a computer with LabView 8.0 software (Scaled Solutions Ltd., U.K) that is set up to automatically control the SI concentration pumped into the system and the flow rates from each pump. Time and pressure drop due to scale formation are recorded. The procedure of dynamic SIs testing consists of four automated stages for each experiment:

- a. A first blank test, where B1 + B2 are pumped into the system at a flowrate of 5.00 mL/min each, without any SI. During this stage, scale is formed rapidly. Normally within 10-20 minutes for CaCO₃ scale and within 10-12 minutes for BaSO₄. Every time scale is formed, it is automatically detected by the system. Then, the coil is saturated with scale deposit, and the system proceeds to clean automatically with EDTA solution (5 wt%) and deionized water, each one for 10 minutes at a flowrate of 9.99 mL/min.
- b. When the cleaning phase is finished, pump 2 switches from cleaning solution to scaling B2, causing a momentary drop in differential pressure. Such momentary drops are observed at the end of each cleaning cycle before new scaling ions are pumped through. Then, a first scale test is initiated, where B1 + B2 are pumped into the system with decreasing concentrations of SI every hour or until scale is formed (FIC). When the performance of the SI is unknown, or a new SI is being tested, the starting concentration during this stage is 100 ppm of SI, followed by 50, 20, 10, 5, 2 and 1 ppm. In this research, these concentrations are used as the starting point for SI testing using static bottle tests.
- c. Repeated scale test, where B1 + B2 are pumped into the system together with the SI concentration before the one that led to scale formation in Stage b., understood as MIC. This step guarantees that the reproducibility of the experiment is acceptable. A difference of ± 5 min between first and second scale tests is tolerable. It has been determined that an 'ideal' MIC should be between 1 to 100 pm⁸¹. However, due to economic reasons, a more practical range is from 1 to 5 ppm. This range is the aim throughout DSR testing.
- d. A second blank test, where only B1 + B2 are injected at a flowrate of 5.00 mL/min each, without any SI.

The four stages in one single run discussed above can be observed in Figure 21 from left to right.

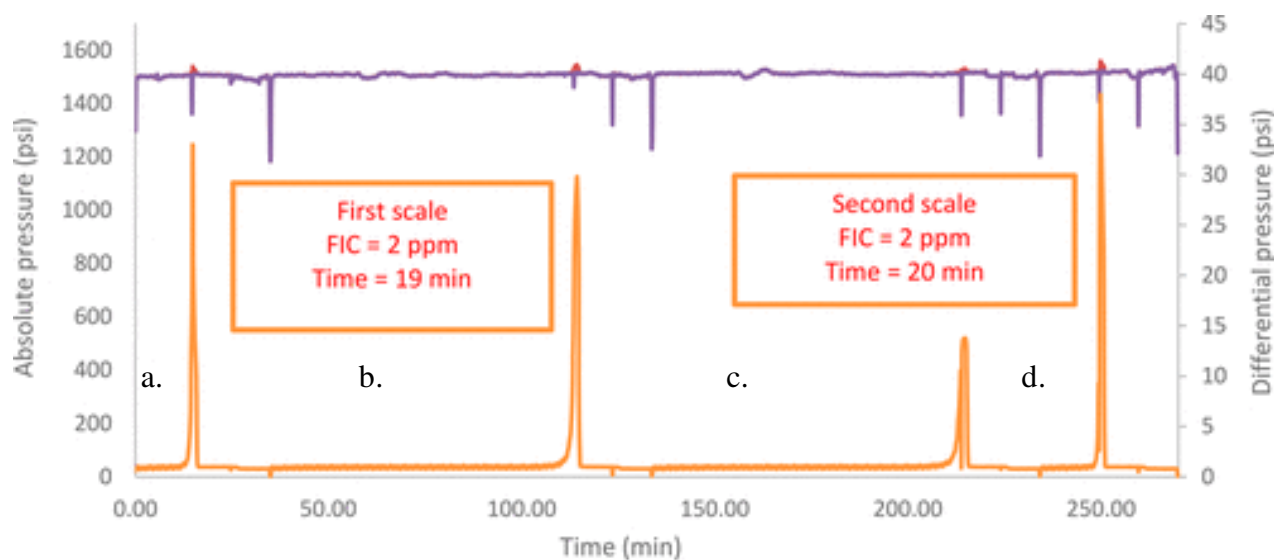


Figure 21. Stages of SI testing in a dynamic scale rig (pressure vs. time).

3.3.4. Thermal stability tests

An important characteristic of SIs evaluated for squeeze applications is their ability to withstand and remain stable at high temperatures for long periods of time, as they would be subject to harsh conditions when injected into the reservoir. Within the commercialized species, polysulfonates have been reported as particularly useful for high-temperature squeeze applications^{1,17}. To evaluate this aspect, 20 mL of 5 wt% solutions of selected SIs were prepared with deionized water, and the pH was adjusted between 4.5 to 5. In a pressure tube, solutions were sparged with nitrogen gas to mimic downhole anaerobic conditions. They were further heated up to 130°C under stirring for 7 days. The obtained solutions were then diluted to 0.1% (1000ppm) and stored in 1 L Schott® bottles. Finally, the scale inhibition performance of the aged solutions was tested by static bottle test method and compared to the respective non-aged SI.

3.3.5. Calcium compatibility tests

Studying the compatibility between SIs and brines is another key factor for squeeze treatment and continuously dosed inhibitors. Usually, formation water contains divalent cations such as Ca^{2+} which at high concentrations could negatively affect the performance of the SI. When this happens, there exists the tendency of formation of Ca^{2+} -SI complexes that precipitate and are not desired during production. Some refer to these complexes as ‘*pseudoscale*’³⁶. In some cases, the presence of Mg^{2+} ions also influence the performance of SIs^{1,30,36}. Thus, if the SI is not compatible with Ca^{2+} or Mg^{2+} , these complexes will be formed instead of inhibiting scale, causing a change in the physical and chemical structure of the SI, leading to formation damage, reduced productivity, low profitability, etc.

From a general perspective, phosphonates are the least compatible with high $\text{Ca}^{2+}/\text{Mg}^{2+}$ concentrations, carboxylates are intermediate, and sulfonates are the most compatible¹. Some aminomethylenephosphonates have been claimed as good calcite and sulfate scale inhibitors with improved compatibility²².

To evaluate the compatibility between Ca^{+2} ions and SIs, different concentrations of SI (100, 1000, 10000, and 50000 ppm) were tested at different Ca^{+2} ions concentrations (100, 1000, and 10000 ppm) together with 30000 ppm of NaCl (3 wt%) to simulate seawater conditions, in 20 mL of deionized water. The pH of the solutions was further adjusted between 4 and 5, and the appearance of the different solutions was observed at mixing, after 30 minutes, 1, 4, and 24 hours of placed in a TS 8056 oven (Termaks, Norway) at 80°C. Scale inhibitors were considered compatible with Ca^{2+} when the appearance of the solution was clear after 24 hours.

3.3.6. Seawater biodegradability tests

The OECD guidelines N° 306, otherwise known as “Biodegradability in Seawater”, is the primary method used in this thesis to determine the biodegradability of the tested scale inhibitors²⁵. All tested SIs were evaluated for biodegradability except **SI-10**. The OECD biodegradability method measures the amount of O_2 consumed by aerobic heterotrophs for assimilation of the SI in question (BOD), as opposed to the theoretical amount of O_2 that would be demanded by the product for complete biochemical oxidation (ThOD). The ratio measured is biodegradability (BD), as shown in Equations 3 and 4.

$$BD (\%) = \frac{\text{mg O}_2/\text{mg SI}}{\text{mg ThOD}/\text{mg SI}} \times 100 \quad \text{Equation 3}$$

$$BD (\%) = \frac{\text{BOD}_{28}}{\text{ThOD}} \times 100 \quad \text{Equation 4}$$

The ThOD of a compound with the empirical formula $\text{C}_c\text{H}_h\text{O}_o\text{N}_n\text{P}_p\text{S}_s$ is directly calculated using Equation 5, where Mm is the molar mass of the tested compound and subscripts are the elemental coefficients. Both the BOD and the ThOD determine the degree of biodegradability. The BOD test is evaluated over 28 days to ensure complete oxidation of the test compound under incubation at 20°C in the dark. According to the OECD method, if $\text{BOD} \geq 0.6 \text{ ThOD}$, then the compound is biodegradable.

$$\text{ThOD} \left(\text{mg O}_2/\text{L} \right) = \frac{16 \left[2c + \frac{1}{2}(h-3n) + 3s + \frac{5}{2}p - o \right]}{Mm} \quad \text{Equation 5}$$

3.3.6.1. Seawater sampling

The seawater was collected by the International Research Institute (NORCE) located in Mekjarvik (Norway) from a non-polluted fjord (salinity $\approx 3.5\%$) ($59^{\circ} 1'N$, $5^{\circ} 37'E$) via a piping system. The temperature of the seawater obtained from a depth of 80 m was approximately $8^{\circ}C$. Sampling was done on May 21st and stored at $4^{\circ}C$ until it was used to set up the experiments the next day. The bottles for collecting were filled approximately $2/3$ of the capacity to maintain sufficient air in the headspace to prevent anaerobic conditions.

3.3.6.2. BOD analysis set up

Before starting the BOD tests, all glassware was autoclaved using a Panasonic MLS-3751 (Osaka, Japan) in order to ensure sterility and avoid cross-contamination while handling samples. The seawater was saturated with O_2 by bubbling compressed air for 20 minutes before setting up the experiments.

Considering a density of 1.033 g/L for the seawater, 1028 g of seawater were weighed into 1 L autoclaved Schott® glass bottles. Consequently, 1 mL of each nutrient solution (A, B, C, D), $10\ \mu\text{L}$ of vitamins, and $10\ \mu\text{L}$ of the amino acid mixture were added to each bottle. Except for the autoclaved seawater used for the negative controls. Appendix C details the nutrient solutions A, B, C, D, as well as the amino acids and vitamins solutions.

Certain amounts of the amended seawater were dosed into 500 mL BOD amber bottles, as shown in Table 8. Moreover, these amber bottles were capped with OxiTop®-C measuring heads (WTW, Germany) and left under incubation on magnetic stir-plates overnight at $20^{\circ}C$, with 2 NaOH pellets in the rubber inserts, serving as CO_2 trap. The next day, the carbon sources (SIs as test compounds and sodium benzoate for the positive control) were added. Finally, the bottles are placed once more in the OxiTop® IS 6 inductive stirring system (WTW, Germany) and connected to a receiver for automatic data recording.

OxiTop® measuring system is based on reading and recording gas pressure changes resulting from microbial degradation. This is, the microorganisms in the sample consume O_2 and form CO_2 (absorbed by the NaOH), creating a value that can be measured as mg/L BOD value. Data collection and analysis occur 28 days later when biodegradation has taken place, and the O_2 concentrations have stabilized.

Table 8. Biodegradation tests: bottles distribution and set up.

Name	C Source	Seawater	A, B, C, and D Solutions (1 mL each)	Amino Acid and Vitamin Solutions (10 µL each)	Replicate
Blank	No C Source	300 mL (310 g) SW	✓	✓	3
Positive Control	1 mL C ₇ H ₅ O ₂ Na 3%	299 mL (309 g) SW	✓	✓	3
Test Compound	1.8 mL SI 1%	298.2 mL (308 g) SW	✓	✓	3 per SI
Negative Control	No C Source	298.2 mL (308 g) autoclaved SW	✗	✗	1 per SI

4. RESULTS AND DISCUSSION

4.1. Project 1

4.1.1. Chemistry

A set of new aliphatic hydroxybisphosphonates SIs with added functional groups have been synthesized via different routes using alendronic acid as starting compound. Alendronic acid (**SI-1**) is a well-known hydroxybisphosphonate drug for treating bone diseases. The low toxicity of alendronic acid motivated us to synthesize potentially environmentally friendly SIs.

First, the amino group of alendronic acid was functionalized with phosphorous acid in the presence of formaldehyde and hydrochloric acid in water via the Moedritzer-Irani reaction to produce the aminomethylenephosphonate **SI-2**. Second, sulfonic acid derivatives were used as reactants to obtain two new hydroxybisphosphonates with attached alkylsulfonates (alkyl = methyl, and ethyl, for **SI-3** and **SI-5**, respectively) to the amino group of alendronic acid. Furthermore, from carboxylic acid starting materials, two carboxyl groups were attached to the amino group of alendronic acid to obtain **SI-4** and **SI-7**. Lastly, **SI-6** was obtained from the reaction of a dicarboxylic acid with alendronic acid. All reactions except the corresponding to **SI-2** were carried out under basic conditions using NaOH.

To characterize the target chemicals, FTIR and NMR spectroscopy techniques were used. FTIR spectra of **SI-1** displayed a broad absorption peak around 3196 cm^{-1} attributed to the NH bond stretching vibration, a broad stretch around 3086 cm^{-1} representing the OH bond, and two peaks at 919 cm^{-1} and 824 cm^{-1} revealing the phosphonate groups ($-\text{PO}_3^-$). For the synthesized compounds, the OH band was further observed around 3300 cm^{-1} without the presence of the NH bond. The FTIR spectrum of **SI-2** displayed strong absorption peaks at 1046 cm^{-1} and 898 cm^{-1} , indicating the presence of the added phosphonate groups in the alendronic acid structure. For **SI-3** and **SI-5**, the S=O absorption peaks were observed between 1027 and 1179 cm^{-1} . The carboxylated compounds **SI-4**, **SI-6**, and **SI-7** revealed C=O peaks around the 1600 cm^{-1} region.

Furthermore, the ^1H NMR spectra of **SI-1** in D_2O displayed a triplet at $\delta 2.96$ ppm attributed to $\text{NH}_2\text{-CH}_2\text{-CH}_2\text{-}$ protons and a characteristic broad peak around $\delta 1.99 - 1.89$ ppm for $-\text{CH}_2\text{-CH}_2\text{-C(OH)(PO}_3\text{H}_2)_2$ protons. All synthesized SIs showed these peaks in their respective ^1H NMR spectra. In addition, the ^{31}P NMR chemical shift (δ) of the phosphonic acid group in **SI-1** and all the modified structures, showed a singlet signal between $\delta 17\text{-}18$ ppm. In the case of **SI-2**, an additional singlet

signal was obtained at δ 7.08 ppm. The results obtained in both FTIR and NMR spectra indicate that all compounds were successfully synthesized.

4.1.2. Static bottle tests

Inhibition efficiencies of aliphatic hydroxybisphosphonates synthesized in this study were screened against gypsum and calcite scales. Doses of SIs of 100, 50, 20, 10, 5, 2, and 1 ppm were evaluated using static bottle tests at 80°C for 5 hours. Detailed data set obtained can be found in Appendix D. Commercial SIs such as PVS, ATMP, and CMI were also tested for comparative purposes.

4.1.2.1. Gypsum scale

All synthesized SIs in this project (**SI-1** to **SI-7**) and commercial SIs were tested for gypsum scale inhibition using static testing at 80°C and 5 hours. Results are provided in Table 9. Results show that all synthesized products gave good to outstanding performance against gypsum formation at the conditions studied. The parent compound, alendronic acid (**SI-1**) showed good performance at high SI concentrations. However, its performance slowly decreased at low concentrations. Table 9 and Figure 22 show that all new SIs improved the performance against gypsum inhibition compared to **SI-1**. This is a reflection that the addition of different functional groups successfully improved scale inhibition performance.

Table 9. Gypsum inhibition performance of commercial SIs and SI-1 to SI-7.

SI concentration (ppm)	% inhibition									
	PVS	ATMP	CMI	SI-1	SI-2	SI-3	SI-4	SI-5	SI-6	SI-7
100	98	97	98	100	100	100	99	95	100	98
50	96	93	94	97	99	97	99	92	100	98
20	95	90	94	96	97	85	99	86	98	97
10	95	87	89	96	96	65	99	68	95	97
5	93	87	82	83	94	42	97	32	93	97
2	91	87	76	82	93	13	97	24	90	94
1	89	85	68	75	80	13	96	15	85	94

To begin with, commercial SIs performed well against the gypsum scale. However, at decreasing concentrations of SI, slight losses of inhibition performance were obtained. Furthermore, an outstanding performance was obtained for carboxylated SIs, **SI-4** and **SI-7**, throughout the whole concentrations range. Both products performed better than commercial SIs, exhibiting more than 90% inhibition at all doses. It has been reported that SIs containing carboxyl groups, specially polymeric, are particularly effective as gypsum inhibitors^{40,82,83}.

SI-6 also showed very good inhibition at all concentrations of SI tested, providing more than 90% inhibition above 2 ppm. However, its performance dropped to 85% at 1 ppm. Compared to the commercial SIs, this is still a good performance as ATMP presented the same inhibition at 1 ppm, while PVS showed 89% inhibition at the same concentration.

The aminomethylenephosphonate **SI-2** also provided very good performance against gypsum formation, remaining above 90% until 2 ppm. **SI-2** also had better performance than all tested commercial SI, except at 1 ppm where its performance dropped to 80%. PVS and ATMP presented higher inhibition performance than **SI-2** at 1 ppm. However, **SI-2** exhibited higher inhibition efficiency (80%) than CMI (68%) at 1 ppm.

The hydroxybisphosphonates with attached alkylsulfonates, **SI-3** and **SI-5**, also showed excellent performance at high concentrations. However, in both cases, inhibition performance dropped continuously at decreasing concentrations until reaching 13% and 15% at 1 ppm for **SI-3** and **SI-5**, respectively. A reason for this may be that sulfonic groups form weaker complexes with surface calcium ions in comparison with carboxylic groups⁸⁴.

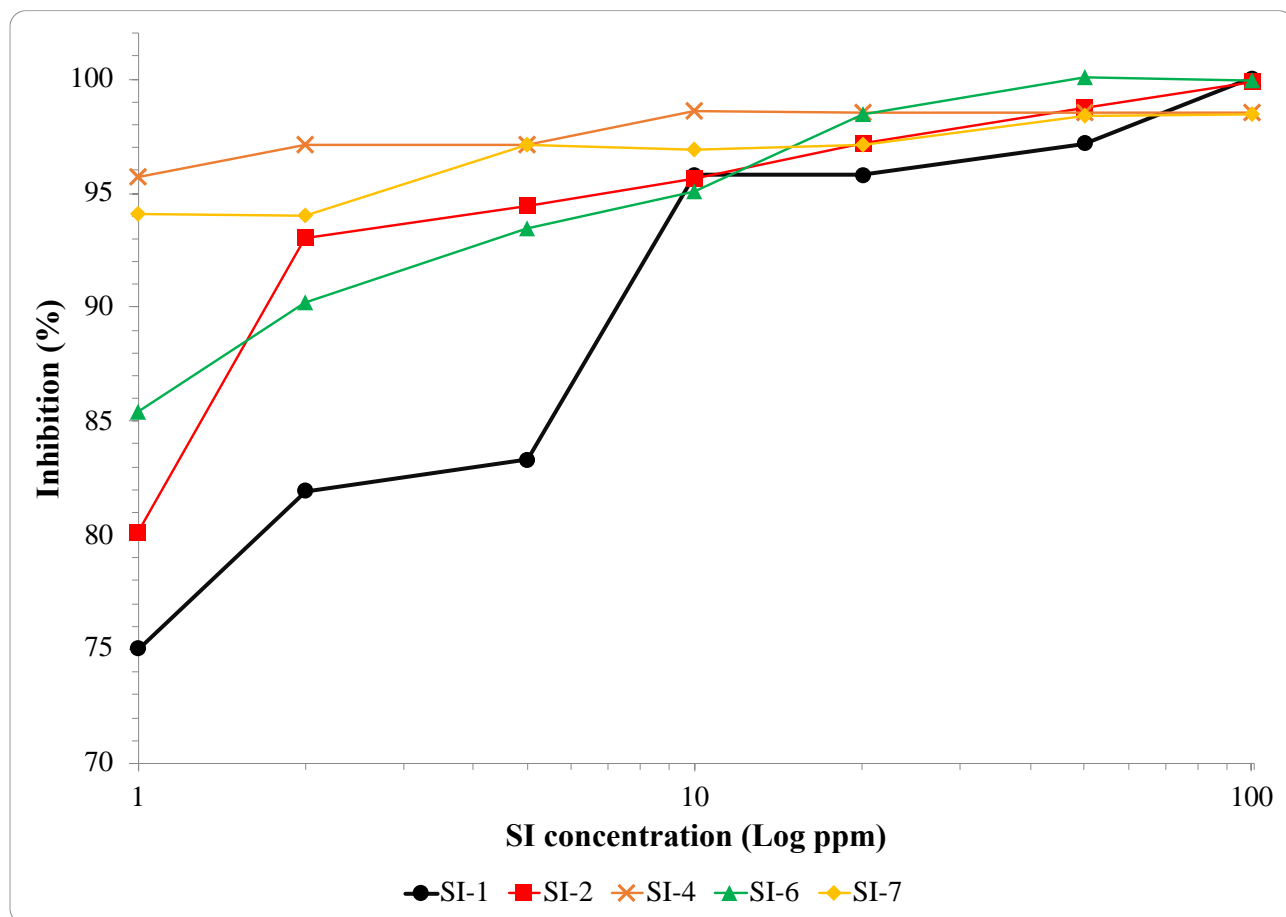


Figure 22. Gypsum inhibition performance of selected SIs.

4.1.2.2. Calcite scale

Results obtained for the performance evaluation against calcite scale of synthesized and commercial SIs using static bottle test at 80°C for 5 hours are shown in Table 10. Not surprisingly, a decrease in performance was obtained for all SIs in contrast to gypsum performance. All commercial SIs showed significant decrease in performance at low concentrations. PVS remained as the SI with highest inhibition performance. Its polymeric structure provides preferential affinity for Ca²⁺ and Mg²⁺ ions than non-polymeric phosphonates³⁰. However, PVS performance dropped from 97% at 100 ppm to 79% at 20 ppm and continued decreasing at lower concentrations. ATMP showed a low inhibition performance, reiterating the fact that its non-polymeric phosphonated structure causes incompatibility between SI and Ca²⁺ ions, leading to precipitation of a Ca²⁺-ATMP complex. This has been similarly reported previously⁸².

Regarding the newly synthesized SIs proposed in this project, **SI-3**, **SI-4**, and **SI-7** presented the best inhibition performance at high concentrations of SI. This is illustrated in Figure 23. All the mentioned SIs improved the inhibition performance at 100 ppm when compared to **SI-1**. Alendronic acid, **SI-1**, presented 76% inhibition at 100 ppm while **SI-3**, **SI-4** and **SI-7** presented an inhibition of more than 80%. However, the performance of all products was reduced at low concentrations of SI.

Table 10. Calcite inhibition performance of commercial SIs and SI-1 to SI-7.

SI concentration (ppm)	% inhibition									
	PVS	ATMP	CMI	SI-1	SI-2	SI-3	SI-4	SI-5	SI-6	SI-7
100	97	85	70	76	56	84	82	75	75	80
50	92	70	59	73	50	71	72	74	67	72
20	79	64	42	63	38	57	63	58	57	64
10	54	59	38	62	34	40	55	32	52	61
5	43	53	16	45	28	27	49	25	41	46
2	12	50	12	26	2	16	16	10	16	19
1	5	28	10	10	0	12	1	4	6	3

As shown in Figure 23, the hydroxybisphosphonate incorporated methylsulfonate, **SI-3**, presented the sharpest decrease in inhibition performance at low concentrations. While **SI-4** and **SI-7** remained closer to the behavior of the parent compound **SI-1**. Except at concentrations of 2 and 1 ppm where the inhibition performance of the synthesized compounds was lower than the obtained for **SI-1**. As similarly discussed in the previous section, the improved performance of carboxylated SIs over the sulfonated SIs, may be due to the higher affinity between carboxyl groups with Ca²⁺ ions. Even though the performance of the ethylsulfonate **SI-5** was lower than **SI-3**, both exhibited a fairly similar trend throughout the entire concentration range examined.

Moreover, **SI-6** performance was not as high as the previously mentioned SIs. However, it exhibited better performance at low concentrations than **SI-5** and had an overall better performance than the commercial CMI. **SI-2** presented the lowest inhibition against this type of scale, presumably due to the incompatibility between the phosphonate groups in its structure and the Ca^{2+} ions in solution. The incompatibility of aminomethylenephosphonates has been previously demonstrated and discussed thoroughly by our research group^{21,47,67,75}.

In general, calcite scale is more difficult to deal with than gypsum scale, as the latter one is readily soluble in water and certain chelants. Therefore, a general decrease in performance within the SIs tested was expected and further obtained, as most SIs exhibited an inhibition around 80% at the highest concentration tested (100 ppm). However, it does not mean that the proposed SIs give a bad performance, but they require further studies under different conditions, e.g., dynamic testing.

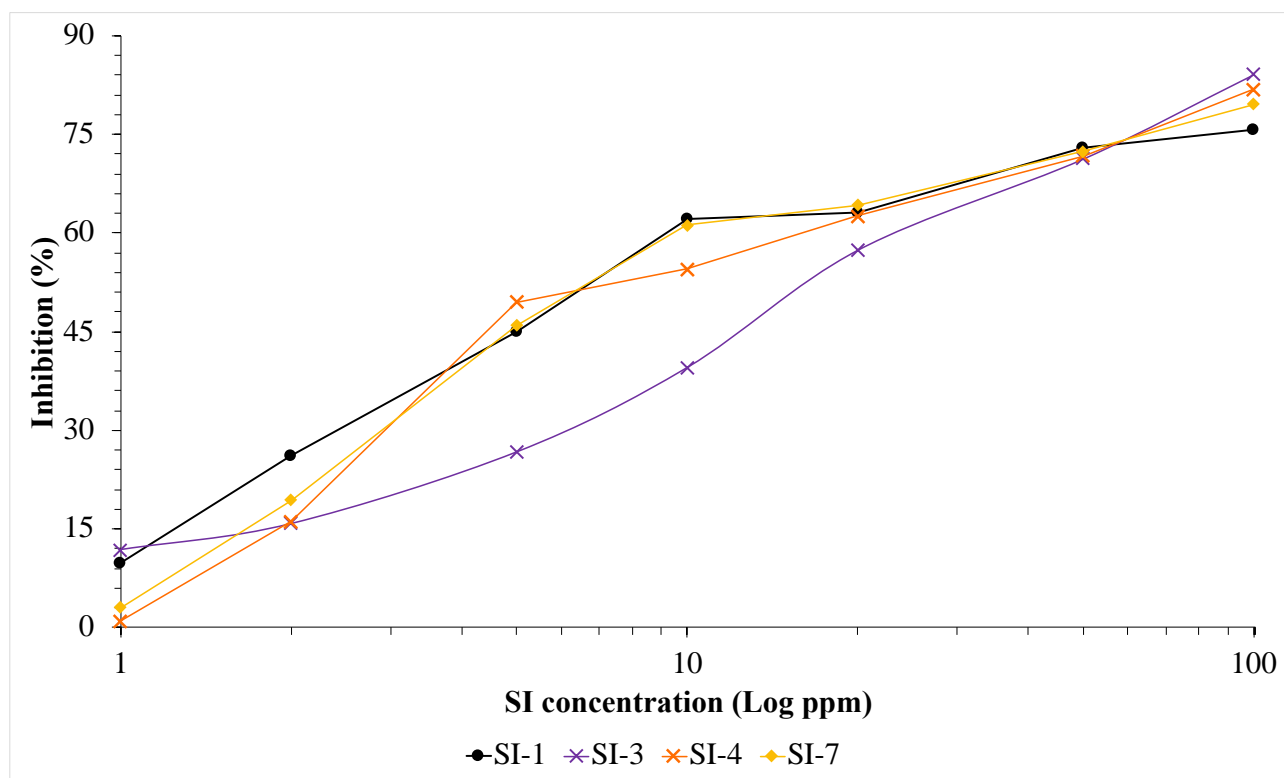


Figure 23. Calcite inhibition performance of selected SIs.

4.1.2.3. Heidrun calcite scale

All compounds mentioned previously throughout this project were also statically tested against calcite scale using a water chemistry based on produced fluids from the Heidrun oilfield in the North Sea. Performance results obtained for the commercial and synthesized products are shown in Table 11.

In this case, it can be observed that PVS showed higher inhibition performance than for the previously tested calcite. This trend could have been obtained due to the slightly higher Mg^{2+} concentration in this brine mixture (265 ppm) with respect to the brine mixture proposed by NACE 0374-2007 (220 ppm). It has been reported that PVS exhibits slight improvements in performance at increased concentrations of Mg^{2+} ions³⁰.

Furthermore, Ca^{2+} concentration in this brine mixture is lower than the calcite-forming brine tested in the previous section. This led to less incompatibility between ATMP and Ca^{2+} ions which is subsequently reflected in the increased performance for this SI.

Table 11. Heidrun calcite inhibition performance of commercial SIs and SI-1 to SI-7.

SI concentration (ppm)	% inhibition									
	PVS	ATMP	CMI	SI-1	SI-2	SI-3	SI-4	SI-5	SI-6	SI-7
100	99	90	100	98	88	100	94	100	100	100
50	97	87	95	97	83	98	92	100	100	97
20	97	97	88	97	69	98	90	98	98	95
10	93	99	79	93	65	97	89	98	95	95
5	93	99	97	92	63	72	77	53	93	91
2	46	85	90	87	54	56	37	30	47	72
1	20	48	28	82	35	5	35	22	40	39

Most of the synthesized SIs presented good inhibition against Heidrun calcite formation. Except for **SI-2**, all inhibitors had very good performance up to 10 and 5 ppm of SI. **SI-2** performance was not outstanding. Presumably, the phosphonated structure made it less compatible with Ca^{2+} ions in solution, which decreases its inhibition efficiency by producing a SI- Ca^{2+} precipitate. **SI-3**, **SI-5**, **SI-6**, and **SI-7** showed better performance than the parent compound **SI-1** at concentrations of 100, 50, 20, and 10 ppm, almost reaching 100% in all cases. However, **SI-3** decreased its inhibition at low concentrations, reaching a minimum inhibition of 5% at 1 ppm. Furthermore, **SI-4** did not reach 100% inhibition at 100 ppm of SI but showed higher inhibition capacity at lower concentrations than **SI-3** and **SI-5**, for example. This can be appreciated in Figure 24. **SI-6** and **SI-7** showed very good performance throughout the whole concentrations range. However, in both cases, the inhibition decreased to nearly 40% at 1 ppm. Again, these results reflect the higher compatibility between carboxyl groups with Ca^{2+} over sulfonate groups⁸⁴.

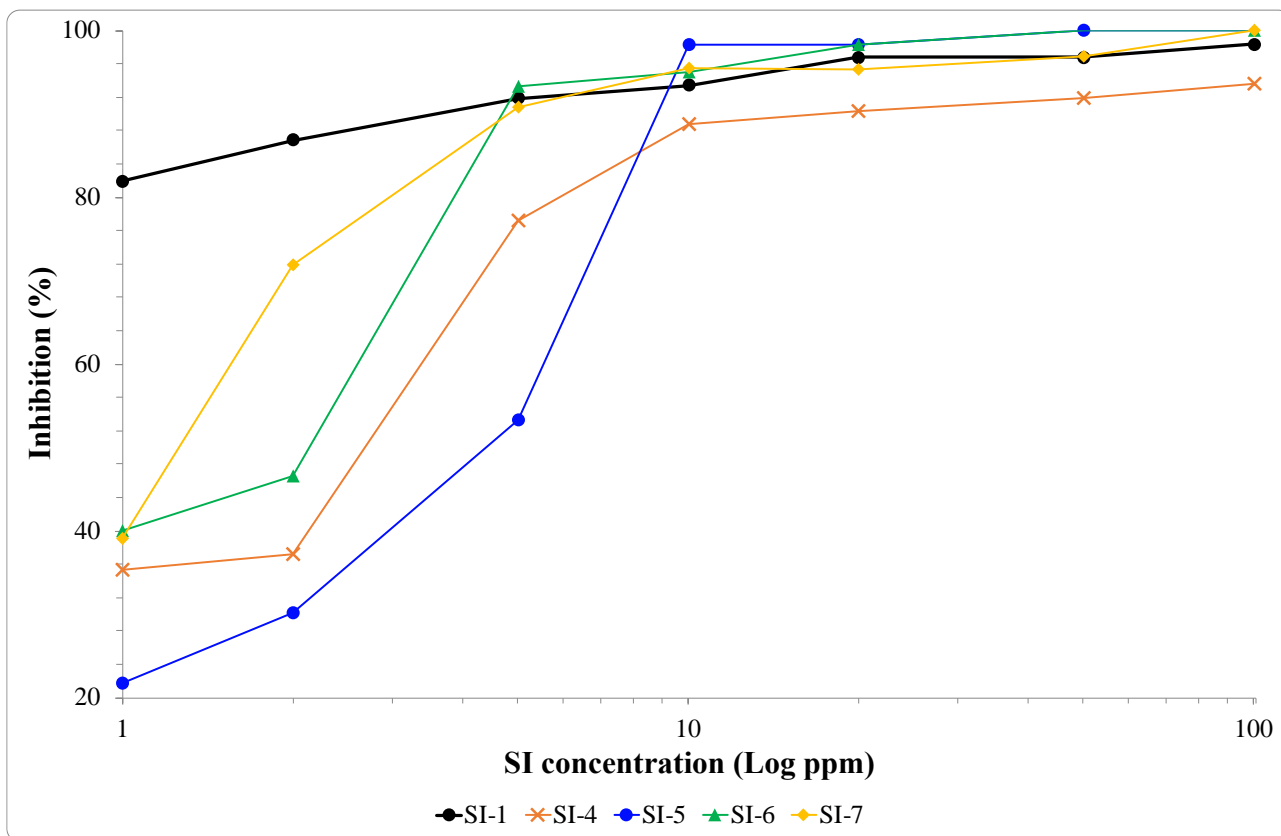


Figure 24. Heidrun calcite inhibition performance of selected SIs.

4.1.3. Calcium compatibility

As discussed previously in Section 3.3.5, an important characteristic to consider when designing SIs is their compatibility with Ca^{2+} (and in some cases, Mg^{2+}) ions. Some SIs, especially phosphonates, tend to form Ca^{2+} -SI complexes which precipitate and could further obstruct the production line. In this research, calcium compatibility of the proposed SIs was evaluated by testing different concentrations of Ca^{2+} (100, 1000, and 10000 ppm) against different concentrations of SI (100, 1000, 10000, and 50000 ppm) at 80°C under static and saline (3% NaCl) conditions. The pH of the solutions was adjusted between 4 and 5. The compatibility between SIs and brines can vary depending on the basic or acidic conditions of the system¹. Furthermore, calcium compatibility was assessed by judging the appearance of the solutions as clear, hazy or precipitate, right after mixing and after 30 minutes, 1 hour, 4 hours, and 24 hours. SIs compatible with Ca^{2+} ions show a clear appearance after 24 hours at 80°C . Calcium compatibility results are provided in Appendix E. However, the SIs most compatible with Ca^{2+} are presented in Table 12.

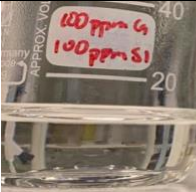
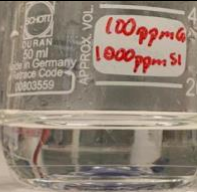
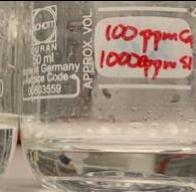
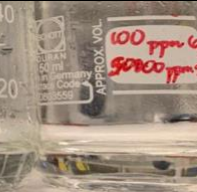
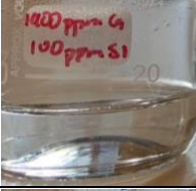
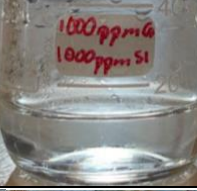
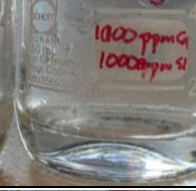

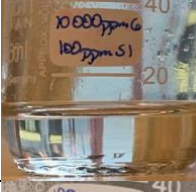

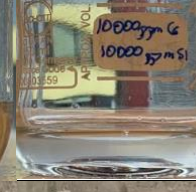
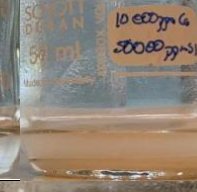
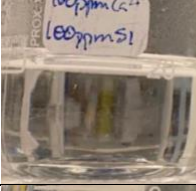
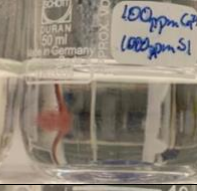
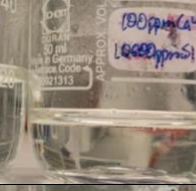

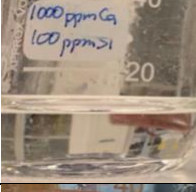
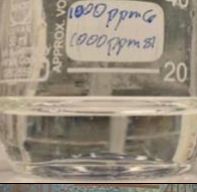
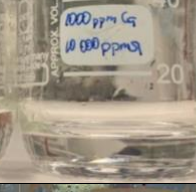
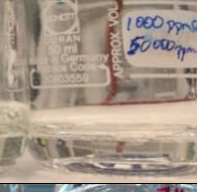

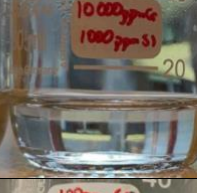


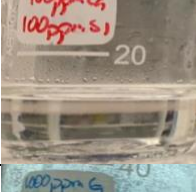


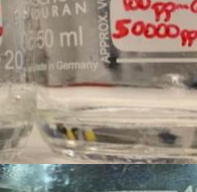




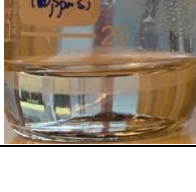
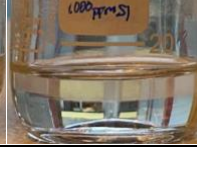
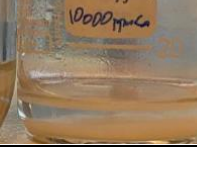
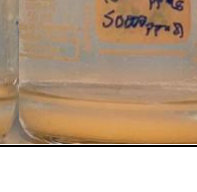
Ca^{2+} compatibility of **SI-1** was previously studied under the same conditions⁶⁷. The phosphonated nature of **SI-1** did not allow good compatibility at 1000 and 10000 ppm Ca^{2+} . At 100 ppm of SI the solutions remained clear after 24 hours. However, when carboxyl groups were attached to the structure (for example, **SI-4** and **SI-7**), an improvement in compatibility was obtained.

In both cases, good compatibility was obtained even at 1000 ppm Ca²⁺ and 50000 ppm of SI. When increasing the Ca²⁺ concentration to 10000 ppm, an improvement in contrast to **SI-1** was also obtained as the samples were clear until 1000 ppm of SI, showing haziness/precipitate only at higher concentrations of Ca²⁺. Finally, the sulfonated **SI-5** exhibited outstanding compatibility with Ca²⁺ ions as solutions remained clear after 24 hours at all Ca²⁺ and SI concentrations. As mentioned in Section 3.3.5, the results obtained correspond with the literature as the addition of carboxyl (**SI-4** and **SI-7**) and sulfonate (**SI-5**) groups improved the compatibility when compared to the single phosphonate SI (**SI-1**)^{1,85}. For further illustration, the appearance after 24 hours of the SIs previously discussed are shown in Table 13.

Table 12. Ca²⁺ tolerance tests at 30000 ppm (3 wt%) NaCl for SI-1, SI-4, SI-5 and SI-7.

SI	Ca ²⁺ dose (ppm)	SI dose (ppm)	pH	Appearance					
				after mixing	30 minutes	1 hour	4 hours	24 hours	
67SI-1	1000	100	-	clear	clear	clear	clear	clear	
		1000	-	clear	hazy	precipitate	precipitate	precipitate	
		10000	-	clear	precipitate	precipitate	precipitate	precipitate	
		50000	-	precipitate	precipitate	precipitate	precipitate	precipitate	
	10000	100	-	clear	clear	clear	clear	clear	
		1000	-	precipitate	precipitate	precipitate	precipitate	precipitate	
		10000	-	precipitate	precipitate	precipitate	precipitate	precipitate	
		50000	-	precipitate	precipitate	precipitate	precipitate	precipitate	
	SI-4	100	100	4.32	clear	clear	clear	clear	clear
			1000	5.02	clear	clear	clear	clear	clear
			10000	4.86	clear	clear	clear	clear	clear
			50000	5.07	clear	clear	clear	clear	clear
1000		100	4.84	clear	clear	clear	clear	clear	
		1000	4.78	clear	clear	clear	clear	clear	
		10000	4.68	clear	clear	clear	clear	clear	
		50000	4.89	clear	clear	clear	clear	clear	
10000		100	4.56	clear	clear	clear	clear	clear	
		1000	4.32	clear	clear	clear	clear	clear	
		10000	4.33	hazy	hazy	hazy	hazy	hazy	
		50000	4.40	hazy	precipitate	precipitate	precipitate	precipitate	
SI-5	100	100	4.03	clear	clear	clear	clear	clear	
		1000	3.80	clear	clear	clear	clear	clear	
		10000	4.48	clear	clear	clear	clear	clear	
		50000	4.64	clear	clear	clear	clear	clear	
	1000	100	5.01	clear	clear	clear	clear	clear	
		1000	4.83	clear	clear	clear	clear	clear	
		10000	4.79	clear	clear	clear	clear	clear	
		50000	4.81	clear	clear	clear	clear	clear	
	10000	100	4.54	clear	clear	clear	clear	clear	
		1000	4.33	clear	clear	clear	clear	clear	
		10000	4.66	clear	clear	clear	clear	clear	
		50000	4.27	clear	clear	clear	clear	clear	
SI-7	100	100	4.83	clear	clear	clear	clear	clear	
		1000	4.60	clear	clear	clear	clear	clear	
		10000	4.38	clear	clear	clear	clear	clear	
		50000	4.34	clear	clear	clear	clear	clear	
	1000	100	4.68	clear	clear	clear	clear	clear	
		1000	4.51	clear	clear	clear	clear	clear	
		10000	4.24	clear	clear	clear	clear	clear	
		50000	4.29	clear	clear	clear	clear	clear	
	10000	100	4.14	clear	clear	clear	clear	clear	
		1000	4.50	clear	clear	clear	clear	clear	
		10000	4.27	hazy	precipitate	precipitate	precipitate	precipitate	
		50000	4.41	hazy	precipitate	precipitate	precipitate	precipitate	

Table 13. Ca²⁺ tolerance tests. Appearance after 24 hours.

SI	Ca ²⁺ dose (ppm)	SI dose (ppm)			
		100	1000	10000	50000
SI-4	100				
	1000				
	10000				
SI-5	100				
	1000				
	10000				
SI-7	100				
	1000				
	10000				

4.1.4. Thermal stability

SI-2, **SI-5**, and **SI-7** were selected as representatives of their respective functional groups for studying thermal stability in this project. 5% solutions of each SI were prepared and sparged with nitrogen to stimulate anaerobic conditions. They were subject to heat over 7 days at 130°C and further evaluated for gypsum and calcite scales as described throughout this project. The complete data set is provided in Appendix D.

4.1.4.1. Gypsum scale

After being exposed to thermal aging under anaerobic conditions, **SI-2**, **SI-5**, and **SI-7** were tested against gypsum scale formation. The obtained results are showed in Table 14.

Table 14. Gypsum inhibition performance of SI-2, SI-5, and SI-7 after thermal aging.

SI concentration (ppm)	%inhibition		
	SI-2*	SI-5*	SI-7*
100	99	88	100
50	97	84	100
20	98	57	100
10	98	54	98
5	97	23	98
2	97	22	95
1	97	21	84

*Tested after heating at 130°C under anaerobic conditions over 7 days.

In Figure 25, the contrast between performances before and after thermal aging of the different SIs tested can be observed. **SI-2** remained relatively stable throughout the whole test after thermal aging. Before thermal aging, **SI-2** dropped its inhibition performance from 93% at 2 ppm to 80% at 1 ppm. However, after thermal aging, this decrease in performance at low concentrations was not obtained. Instead, scale inhibition performance of **SI-2** remained above 95% at all concentrations evaluated after thermal aging. This suggests that the aminomethylenephosphonate **SI-2** was thermally stable against gypsum inhibition.

Unexpectedly, the ethylsulfonate **SI-5** presented a considerable decrease in performance along the whole concentrations range. Usually, sulfonate groups are expected to provide an improvement in calcium compatibility and thermal stability. However, stability against gypsum scale formation was not obtained from **SI-5**. A low affinity between Ca^{2+} ions and sulfonic group has been reported and it may be reason behind the results obtained⁸⁴.

On the contrary, the carboxylated **SI-7** did not lose inhibition performance after thermal aging. Before thermal aging, 94% inhibition was obtained at 1 ppm for **SI-7**. This further changed to 84% after thermal aging. However, inhibition remained above 95% above 2 ppm of **SI-7** after thermal aging which is still an acceptable result.

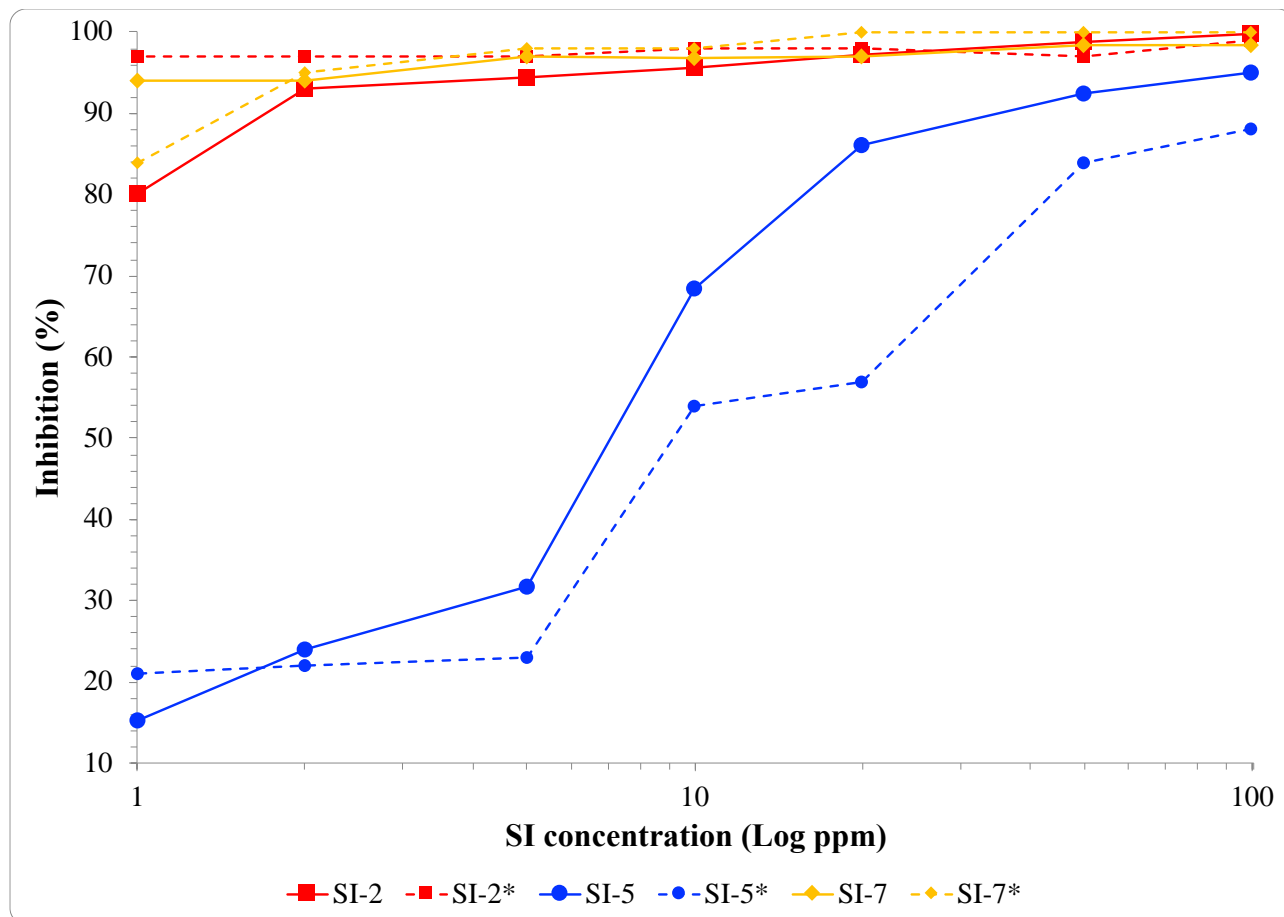


Figure 25. Gypsum inhibition performance of SI-2, SI-5 and SI-7 after thermal aging. (*compound tested after thermal aging).

4.1.4.2. Calcite scale

Calcite inhibition performance of **SI-2**, **SI-5**, and **SI-7** after thermal aging under anaerobic conditions over 7 days are presented in Table 15.

Table 15. Calcite inhibition performance of SI-2, SI-5 and SI-7 after thermal aging.

SI concentration (ppm)	%inhibition		
	SI-2*	SI-5*	SI-7*
100	77	83	69
50	64	77	64
20	59	57	61
10	54	35	60
5	33	22	56
2	17	3	48
1	5	2	45

*Tested after heating at 130°C under anaerobic conditions over 7 days

After thermal aging, **SI-2** presented an increase in performance throughout the concentrations range examined. This can be further appreciated in Figure 26. Before thermal aging, the maximum inhibition exhibited by **SI-2** was 56% at 100 ppm of SI. However, after thermal aging, a 77% inhibition was obtained at the same concentration. A similar trend was obtained even at low concentrations of SI. For example, before thermal aging, the inhibition performance of **SI-2** was 0% and 2% at 1 and 2 ppm, respectively. While after thermal aging, this increased to 5% and 17%.

Furthermore, in the case of **SI-5**, inhibition performance remained relatively stable from 100 to 10 ppm. However, more noticeable decreases were observed at 2 and 1 ppm. Before thermal aging, inhibitions of 10% and 4% were obtained at 2 and 1 ppm, respectively. While after thermal aging, a decrease to 3% and 2% were obtained.

A variation in the performance of **SI-7** was obtained after thermal aging. A slight decrease in performance was obtained between 100 and 10 ppm when comparing to the performance before thermal aging. The maximum performance exhibited by **SI-7** before thermal aging was 80% at 100 ppm, while after thermal aging it presented 69% at the same concentration. However, noticeable improvements were obtained from 5 ppm of SI and below. At the lowest concentration, 1 ppm, the performance before thermal aging was 3%. While after thermal aging, it remained at 45%.

Explanations behind the improvement in performance of SIs after thermal aging are still unidentified. Therefore, further research is needed. Not all compounds show improved performance after thermal aging. Thus, it is mostly hypothesized that it could be due to changes in the chemical structure. Furthermore, it is important to remember that in general terms, calcite scale is more difficult to deal with than the gypsum scale and this also influences the relatively poor performance of the different SIs. However, it would be ideal to study the performance of these chemicals under dynamic conditions, as static bottle tests are only used as a starting point in the evaluation of SIs.

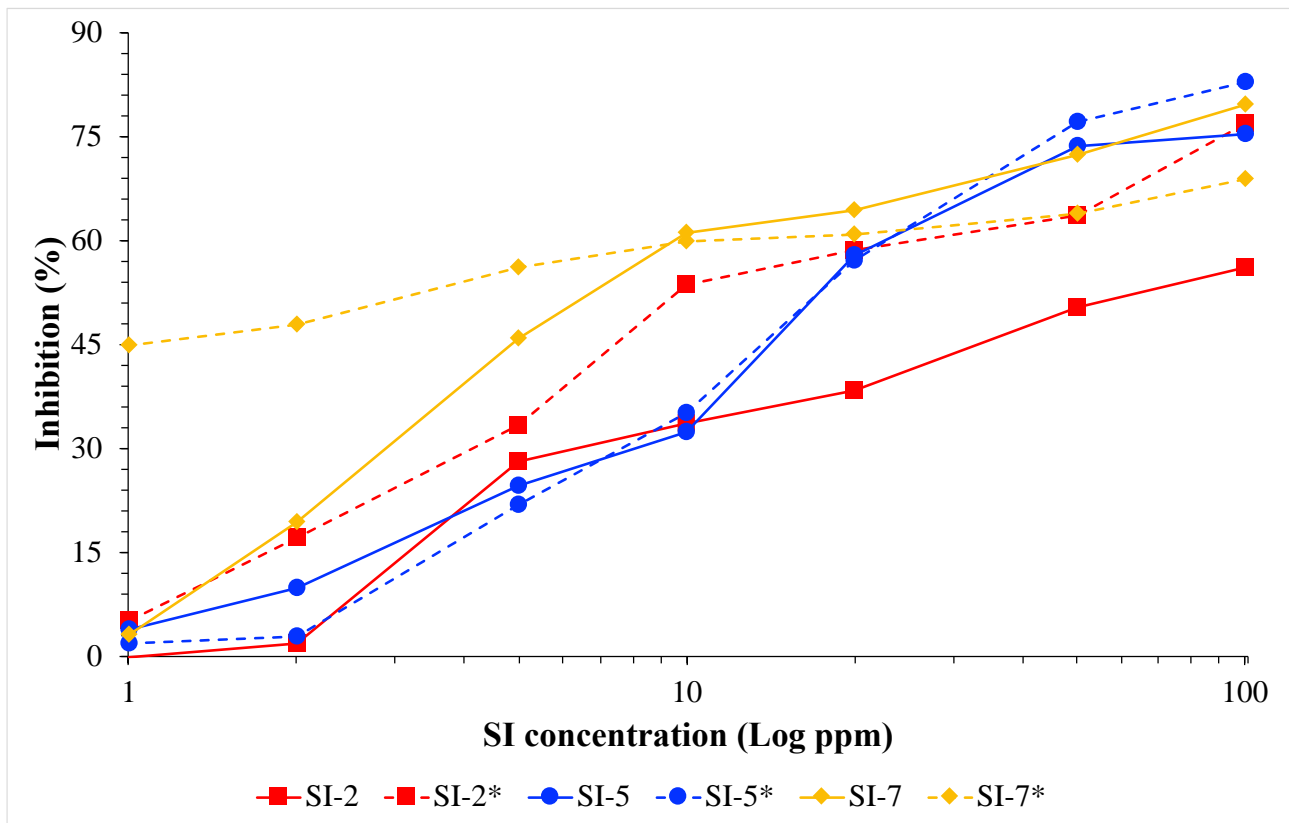


Figure 26. Calcite inhibition performance of SI-2, SI-5 and SI-7 after thermal aging. (*compound tested after thermal aging).

4.1.4.3. Heidrun calcite scale

Table 16 presents the inhibition performance of SI-2, SI-5, and SI-7 after thermal aging under anaerobic conditions over 7 days, against calcite inhibition using synthetic brines with ionic composition from the Heidrun oilfield in the North Sea.

Table 16. Heidrun calcite inhibition performance of SI-2, SI-5, and SI-7 after thermal aging.

SI concentration (ppm)	%inhibition		
	SI-2*	SI-5*	SI-7*
100	81	97	100
50	72	97	100
20	72	97	97
10	66	94	94
5	63	56	94
2	50	38	66
1	44	32	54

*Tested after heating at 130°C under anaerobic conditions over 7 days

In Figure 27 can be appreciated the comparison between the performances obtained before and after thermal aging of the studied SIs. SI-2 presented a relatively stable inhibition against the Heidrun calcite scale after thermal aging. However, slight decreases in performance were obtained from 100 to 50 ppm. Before thermal aging, 88% efficiency decreased to 83% while after thermal aging the samples showed a decrease from 81% to 72% inhibition.

It is important to remark that the phosphonated structure of **SI-2** does not allow good compatibility with Ca^{2+} ions, forming a complex precipitate at high concentrations of SI, a reason why a poor inhibition performance is usually obtained within this range. However, as the concentration of the SI decreased, a more stable performance was obtained when compared to the performance obtained before thermal aging. Additionally, before thermal aging, 35% inhibition was obtained at 1 ppm. While after thermal aging, a slight increase to 44% of calcite inhibition was obtained.

Furthermore, **SI-5** presented a stable inhibition performance throughout the test. Up to 10 ppm, both performances before and after thermal aging, remained above 90% inhibition, but after thermal aging they were slightly lower. From 5 ppm and below, the performance after thermal aging slightly improved, finally presenting 32% inhibition in contrast to 22% inhibition before thermal aging. The sulfonic group in **SI-5** is assumed to have the responsibility in providing this stability which is observed in both variants of the calcite scale.

SI-7 was also stable at all concentrations examined after thermal aging. Its performance resulted slightly higher at high concentrations. For example, at 50 ppm showed 100% inhibition after thermal aging, while before thermal aging it presented 97%. Even though at 2 ppm the inhibition dropped from 72% before thermal aging to 66% after thermal aging, it resulted higher at 1 ppm (54%) than the non-aged sample (39%).

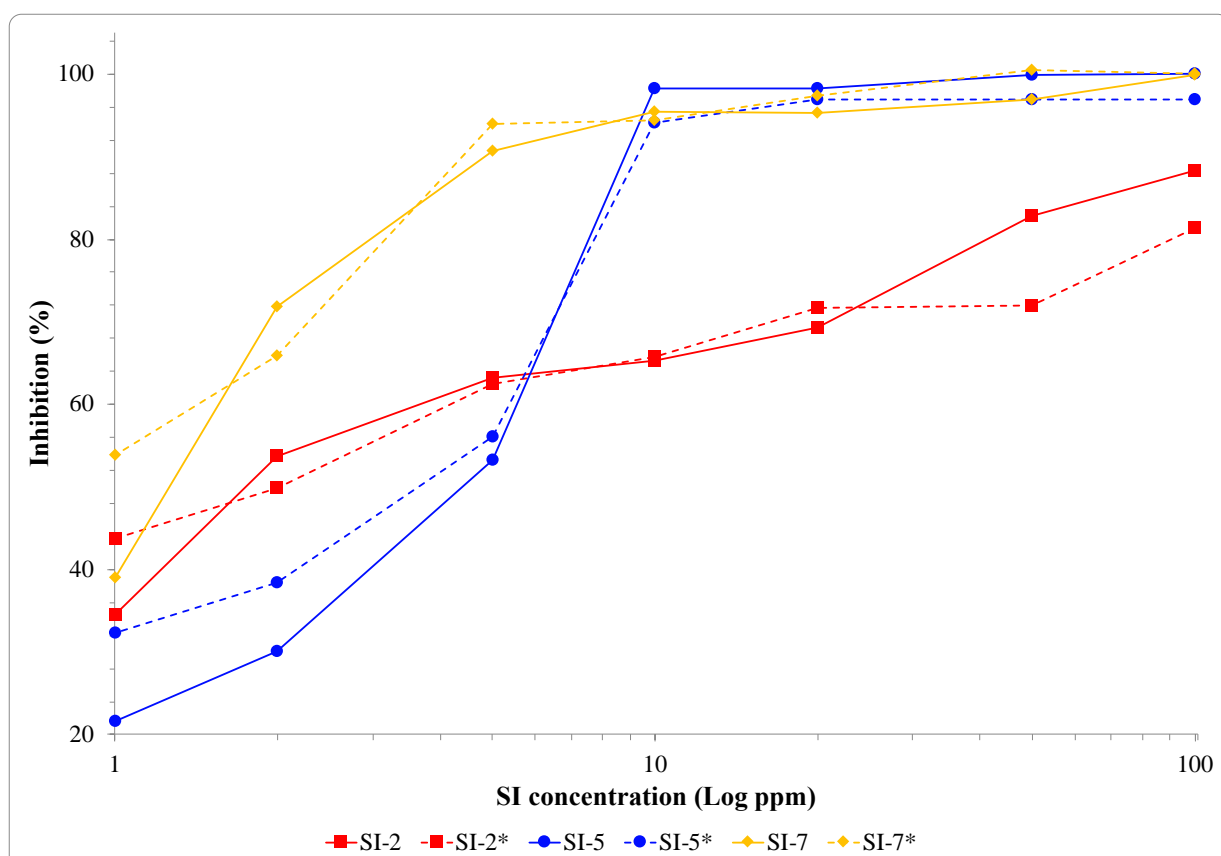


Figure 27. Heidrun calcite inhibition performance of SI-2, SI-5, and SI-7 after thermal aging. (*compound tested after thermal aging).

4.2. Project 2

4.2.1. Chemistry

Three SIs with nitrogen-free phosphonate groups were studied as antiscaling agents in this project. First, the commercial and natural product antibiotic fosfomycin (**SI-8**), was tested as SI for oilfield conditions. Second, its orally bioavailable derivative, fosfomycin trometamol (**SI-9**), was synthesized according to the European Patent 1 762 573 A1, where the reaction between fosfomycin disodium salt (**SI-8**) and a tromethamine acid salt with oxalic acid is carried out in substantially alcoholic media⁷⁰. Finally, due to the instability of **SI-8** in acidic media, it was desired to hydrolyze the epoxide ring to obtain an aliphatic compound and compare their performances as new nitrogen-free phosphonated SI (**SI-10**). This reaction consisted of bringing the pH of a fosfomycin solution down to 3 under reflux conditions at high temperatures.

The structures of the compounds in question were characterized using NMR and FTIR spectroscopies. In the FTIR spectra of **SI-8**, a sharp absorption peak is shown at 1089 cm⁻¹, attributed to the phosphonate group. As expected, there were no easily distinguishable IR bands for the CO bond of the epoxide. Instead, this structure can be further confirmed by the absence of an OH band (3200-3700 cm⁻¹) and a C=O band (1650-1800 cm⁻¹). The FTIR spectra of **SI-9** showed a strong, broadband at 3048 cm⁻¹ representing the NH stretching vibration and further at 2945 and 2822 cm⁻¹, the OH stretch. A characteristic peak for the phosphonate group was present at 1035 cm⁻¹. In the case of **SI-10**, a broad OH stretch was obtained at 3249 cm⁻¹, and a sharp absorption peak at 1041 cm⁻¹ was attributed to the phosphonate group.

The ¹H NMR for **SI-8** in D₂O, displayed multiple peaks in the range δ 3.20 - 3.13 ppm, which represent the -CH-CH₃ proton. In the range δ 2.75-2.69 ppm, a doublet-doublet peak is observed due to the -CH-PO₃H₂ proton. Finally, a very sharp doublet is displayed at δ 1.38 and δ 1.37 ppm representing the methyl group (-CH-CH₃). In the case of **SI-9**, a sharp singlet peak is displayed at δ 3.60 ppm representing the methylene groups (CH₂(OH))₂-C(NH₂)-CH₂-. Furthermore, the determining factor in differentiating **SI-10** from **SI-8**, was the chemical shift obtained in the ³¹P NMR spectra. While **SI-8** showed a singlet signal at δ 9.99 ppm, **SI-9** and **SI-10** shifted the signal to δ 12.29 ppm and δ 17.33 ppm, respectively.

4.2.2. Static bottle tests

Inhibition efficiency of nitrogen-free phosphonates was screened against gypsum and calcite scales. Different doses of SIs of 100, 50, 20, 10, 5, 2, and 1 ppm were evaluated using static bottle tests at 80°C for 5 hours. Detailed data set obtained can be found in Appendix H. A commercial SI, HPAA, was also tested under the same conditions to compare the performance of our proposed SIs with a commercially available product that possesses a similar chemical structure.

4.2.2.1. Gypsum scale

Inhibition performance against gypsum scale of the commercial scale inhibitor HPAA and the synthesized SIs using static bottle tests are shown in Table 17. The inhibition behavior of the tested SIs is further represented in Figure 28.

Table 17. Gypsum inhibition performance of HPAA and SI-8 to SI-10.

SI concentration (ppm)	%inhibition			
	HPAA	SI-8	SI-9	SI-10
100	97	98	91	95
50	93	94	67	92
20	91	85	47	86
10	81	31	19	78
5	63	19	11	63
2	37	4	5	40
1	32	4	0	25

From a general perspective, the proposed scale inhibitors showed good performance for gypsum inhibition. **SI-8** showed only about 1% better performance than HPAA at 100 and 50 ppm, at 20 ppm it still showed relatively good performance of 85% gypsum inhibition, but this unfortunately dropped down to 31% at 10 ppm. The poor performance of HPAA against the gypsum scale, presumably attributed to its low molecular weight and/or poor adsorption of the SI on gypsum crystallites has been reported⁸². In the case of **SI-9**, good inhibition of 91% was obtained at 100 ppm. However, it continuously dropped throughout the whole test until reaching <10% inhibition at 2 and 1 ppm.

SI-10 showed the best inhibition performance of the synthesized SIs, behaving similarly to the commercial HPAA. Even at low concentrations, **SI-10** showed certain inhibition of 63% at 5 ppm of SI, same as HPAA. However, at 1 ppm, **SI-10** showed 25% inhibition while HPAA was slightly higher at 32% inhibition.

Furthermore, in Figure 28 can be observed that HPAA remained as the SI with the highest inhibition performance against the gypsum scale. However, **SI-10** showed good performance throughout all concentrations of SIs tested. **SI-8** and **SI-9** showed good performance only at the highest concentrations of SI. The slightly different performance between HPAA and **SI-10** is attributed to the presence of the carboxyl group in the structure of HPAA. The presence of this functional group allows more and stronger interactions between SI and ions in the solution, which translates to a better inhibition performance.

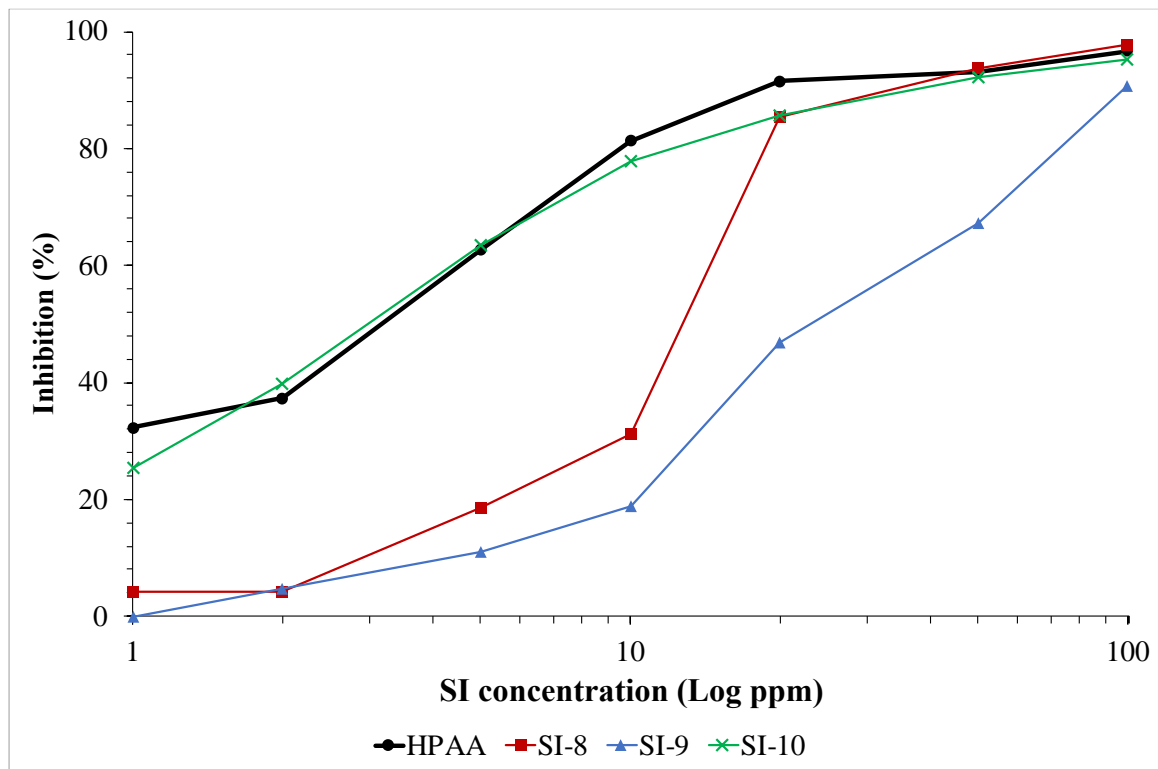


Figure 28. Gypsum inhibition performance of HPAA and SI-8 to SI-10.

4.2.2.2. Calcite scale

Table 18 shows the inhibition performance of the studied SIs against the calcite scale using static bottle tests. The representation in Figure 29 shows a similar trend as the obtained for the gypsum scale, where HPAA remained as the SI with the highest inhibition performance, followed by **SI-10**.

Table 18. Calcite inhibition performance of HPAA and SI-8 to SI-10.

SI concentration (ppm)	%inhibition			
	HPAA	SI-8	SI-9	SI-10
100	71	43	48	62
50	57	22	18	42
20	34	17	6	17
10	29	8	1	12
5	18	8	0	9
2	3	4	0	6
1	1	1	0	1

HPAA presented 71 and 57% inhibition at concentrations of 100 and 50 ppm of SI, remaining above 20% until 10 ppm. **SI-8**, **SI-9**, and **SI-10** showed only about 43%, 48%, and 62% inhibition at 100 ppm, respectively. However, **SI-8** dropped its inhibition to 22% at 50 ppm and further to 17% at 20 ppm, while **SI-9** instantly dropped to 18% at 50 ppm. Both **SI-8** and **SI-9** presented an inhibition below 10% from 10 and 20 ppm, respectively. In the case of **SI-10**, a fair 62% was obtained at 100 ppm dropping to 42% and 17% at 50 and 20 ppm, respectively.

As similarly obtained for the gypsum scale, **SI-10** showed an improvement in inhibition compared to **SI-8**. This is presumably because **SI-10** is a linear structure with a hydroxyl group that could provide extra binding capabilities in contrast to the epoxide ring of **SI-8**. At the same time and as mentioned in Section 4.2.2.1, the structure of **SI-10** is the most analogous to HPAA except for the carboxyl group. Due to this functional group, HPAA provides an inhibition of more than 10% at concentrations up to 5 ppm which is not the case of **SI-8** or **SI-10**. Same as for gypsum, it was expected that **SI-9** provided better performance than **SI-9** due to the presence of the diverse amino, hydroxyl, and phosphonate groups in its structure, but this was not the case.

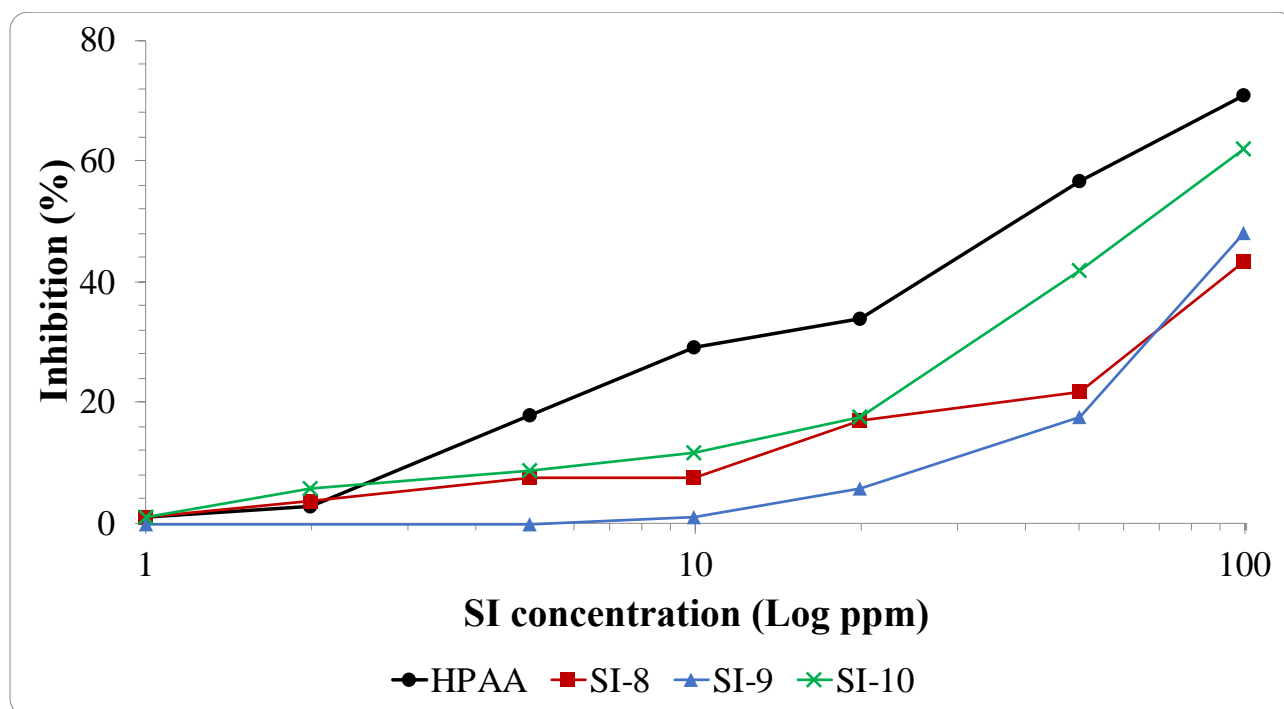


Figure 29. Calcite inhibition performance of HPAA and SI-8 to SI-10.

In general, it was expected to obtain good inhibition performance from all compounds against calcite scale. However, it is relevant to remark that the divalent cation concentrations in this mixed brine are 1657 ppm Ca^{2+} and 220 ppm Mg^{2+} while the mixed gypsum brine composition is 1514 ppm Ca^{2+} . This is of relevant importance as the inhibition efficiency of some SIs is negatively affected at high Ca^{2+} concentrations. Furthermore, it has also been stated that the presence of Mg^{2+} ions in some cases negatively affects the inhibition efficiency behavior of SIs, especially in phosphonated SIs³⁰.

4.2.2.3. Heidrun calcite scale

Results of inhibition performance against the Heidrun calcite scale are presented in Table 19. In this case, good inhibition performance was obtained for all tested SIs at high concentrations. HPAA inhibition efficiency remained above 90% until 5 ppm, this further dropped to 36% and 13% at 2 and 1 ppm, respectively.

Table 19. Heidrun calcite inhibition performance of HPAA and SI-8 to SI-10.

SI concentration (ppm)	%inhibition			
	HPAA	SI-8	SI-9	SI-10
100	100	92	68	97
50	98	71	55	73
20	97	49	34	61
10	95	38	24	42
5	95	32	18	15
2	36	24	15	0
1	13	24	13	0

The results are further illustrated in Figure 30. **SI-8** showed 92% inhibition at 100 ppm. However, this decreased to 71% at 50 ppm. For **SI-9**, 68% inhibition was obtained at 100 ppm, further at 50 ppm the inhibition dropped to 55% and continuously decreased at lower concentrations, resulting as the poorest SI against this type of scale. **SI-10** was the proposed SI that showed the highest inhibition against calcite, presenting 97% inhibition at 100 ppm. Although the overall performance was not relatively similar to the commercial HPAA throughout the whole concentrations range, it still exhibited adequate inhibition.

Furthermore, testing conditions most likely influenced the scale inhibitors performance compared to standard calcite. For standard calcite, Ca^{2+} concentration in the mixed brine is 1657 ppm and Mg^{2+} concentration is 220 ppm. For Heidrun calcite, Ca^{2+} concentration is 1020 ppm and Mg^{2+} concentration is 265 ppm. Although Mg^{2+} concentration for Heidrun conditions is slightly higher than the proposed by NACE Standard TM0374-2007, it did not seem to negatively affect the inhibition performance of the tested SIs. This may be due to the lower Ca^{2+} concentration for Heidrun water chemistry, as the harmful effect of Mg^{2+} ions on the inhibition efficiency is stronger at higher Ca^{2+} concentrations³⁰.

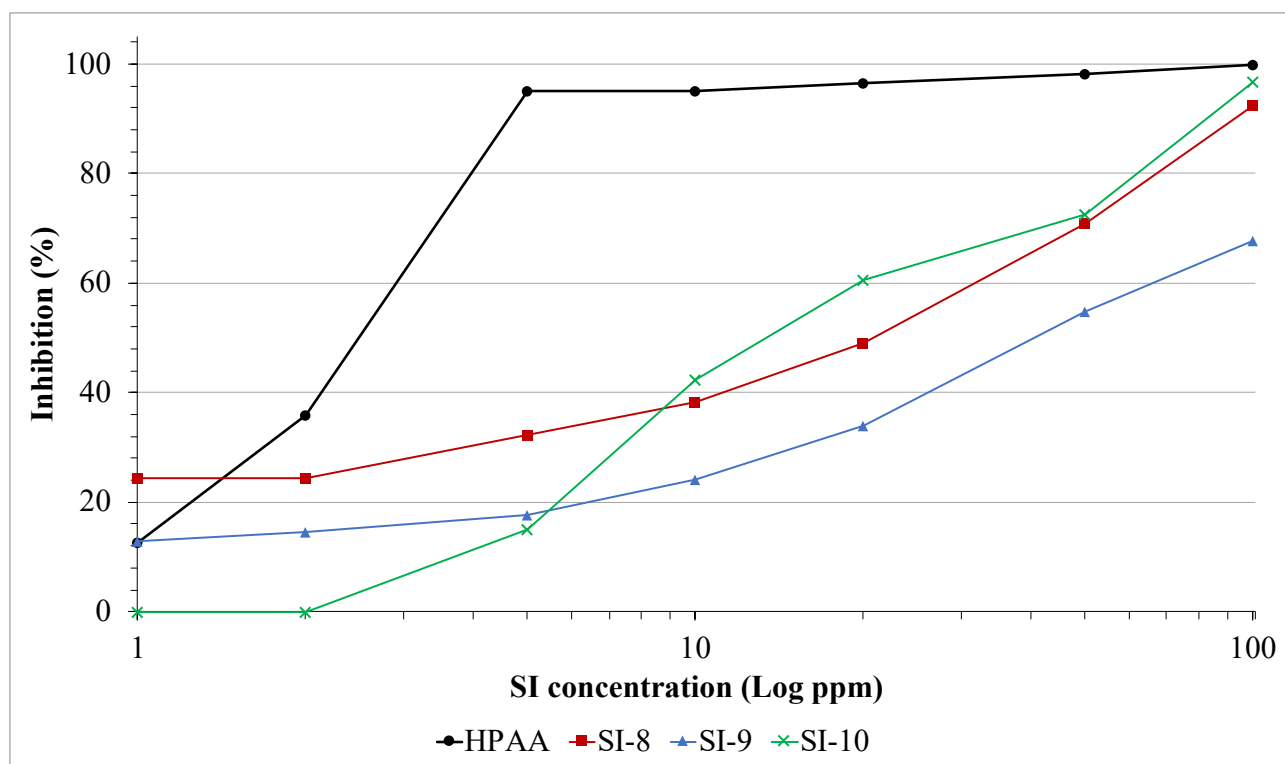


Figure 30. Heidrun calcite inhibition performance of HPAA and SI-8 to SI-10.

4.2.3. Calcium compatibility

Calcium tolerance of the proposed SIs in this project was evaluated as discussed previously in Sections 3.3.5. and 4.1.3. A summary of the results obtained is presented in Table 20.

Initially, **SI-8** and **SI-9** presented outstanding compatibility at all concentrations of Ca^{2+} and SI evaluated. The presence of ether linkages in their structures may enhance the ability to overcome complexing with Ca^{2+} ions^{14,22}. Furthermore, the compatibility of HPAA was evaluated for further comparison with **SI-10**, as both present analogous structures. HPAA presented very low compatibility at concentrations above 1000 ppm Ca^{2+} and 10000 ppm of SI. Even at 10000 ppm Ca^{2+} and 1000 ppm SI, the precipitate was obtained after 30 minutes at 80°C. In contrast, **SI-10** exhibited better performance than HPAA. For **SI-10**, all samples were clear after 24 hours except the correspondent to 50000 ppm **SI-10** at 1000 and 10000 ppm SI. Moreover, at 10000 ppm Ca^{2+} and 10000 ppm **SI-10**, the solution turned hazy after 30 minutes at 80°C. However, a precipitate was never obtained for any of these samples. All these observations are presented in Table 21.

As discussed earlier, the presence of carboxyl groups in phosphonated SIs enhances the complexing abilities of the SI with Ca^{2+} ions. However, that is not the case for a small molecule like HPAA. The compatibility of HPAA in contrast to SIs with increased chain length has been reported, showing that HPAA remains within the SIs with least Ca^{2+} tolerance¹⁴. Nevertheless, even though **SI-10** only contains a hydroxyl group, an improvement in Ca^{2+} compatibility was obtained.

It has also been reported that the existence of hydroxyl groups on the side chains of SIs enhances the complexing abilities for Ca^{2+} ⁸⁵.

Table 20. Ca^{2+} tolerance tests at 30000 (3 wt%) NaCl for SI-8, SI-9, SI-10 and HPAA.

SI	Ca^{2+} dose (ppm)	SI dose (ppm)	pH	Appearance				
				after mixing	30 minutes	1 hour	4 hours	24 hours
*SI-8	10000	100	4.82	clear	clear	clear	clear	clear
		1000	4.81	clear	clear	clear	clear	clear
		10000	4.58	clear	clear	clear	clear	clear
		50000	4.41	clear	clear	clear	clear	clear
*SI-9	10000	100	4.61	clear	clear	clear	clear	clear
		1000	4.46	clear	clear	clear	clear	clear
		10000	4.35	clear	clear	clear	clear	clear
		50000	4.30	clear	clear	clear	clear	clear
SI-10	100	100	4.80	clear	clear	clear	clear	clear
		1000	4.43	clear	clear	clear	clear	clear
		10000	3.95	clear	clear	clear	clear	clear
		50000	4.58	clear	clear	clear	clear	clear
	1000	100	4.88	clear	clear	clear	clear	clear
		1000	4.33	clear	clear	clear	clear	clear
		10000	5.10	clear	clear	clear	clear	clear
		50000	5.26	hazy	hazy	hazy	hazy	hazy
	10000	100	4.45	clear	clear	clear	clear	clear
		1000	4.10	clear	clear	clear	clear	clear
		10000	5.30	clear	hazy	hazy	hazy	hazy
		50000	4.18	hazy	hazy	hazy	hazy	hazy
HPAA	100	100	4.02	clear	clear	clear	clear	clear
		1000	3.95	clear	clear	clear	clear	clear
		10000	4.54	clear	clear	clear	clear	clear
		50000	4.42	clear	clear	clear	clear	clear
	1000	100	4.05	clear	clear	clear	clear	clear
		1000	4.30	clear	clear	clear	clear	clear
		10000	4.55	hazy	precipitate	precipitate	precipitate	precipitate
		50000	4.64	hazy	precipitate	precipitate	precipitate	precipitate
	10000	100	5.03	clear	clear	clear	clear	clear
		1000	4.48	hazy	precipitate	precipitate	precipitate	precipitate
		10000	4.18	hazy	precipitate	precipitate	precipitate	precipitate
		50000	4.26	hazy	precipitate	precipitate	precipitate	precipitate

*Tests for 100 and 1000 ppm Ca^{2+} were not performed due to outstanding compatibility at highest concentration of calcium ions.

Table 21. Ca²⁺ tolerance tests. Appearance after 24 hours.

SI	Ca ²⁺ dose (ppm)	SI dose (ppm)			
		100	1000	10000	50000
SI-8	10000				
HPAA	1000				

4.2.4. Thermal stability

For this section, all the SIs were subject to heating at 130°C over 7 days under anaerobic conditions and further tested for gypsum and calcite inhibition. The complete data set is provided in Appendix H.

4.2.4.1. Gypsum scale

The inhibition performance against gypsum scale for all compounds discussed in this project after being subject to high temperatures over a period of 7 days is shown in Table 22 and further illustrated in Figure 31.

Table 22. Gypsum inhibition performance of HPAA and SI-8 to SI-10 after thermal aging.

SI concentration (ppm)	%inhibition			
	HPAA*	SI-8*	SI-9*	SI-10*
100	92	81	98	98
50	90	43	84	96
20	82	16	36	89
10	80	12	33	73
5	70	8	23	69
2	66	7	17	63
1	60	4	12	38

* Tested after heating at 130°C under anaerobic conditions over 7 days.

The performance of HPAA after thermal aging remained stable at all concentrations of SI when compared to the non-aged sample. Inhibition performance was shown to be higher for HPAA before thermal aging until it dropped from 81% at 10 ppm to 63% at 5 ppm. After thermal aging, the inhibition dropped from 80% at 10 ppm to 70% at 5 ppm but remained within 60% at 1 ppm. While, before thermal aging, HPAA exhibited 37 and 32% inhibition at 2 and 1 ppm, respectively.

SI-8 presented a decrease in its inhibition performance after thermal aging. Before thermal aging, it presented 98% and 94% inhibition at 100 and 50 ppm, respectively. However, after thermal aging these values dropped to 81% and 43%. Throughout the whole concentrations range, the inhibition performance was lower after thermal aging, except at 2 ppm, where it increased from 4% before thermal aging, to 7% after thermal aging. However, this is not a significant change.

Furthermore, **SI-9** showed an improvement in performance after thermal aging at all concentrations. A 98% performance was obtained at 100 ppm, this dropped continuously reaching <20% at 2 ppm, while the non-aged **SI-9** presented 19% inhibition at 10 ppm.

SI-10 inhibition also improved after thermal aging even at low concentrations of SI. It even reached higher inhibition than HPAA at 100, 50, and 20 ppm of SI. However, from 10 ppm, inhibition performance of **SI-10** remained slightly lower than that of HPAA.

In general terms, the performance trend of SIs remained relatively stable after thermal aging. **SI-9** presented a higher inhibition performance than before thermal aging and at the same time higher than **SI-8** after thermal aging. The performance between **SI-10** and HPAA also remained similar throughout all concentrations. However, HPAA still remains as the SI with the best performance of all products tested. Reasons behind the fact of obtaining a better performance after thermal aging are unknown, and thus, more research is needed. Not all compounds show better performance after thermal aging. Therefore, it is mostly hypothesized that could be due to changes in the chemical structure.

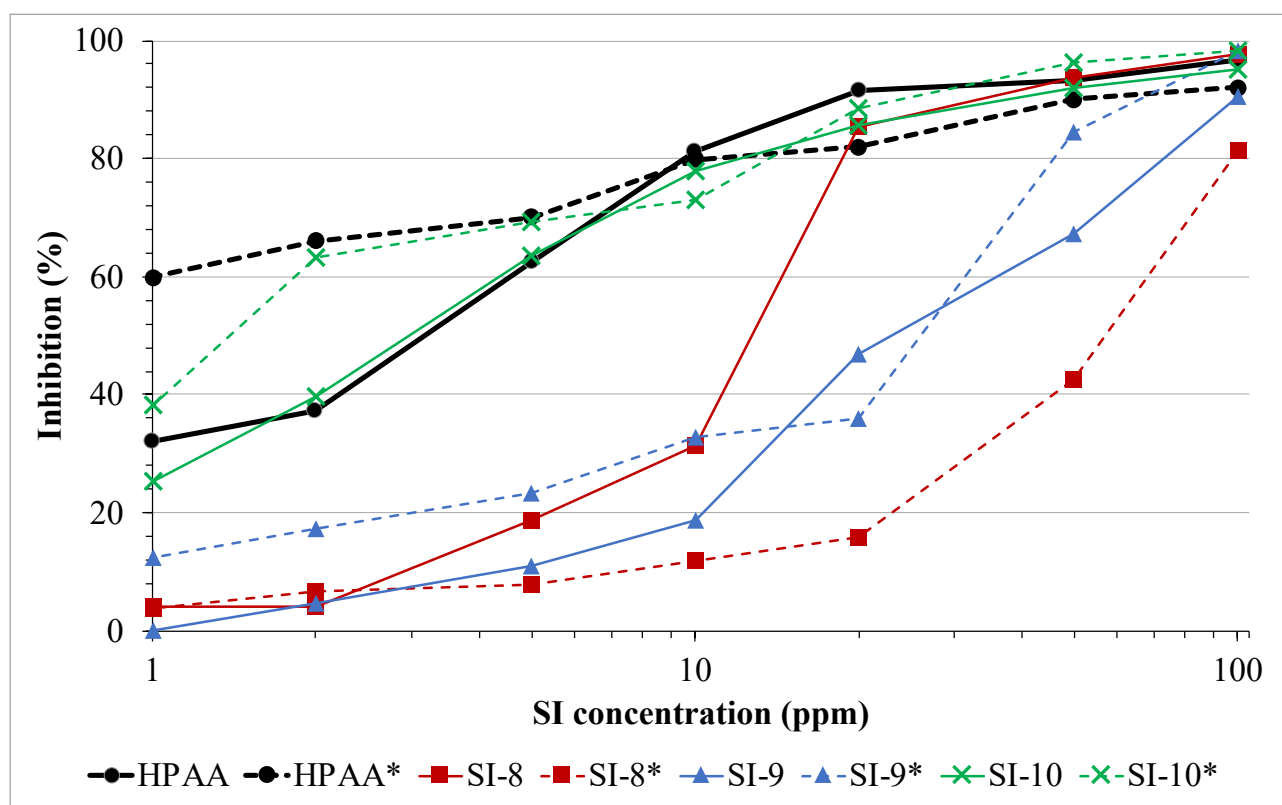


Figure 31. Gypsum inhibition performance of HPAA and SI-8 to SI-10 after thermal aging. (*compound tested after thermal aging).

4.2.4.2. Calcite scale

As can be observed in Table 23, thermal aging did not have a significant negative effect on the performance against calcite scale of the synthesized SIs compared to the pre-aging test, except for **SI-10**. However, in both cases the performance of all compounds was not enough to fully inhibit calcite formation, even at high concentrations of SI. Once again, HPAA presented the highest inhibition performance, showing 75% at 100 ppm and 64% at 50 ppm of SI. While before thermal aging, the performance remained at 71 and 57% inhibition at same concentrations, respectively.

After thermal aging, **SI-8** showed an overall improvement in performance compared to the non-aged sample. Before thermal aging, **SI-8** presented 43% inhibition at 100 ppm. After thermal aging, it improved to 59%. However, in both cases, the performance dropped to 22% at 50 ppm and 20 ppm, before and after thermal aging, respectively. For the non-aged **SI-8**, the inhibition remained under 20% below 20 ppm of SI, while after thermal aging this happened from 10 ppm.

At 100 ppm, **SI-9** showed 48% and 60% inhibition performance before and after thermal aging, respectively. However, it decreased to less than 10% at 20 ppm in both cases. Therefore, the contribution of this product for scale inhibition is not significant. At 100 ppm, **SI-10** presented a decline in performance from 62% before thermal aging to 57% after thermal aging. Before thermal aging it dropped to 42% at 50 ppm and further down to 17% at 20 ppm. While after thermal aging at 50 ppm the performance decreased to 25% at 50 ppm and further to 8% at 20 ppm.

Results in Figure 32 show that the studied SIs are not thermally stable as they present variations in performance before and after thermal aging. **SI-10** experienced a poor performance after thermal aging while HPAA, **SI-8** and **SI-9** presented a slight improvement. However, as similarly obtained in the calcite tests before thermal aging, none of the evaluated SIs presented excellent inhibition performance for this type of scale. The effects of high Ca^{2+} concentration and the presence of Mg^{2+} in the brine mixture plus the effect of the thermal aging that could cause changes in the chemical structures of the SIs proposed, may have accumulated and are reflected in the unexpected, obtained results.

Table 23. Calcite inhibition performance of HPAA and SI-8 to SI-10 after thermal aging.

SI concentration (ppm)	% inhibition			
	HPAA*	SI-8*	SI-9*	SI-10*
100	75	59	60	57
50	64	46	33	25
20	46	22	9	8
10	23	14	3	5
5	16	12	3	1
2	3	11	1	1
1	1	8	2	0

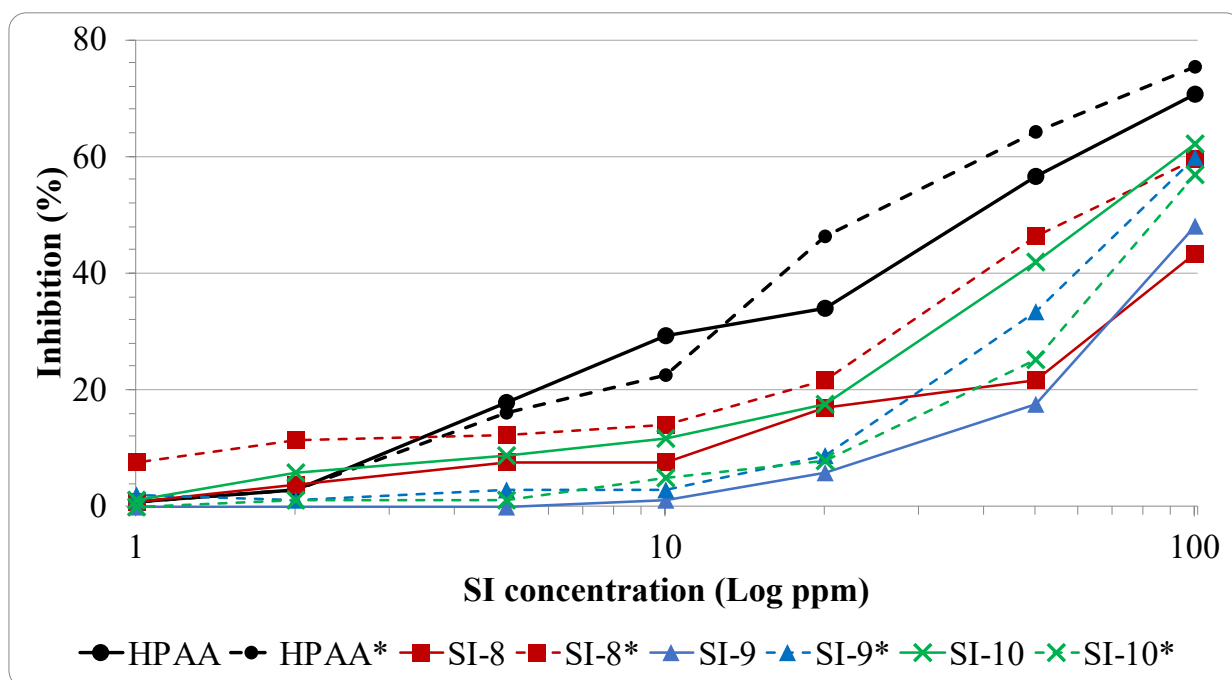


Figure 32. Calcite inhibition performance of HPAA and SI-8 to SI-10 after thermal aging. (*compound tested after thermal aging).

4.2.4.3. Heidrun calcite scale

Results of inhibition performance against calcite scale using Heidrun oilfield water chemistry are shown in Table 24 and further represented in Figure 33.

Table 24. Heidrun calcite inhibition performance of HPAA and SI-8 to SI-10 after thermal aging.

SI concentration (ppm)	% inhibition			
	HPAA*	SI-8*	SI-9*	SI-10*
100	82	92	95	90
50	72	85	90	86
20	93	77	82	60
10	79	49	6	49
5	48	20	0	28
2	34	16	0	22
1	7	3	0	11

In general terms, HPAA exhibited a decrease in inhibition performance throughout all concentrations range. At 100 and 50 ppm, HPAA presented a low inhibition performance which increased to 93% at 20 ppm. This behavior may have happened due to incompatibility of the thermal aged HPAA with divalent ions present in the solution. Even though HPAA is compatible with Ca^{2+} at 100 ppm, the influence of other divalent ions such as Mg^{2+} and Sr^{2+} could have affected the performance of this SI after thermal aging. Therefore, precipitate may form due to incompatibility between the SI and the ions in the solution, affording low inhibition values.

Furthermore, **SI-8** remained stable at 100 ppm after thermal aging, affording 92% of inhibition performance. This value dropped to 85% at 50 ppm and further down to 77% at 20 ppm. Before thermal aging it presented 71% at 50 ppm and 24% inhibition at 1 ppm. While after thermal aging only 3% inhibition was obtained at 1 ppm. A similar situation was observed for **SI-9**, where an improvement in inhibition performance was obtained at high concentrations of SI. Before thermal aging, **SI-9** presented 68%, 55%, and 34% inhibition at 100, 50, and 20 ppm respectively. After thermal aging, these values increased to 95%, 90% and 82% at the same concentrations of SI. However, at lower concentrations, the performance was negligible after thermal aging.

SI-10 showed slightly different trends before and after thermal aging at 100 and 50 ppm. Before thermal aging, a maximum inhibition efficiency of 97% at 100 ppm was obtained, followed by 73% inhibition at 50 ppm. While after thermal aging, 90% inhibition was obtained at 100 ppm and 86% at 50 ppm. However, from 20 ppm, the inhibition remained relatively constant between both studies, reaching 0% inhibition at 2 ppm before thermal aging. The thermal aged sample presented 11% inhibition at 1 ppm. Furthermore, emphasis is still made in the similarities between chemical structures of HPAA and **SI-10**. **SI-10** presented higher inhibition performance and compatibility with Heidrun brines than HPAA after thermal aging. Therefore, it could be said that **SI-10** resulted more thermally stable at higher concentrations of SI than HPAA.

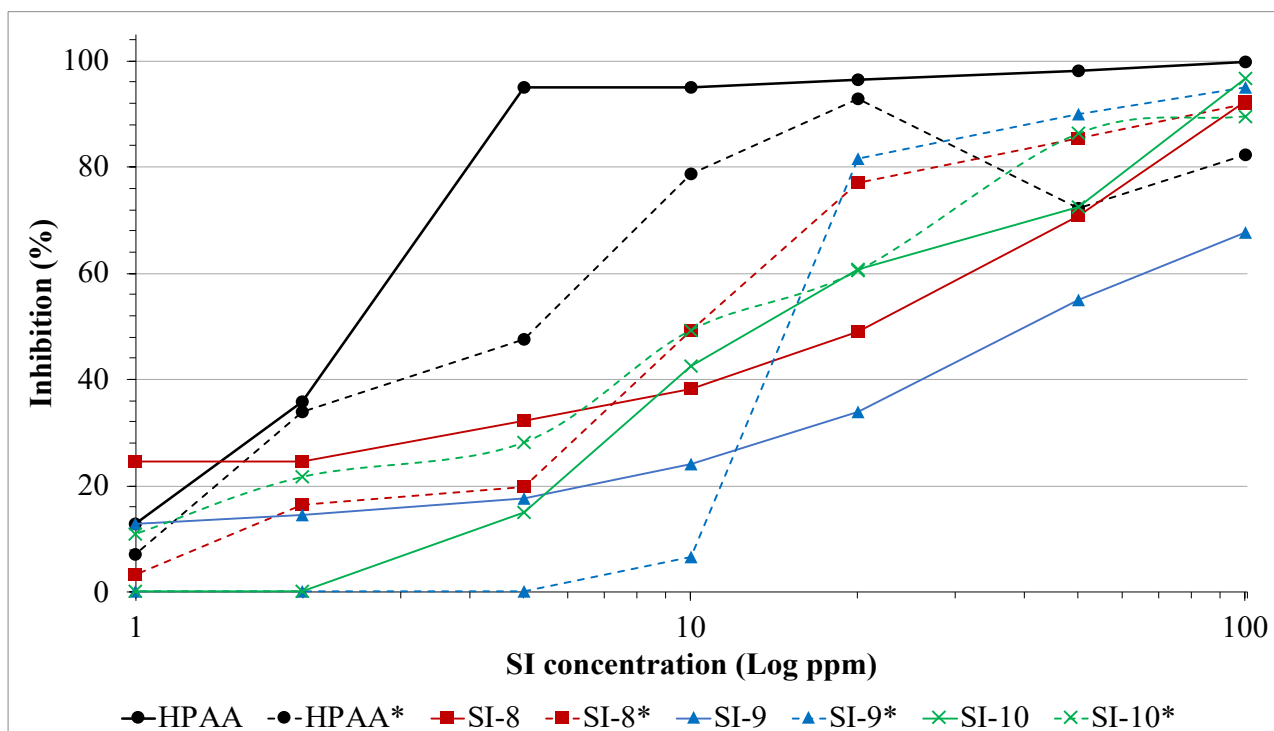


Figure 33. Heidrun calcite inhibition performance of HPAA and SI-8 to SI-10 after thermal aging. (*compound tested after thermal aging).

4.3. Seawater biodegradability

Biodegradability of synthesized products from **SI-1** to **SI-9** was tested according to the OECD 306 protocol using the closed bottle method over 28 days, as described in Section 3.3.6. Complete nitrification was considered during the analysis. BOD of the blank tests was removed from the BOD of the test compounds to avoid overestimating biodegradability. Final biodegradability results are presented in Figure 34.

The biodegradability of a compound is contingent upon its functional groups, ease of uptake and metabolism, redox states, substrate competition, and the microorganisms used together with their adaptation. The reason behind a low biodegradability may stem from any of these factors or a combination of them.

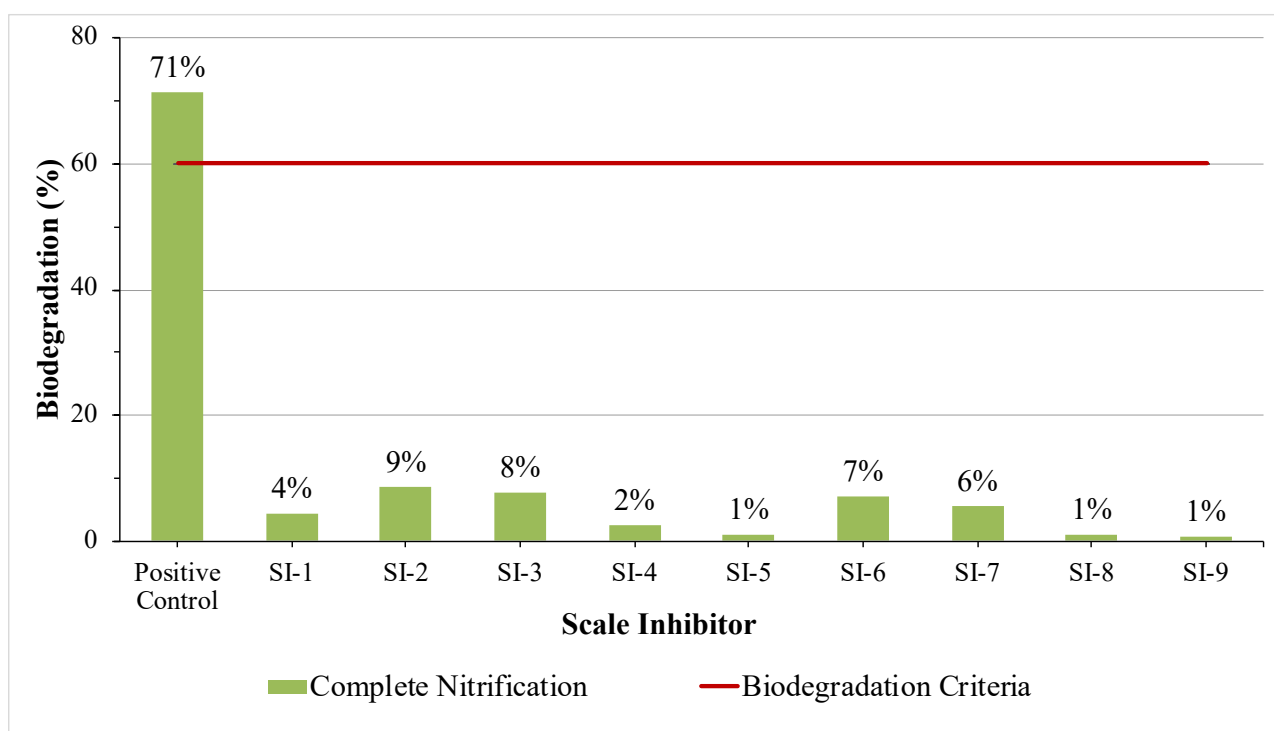


Figure 34. Seawater biodegradability performance of SI-1 to SI-9.

Compounds lacking in nitrogen (positive control and **SI-8**) only have carbon (and phosphorous, in the case of **SI-8**) available for assimilation and catabolism. That being said, the presence of amine groups in the structure of SIs (e.g., **SI-9**) are expected to be more susceptible to hydrolysis and uptake as opposed to lone phosphonates. The C-P bond in phosphonates is extremely stable and requires a lot of energy to assimilate and break down⁵⁸. Furthermore, **SI-8** and **SI-9** have shown the ability to inhibit normal bacterial cell wall growth by resisting peptidoglycan formation, which is potentially the reason behind obtaining a biodegradability of only 1%⁸⁶⁻⁹⁰.

In general, all SIs tested have branched structures, which may also negatively affect biodegradation as opposed to simpler structures. Organic metal complexing agents such as phosphonates and aminophosphonates have shown low acute toxicity concentrations as well as minimal bioconcentration factors⁹¹. Therefore, it is most probable that the low biodegradability is attributed to low assimilative and catabolic activity towards these SIs in order to break them into CO₂. Some bacteria, however, possess a *C-P lyase enzyme* on their membranes which allows them to cleave the C-P bond and use it for growth. Among these bacteria are *E. coli*, *B. megaterium*, and *P. stutzeri*⁵⁸. So, aquatic environments low in these consortia will lead to lower levels of biodegradability for compounds such as **SI-1** to **SI-9**. It is most probable that the fate of organophosphates is the sediments of the receiving water bodies⁹¹.

SI-3 and **SI-5** are the only two compounds that contain sulphur. Both compounds present the same structure with the exception that **SI-3** presents a methylene sulfonate attached to the amino group of **SI-1**, while **SI-5** carries an ethylene sulfonate. The extra methylene in **SI-5** brought down the biodegradability from 8% (**SI-3**) to 1%, reiterating that larger compounds would require more complex bioprocesses for microbial organisms to biodegrade them.

A compound is assumed to biodegrade by heterotrophs if $BOD_{SI} \geq 0.6 ThOD_{SI}$ ²⁵. Now, in the case of the compounds synthesized and tested (**SI-1** to **SI-9**) their BOD is much less than 60% of their ThOD. Therefore, we can conclude that all compounds are extremely poor biodegradable except for the positive control used (C₇H₅O₂Na). Biodegradability for other organophosphates have been shown, on average, to be higher than those obtained in this study⁵⁸. However, they also remain non-biodegradable. The highest biodegradability was attained by **SI-2** at 9%.

It may also be relevant to remark that the biodegradation obtained for the positive control (71%) is slightly lower than values obtained previously by our research group, where it is usually around 90%²². These results do not necessarily indicate that the products in question are not biodegradable, just that further tests should be considered, as the OECD 306 protocol serves as a preliminary test²⁵.

5. CONCLUSIONS

In this thesis, a broad set of aliphatic hydroxybisphosphonates SIs with attached phosphonate, carboxylate, and sulfonate groups (**SI-1** to **SI-7**) as well as SIs with nitrogen-free phosphonate groups (**SI-8** to **SI-10**) were evaluated as potential oilfield SIs. Due to the unavailability of the Dynamic Scale Rig, it was needed to set up a static bottle test protocol for the first time in our research group. This was carried out successfully and a standard operating procedure is provided in case of future need. Even though static bottle tests are not as reliable as dynamic tests (less accurate and reproducible results if SIs are not compatible with high concentrations of Ca^{2+} ions), static tests still provide a good and inexpensive prediction of inhibition performance.

Results obtained throughout this research were successful in answering the research objectives proposed in Section 1.1. The following conclusions are drawn from this study:

- SIs containing carboxylate groups (**SI-4** and **SI-7**) exhibit good to excellent gypsum and calcite inhibition performance.
- SIs containing sulfonate groups (**SI-3** and **SI-5**) exhibit medium to good calcite inhibition and poor gypsum inhibition.
- Obvious correlation between poor inhibition performance in static bottle tests and low Ca^{2+} compatibility for SIs with aminomethylenephosphonate groups due to formation of Ca^{2+} -SI complex, e.g., **SI-2**.
- **SI-2** and **SI-7** inhibition performance against gypsum and calcite scales remained stable after thermal aging. However, the **SI-5** performance after thermal aging only remained stable against calcite formation.
- Ca^{2+} compatibility of **SI-1** improved when attaching carboxylate and sulfonate groups to create the new SIs. Results can be ranked as follows: **SI-5** > **SI-4** > **SI-7** > **SI-3** > **SI-6** > **SI-2** > **SI-1**.
- HPAA and **SI-10** presented similar performance against gypsum and calcite due to their analogous structures. However, HPAA remained higher due to the presence of the carboxylate group in its structure. **SI-10** provided an improvement in Ca^{2+} compatibility in contrast to HPAA, as well as a better inhibition performance than **SI-8** and **SI-9** for all scales evaluated.

- **SI-8** and **SI-9** did not show an outstanding performance against gypsum and calcite scales. Nevertheless, both remained within the most compatible SIs with Ca^{2+} ions evaluated in this research.
- In general terms, better performance for Heidrun calcite than standard calcite was obtained. Presumably because the 50:50 standard brine presents higher Ca^{2+} concentration (1657 ppm) than the 50:50 Heidrun brine (1020 ppm), and the influence of Mg^{2+} ions at high concentrations of Ca^{2+} could negatively affect the SIs efficiency by enhancing incompatibility with scale forming brines.

The results obtained highlight the complications of designing efficient, economically feasible, and biodegradable SIs. Several SIs evaluated throughout this project presented a very good performance against calcite and gypsum formation, as well as good calcium compatibility and thermal stability. However, the biodegradability of all compounds according to the OECD 306 protocol remained below the biodegradation criteria established by discharge regulations in the North Sea. Nonetheless, acute toxicity and bioaccumulation studies would provide more insights into the ability of the proposed compounds to mineralize within the environment. Furthermore, it would be of use to investigate further the performance of the SIs proposed under HTHP conditions (e.g., DSR) to determine the potential of the SIs to be used in continuous injection or squeeze treatments.

6. FUTURE RESEARCH

The following future research recommendations are derived from the thesis work provided.

- a. Further assessment of the SIs presented using the HPDTBT for calcite and barite inhibition.
This was the main methodology of the thesis but had to unfortunately be replaced due to technical issues in the DSR apparatus.
- b. Due to the different problems faced throughout this research derived from the unavailability of DSR equipment, studying the performance of scale inhibitors using other approaches such as the KTT and/or conductivity methods is highly encouraged.
- c. Using molecular dynamics (MD) to simulate interactions between SIs and alkali earth scale. This alongside scanning electron microscopy (SEM), can reveal inhibition mechanisms as well as modifications in the crystalline morphology in the presence of SIs.

7. REFERENCES

- (1) Kelland, M. A. *Production Chemicals for the Oil and Gas Industry*, Second edition.; CRC Press: Boca Raton, FL, 2014.
- (2) Mady, M. F.; Kelland, M. A. Overview of the Synthesis of Salts of Organophosphonic Acids and Their Application to the Management of Oilfield Scale. *Energy Fuels* **2017**, *31* (5), 4603–4615. <https://doi.org/10.1021/acs.energyfuels.7b00708>.
- (3) NACE International. *Laboratory Screening Tests to Determine the Ability of Scale Inhibitors to Prevent the Precipitation of Calcium Sulfate and Calcium Carbonate from Solution (for Oil and Gas Production Systems)*; NACE International: Houston, Tex., 2001.
- (4) Kumar, S.; Naiya, T. K.; Kumar, T. Developments in Oilfield Scale Handling towards Green Technology-A Review. *Journal of Petroleum Science and Engineering* **2018**, *169*, 428–444. <https://doi.org/10.1016/j.petrol.2018.05.068>.
- (5) Safari, M.; Golefatan, A.; Jamialahmadi, M. Inhibition of Scale Formation Using Silica Nanoparticle. *Journal of Dispersion Science and Technology* **2014**, *35* (10), 1502–1510. <https://doi.org/10.1080/01932691.2013.840242>.
- (6) Olajire, A. A. A Review of Oilfield Scale Management Technology for Oil and Gas Production. *Journal of Petroleum Science and Engineering* **2015**, *135*, 723–737. <https://doi.org/10.1016/j.petrol.2015.09.011>.
- (7) Lee, S. Effect of Operating Conditions on CaSO₄ Scale Formation Mechanism in Nanofiltration for Water Softening. *Water Research* **2000**, *34* (15), 3854–3866. [https://doi.org/10.1016/S0043-1354\(00\)00142-1](https://doi.org/10.1016/S0043-1354(00)00142-1).
- (8) Demadis, K. D.; Stavgianoudaki, N.; Grossmann, G.; Gruner, M.; Schwartz, J. L. Calcium–Phosphonate Interactions: Solution Behavior and Ca²⁺ Binding by 2-Hydroxyethylimino-Bis-(Methylenephosphonate) Studied by Multinuclear NMR Spectroscopy. *Inorg. Chem.* **2009**, *48* (9), 4154–4164. <https://doi.org/10.1021/ic802400r>.
- (9) Bhuiyan, A. H.; Hossain, S. Petrographic Characterization and Diagenetic Evaluation of Reservoir Sandstones from Smørbukk and Heidrun Fields, Offshore Norway. *Journal of Natural Gas Geoscience* **2020**, *5* (1), 11–20. <https://doi.org/10.1016/j.jnggs.2019.12.001>.
- (10) Al Jaber, J.; Bageri, B. S.; Adebayo, A. R.; Patil, S.; Barri, A.; Salin, R. B. Evaluation of Formation Damages during Filter Cake Deposition and Removal Process: The Effect of Primary Damage on Secondary Damage. *Petroleum Science* **2021**, S1995822621000091. <https://doi.org/10.1016/j.petsci.2021.07.004>.
- (11) Dydo, P.; Turek, M.; Ciba, J. Scaling Analysis of Nanofiltration Systems Fed with Saturated Calcium Sulfate Solutions in the Presence of Carbonate Ions. *Desalination* **2003**, *159* (3), 245–251. [https://doi.org/10.1016/S0011-9164\(03\)90076-2](https://doi.org/10.1016/S0011-9164(03)90076-2).

- (12) Jafar M., M. A. A Review of Green Scale Inhibitors: Process, Types, Mechanism and Properties. *Coatings* **2020**, *10* (10), 928. <https://doi.org/10.3390/coatings10100928>.
- (13) Frenier, W. W.; Ziauddin, M. *Formation, Removal, and Inhibition of Inorganic Scale in the Oilfield Environment*; Society of Petroleum Engineers: Richardson, Texas, 2008.
- (14) Amjad, Z.; Landgraf, R. T.; Penn, J. L. Calcium Sulfate Dihydrate (Gypsum) Scale Inhibition by PAA, PAPEMP, and PAA/PAPEMP Blend. *Int. J. Corros. Scale Inhib.* **2014**, *3* (1), 035–047. <https://doi.org/10.17675/2305-6894-2014-3-1-035-047>.
- (15) Fink, J. *Petroleum Engineer's Guide to Oil Field Chemicals and Fluids*, Second Edition.; Elsevier: United States, 2015.
- (16) Duccini, Y.; Dufour, A.; Harm, W. M.; Sanders, T. W.; Weinstein, B. High Performance Oilfield Scale Inhibitors; 1997.
- (17) Craddock, H. A. *Oilfield Chemistry and Its Environmental Impact*; Wiley: Hoboken, 2018.
- (18) Mpelwa, M.; Tang, S. F. State of the Art of Synthetic Threshold Scale Inhibitors for Mineral Scaling in the Petroleum Industry: A Review. *Pet. Sci.* **2019**, *16* (4), 830–849. <https://doi.org/10.1007/s12182-019-0299-5>.
- (19) Meyers, K. O.; Skillman, H. L. The Chemistry and Design of Scale Inhibitor Squeeze Treatments; Society of Petroleum Engineers: Phoenix, Arizona, 1985. <https://doi.org/10.2118/13550-MS>.
- (20) Amjad, Z. Calcium Sulfate Dihydrate (Gypsum) Scale Formation on Heat Exchanger Surfaces: The Influence of Scale Inhibitors. *Journal of Colloid and Interface Science* **1988**, *123* (2), 523–536. [https://doi.org/10.1016/0021-9797\(88\)90274-3](https://doi.org/10.1016/0021-9797(88)90274-3).
- (21) Mady, M. F.; Bagi, A.; Kelland, M. A. Synthesis and Evaluation of New Bisphosphonates as Inhibitors for Oilfield Carbonate and Sulfate Scale Control. *Energy Fuels* **2016**, *30* (11), 9329–9338. <https://doi.org/10.1021/acs.energyfuels.6b02117>.
- (22) Mady, M. F.; Bayat, P.; Kelland, M. A. Environmentally Friendly Phosphonated Polyetheramine Scale Inhibitors—Excellent Calcium Compatibility for Oilfield Applications. *Ind. Eng. Chem. Res.* **2020**, *59* (21), 9808–9818. <https://doi.org/10.1021/acs.iecr.0c01636>.
- (23) Liu, D.; Dong, W.; Li, F.; Hui, F.; Lédion, J. Comparative Performance of Polyepoxysuccinic Acid and Polyaspartic Acid on Scaling Inhibition by Static and Rapid Controlled Precipitation Methods. *Desalination* **2012**, *304*, 1–10. <https://doi.org/10.1016/j.desal.2012.07.032>.
- (24) Wilson, D.; Harris, K. Development Of A “Green” Hydrothermally Stable Scale Inhibitor For Topside And Squeeze Treatment; 2010; p 13.
- (25) Organisation for Economic Co-operation and Development. *Test N^o. 306: Biodegradability in Seawater*; OECD Publishing: Paris, 1992.

- (26) Sorbie, K. S.; Laing, N. How Scale Inhibitors Work: Mechanisms of Selected Barium Sulphate Scale Inhibitors Across a Wide Temperature Range; UK, 2004. <https://doi.org/10.2118/87470-MS>.
- (27) NACE international. *Dynamic Scale Inhibitor Evaluation Apparatus and Procedures in Oil and Gas Production*; Houston, Texas, 2005.
- (28) Khamis, E.; Abd-El-Khalek, D. E.; Abdel-Kawi, M. A.; Anwar, J. M. Scale Inhibition in Industrial Water Systems Using Chitosan-alginate Mixture. *Water and Environment Journal* **2021**, wej.12704. <https://doi.org/10.1111/wej.12704>.
- (29) Zhang, H.; Cai, Z.; Jin, X.; Sun, D.; Wang, D.; Yang, T.; Zhang, J.; Han, X. Preparation of Modified Oligochitosan and Evaluation of Its Scale Inhibition and Fluorescence Properties. *J. Appl. Polym. Sci.* **2015**, 132 (37), n/a-n/a. <https://doi.org/10.1002/app.42518>.
- (30) Graham, G. M.; Boak, L. S.; Sorbie, K. S. The Influence of Formation Calcium and Magnesium on the Effectiveness of Generically Different Barium Sulphate Oilfield Scale Inhibitors. *SPE Production & Facilities* **2003**, 18 (01), 28–44. <https://doi.org/10.2118/81825-PA>.
- (31) Jordan, M. M.; Sorbie, K. S.; Graham, G. M.; Taylor, K.; Hourston, K. E.; Hennessey, S. The Correct Selection and Application Methods for Adsorption and Precipitation Scale Inhibitors for Squeeze Treatments in North Sea Oilfields; SPE: Lafayette, Louisiana, 1996; p 20. <https://doi.org/10.2118/31125-MS>.
- (32) Shakkthivel, P.; Vasudevan, T. Acrylic Acid-Diphenylamine Sulphonic Acid Copolymer Threshold Inhibitor for Sulphate and Carbonate Scales in Cooling Water Systems. *Desalination* **2006**, 197 (1–3), 179–189. <https://doi.org/10.1016/j.desal.2005.12.023>.
- (33) Al-Roomi, Y. M.; Hussain, K. F. Application and Evaluation of Novel Acrylic Based CaSO₄ Inhibitors for Pipes. *Desalination* **2015**, 355, 33–44. <https://doi.org/10.1016/j.desal.2014.10.010>.
- (34) Al-Roomi, Y. M.; Hussain, K. F. Antiscaling Properties of Novel Maleic-Anhydride Copolymers Prepared via Iron (II) - Chloride Mediated ATRP. *J. Appl. Polym. Sci.* **2014**, 131 (4). <https://doi.org/10.1002/app.39827>.
- (35) Lu, H.; Gu, Z.; Underwood, T.; Guo, B. The Development of Novel Laboratory Test Method on Evaluation of Scale Inhibition and Dispensancy for Downstream Water Treatment Applications; 2020.
- (36) Baugh, T. D.; Lee, J.; Winters, K.; Waters, J.; Wilcher, J. A Fast and Information-Rich Test Method for Scale Inhibitor Performance; OTC: Houston, Texas, USA, 2012. <https://doi.org/10.4043/23150-MS>.
- (37) Brooks, J.; Lu, H.; Barber, M. Kinetic Turbidity Test Method for Scale Inhibitor Evaluation on Multifunctional Scales; 2021.

- (38) Senthilmurugan, B.; Radhakrishnan, J. S.; Arana, V.; Al-Foudari, M. High Temperature Kinetic Scale Inhibitor for Flow Assurance Application. *International Journal of Petroleum Science and Technology* **2019**, *13*, 21–38.
- (39) Drela, I.; Falewicz, P.; Kuczkowska, S. New Rapid Test for Evaluation of Scale Inhibitors. *Water Research* **1998**, *32* (10), 3188–3191. [https://doi.org/10.1016/S0043-1354\(98\)00066-9](https://doi.org/10.1016/S0043-1354(98)00066-9).
- (40) Abd-El-Khalek, D. E.; Abd-El-Nabey, B. A.; Abdel-kawi, M. A.; Ebrahim, Sh.; Ramadan, S. R. The Inhibition of Crystal Growth of Gypsum and Barite Scales in Industrial Water Systems Using Green Antiscalant. *Water Supply* **2019**, *19* (7), 2140–2146. <https://doi.org/10.2166/ws.2019.094>.
- (41) Khamis, E.; Abd-El-Khalek, D. E.; Abdel-Kawi, M. A.; Anwar, J. M. New Application of Brown Sea Algae as an Alternative to Phosphorous-Containing Antiscalant. *Environmental Technology* **2020**, 1–10. <https://doi.org/10.1080/09593330.2020.1797898>.
- (42) Mady, M. F.; Rehman, A.; Kelland, M. A. Synthesis and Study of Modified Polyaspartic Acid Coupled Phosphonate and Sulfonate Moieties As Green Oilfield Scale Inhibitors. *Ind. Eng. Chem. Res.* **2021**, *60* (23), 8331–8339. <https://doi.org/10.1021/acs.iecr.1c01473>.
- (43) de Morais, S. C.; de Lima, D. F.; Ferreira, T. M.; Domingos, J. B.; de Souza, M. A. F.; Castro, B. B.; Balaban, R. de C. Effect of pH on the Efficiency of Sodium Hexametaphosphate as Calcium Carbonate Scale Inhibitor at High Temperature and High Pressure. *Desalination* **2020**, *491*, 114548. <https://doi.org/10.1016/j.desal.2020.114548>.
- (44) Fernandes, R. S.; Beserra, N. L. R.; Souza, M. A. F.; Lima, D. F.; Castro, B. B.; Balaban, R. C. Experimental and Theoretical Investigation of a Copolymer Combined with Surfactant for Preventing Scale Formation in Oil Wells. *Journal of Molecular Liquids* **2020**, *318*, 114036. <https://doi.org/10.1016/j.molliq.2020.114036>.
- (45) Senthilmurugan, B.; Ghosh, B.; Kundu, S. S.; Haroun, M.; Kameshwari, B. Maleic Acid Based Scale Inhibitors for Calcium Sulfate Scale Inhibition in High Temperature Application. *Journal of Petroleum Science and Engineering* **2010**, *75* (1–2), 189–195. <https://doi.org/10.1016/j.petrol.2010.11.002>.
- (46) Tube Blocking & Dynamic Scaling <http://scaledsolutions.co.uk/products-services/equipment-design-build/tube-blocking-rig/> (accessed 2020 -12 -14).
- (47) Mady, M. F.; Fevang, S.; Kelland, M. A. Study of Novel Aromatic Aminomethylenephosphonates as Oilfield Scale Inhibitors. *Energy Fuels* **2019**, *33* (1), 228–237. <https://doi.org/10.1021/acs.energyfuels.8b03531>.
- (48) Di Toto, R. A.; Bruyneel, F.; Parravicini, D.; Kan, A. T.; Tomson, M. B.; Yan, F. Development of the First Readily Biodegradable OECD 306 Phosphonated Amino Acid Chemistry for the Control of Calcium Carbonate and Calcium Sulphate in HTHP and UHT Unconventional Productions; Society of Petroleum Engineers: UK, 2018. <https://doi.org/10.2118/190733-MS>.

- (49) Kelland, M. A.; Mady, M. F.; Lima-Eriksen, R. Kidney Stone Prevention: Dynamic Testing of Edible Calcium Oxalate Scale Inhibitors. *Crystal Growth & Design* **2018**, *18* (12), 7441–7450. <https://doi.org/10.1021/acs.cgd.8b01173>.
- (50) Azizi, J.; Shadizadeh, S. R.; Khaksar Manshad, A.; Mohammadi, A. H. A Dynamic Method for Experimental Assessment of Scale Inhibitor Efficiency in Oil Recovery Process by Water Flooding. *Petroleum* **2019**, *5* (3), 303–314. <https://doi.org/10.1016/j.petlm.2018.07.004>.
- (51) Baraka-Lokmane, S.; Sorbie, K.; Poisson, N.; Kohler, N. Can Green Scale Inhibitors Replace Phosphonate Scale Inhibitors?: Carbonate Coreflooding Experiments. *Petroleum Science and Technology* **2009**, *27* (4), 427–441. <https://doi.org/10.1080/10916460701764605>.
- (52) Barber, M.; Heath, S. A New Approach to Testing Scale Inhibitors in Mild Scaling Brines – Are Dynamic Scale Loop Tests Needed?; SPE: USA, 2019. <https://doi.org/10.2118/193580-MS>.
- (53) Zeng, J.; Wang, F.; Zhou, C.; Gong, X. Molecular Dynamics Simulation on Scale Inhibition Mechanism of Polyepoxysuccinic Acid to Calcium Sulphate. *Chinese Journal of Chemical Physics* **2012**, *25* (2), 219–225. <https://doi.org/10.1088/1674-0068/25/02/219-225>.
- (54) Cui, C.; Zhang, S. Synthesis, Characterization and Performance Evaluation of an Environmentally Benign Scale Inhibitor IA/AMPS Co-Polymer. *New J. Chem.* **2019**, *43* (24), 9472–9482. <https://doi.org/10.1039/C9NJ01355E>.
- (55) Zhang, H.; Luo, X.; Lin, X.; Tang, P.; Lu, X.; Yang, M.; Tang, Y. Biodegradable Carboxymethyl Inulin as a Scale Inhibitor for Calcite Crystal Growth: Molecular Level Understanding. *Desalination* **2016**, *381*, 1–7. <https://doi.org/10.1016/j.desal.2015.11.029>.
- (56) OSPAR Commission <https://www.ospar.org/about> (accessed 2021 -07 -04).
- (57) Organisation for Economic Co-operation and Development. *Test No. 117: Partition Coefficient (n-Octanol/Water), HPLC Method*; OECD Publishing: Paris, 2004.
- (58) Studnik, H.; Liebsch, S.; Forlani, G.; Wiczorek, D.; Kafarski, P.; Lipok, J. Amino Polyphosphonates – Chemical Features and Practical Uses, Environmental Durability and Biodegradation. *New Biotechnology* **2015**, *32* (1), 1–6. <https://doi.org/10.1016/j.nbt.2014.06.007>.
- (59) Rott, E.; Steinmetz, H.; Metzger, J. W. Organophosphonates: A Review on Environmental Relevance, Biodegradability and Removal in Wastewater Treatment Plants. *Science of The Total Environment* **2018**, *615*, 1176–1191. <https://doi.org/10.1016/j.scitotenv.2017.09.223>.
- (60) Bolívar, G.; Colina, M.; Delgado, B.; Mendizabal, E. The Effect of Carboxymethyl Chitosan on Calcium Carbonate Precipitation in Synthetic Brines. *J. Mex. Chem. Soc.* **2021**, *65* (1). <https://doi.org/10.29356/jmcs.v65i1.1429>.

- (61) Zhu, A.; Chan-Park, Mary. B.; Dai, S.; Li, L. The Aggregation Behavior of O-Carboxymethylchitosan in Dilute Aqueous Solution. *Colloids and Surfaces B: Biointerfaces* **2005**, *43* (3–4), 143–149. <https://doi.org/10.1016/j.colsurfb.2005.04.009>.
- (62) Kean, T.; Thanou, M. Biodegradation, Biodistribution and Toxicity of Chitosan. *Advanced Drug Delivery Reviews* **2010**, *62* (1), 3–11. <https://doi.org/10.1016/j.addr.2009.09.004>.
- (63) Kumar, T.; Vishwanatham, S.; Kundu, S. S. A Laboratory Study on Pteroyl-L-Glutamic Acid as a Scale Prevention Inhibitor of Calcium Carbonate in Aqueous Solution of Synthetic Produced Water. *Journal of Petroleum Science and Engineering* **2010**, *71* (1–2), 1–7. <https://doi.org/10.1016/j.petrol.2009.11.014>.
- (64) Abdel-Gaber, A. M.; Abd-El-Nabey, B. A.; Khamis, E.; Abd-El-Khalek, D. E. Investigation of Fig Leaf Extract as a Novel Environmentally Friendly Antiscalent for CaCO₃ Calcareous Deposits. *Desalination* **2008**, *230* (1–3), 314–328. <https://doi.org/10.1016/j.desal.2007.12.005>.
- (65) Suharso; Buhani; Bahri, S.; Endaryanto, T. Gambier Extracts as an Inhibitor of Calcium Carbonate (CaCO₃) Scale Formation. *Desalination* **2011**, *265* (1–3), 102–106. <https://doi.org/10.1016/j.desal.2010.07.038>.
- (66) Barbosa, J. S.; Almeida Paz, F. A.; Braga, S. S. Bisphosphonates, Old Friends of Bones and New Trends in Clinics. *J. Med. Chem.* **2021**, *64* (3), 1260–1282. <https://doi.org/10.1021/acs.jmedchem.0c01292>.
- (67) Mady, M. F.; Rehman, A.; Kelland, M. A. Synthesis and Antiscalting Evaluation of Novel Hydroxybisphosphonates for Oilfield Applications. *ACS Omega* **2021**, *6* (9), 6488–6497. <https://doi.org/10.1021/acsomega.1c00379>.
- (68) Mady, M. F.; Kelland, M. A. Review of Nanotechnology Impacts on Oilfield Scale Management. *ACS Appl. Nano Mater.* **2020**, *3* (8), 7343–7364. <https://doi.org/10.1021/acsanm.0c01391>.
- (69) Ji-jiang, G.; Yang, W.; Gui-cai, Z.; Ping, J.; Mingqin, S. Investigation of Scale Inhibition Mechanisms Based on the Effect of HEDP on Surface Charge of Calcium Carbonate. *Tenside Surfactants Detergents* **2016**, *53* (1), 29–36. <https://doi.org/10.3139/113.110407>.
- (70) Casazza, B. A Process for the Preparation of Fosfomycin Salts. EP 1 762 573 A1, March 14, 2007.
- (71) Okada, M. Chemical Syntheses of Biodegradable Polymers. *Progress in Polymer Science* **2002**, *27* (1), 87–133. [https://doi.org/10.1016/S0079-6700\(01\)00039-9](https://doi.org/10.1016/S0079-6700(01)00039-9).
- (72) Irani, K. R. The Direct Synthesis of *α*-Aminomethylphosphonic Acids. Mannich-Type Reactions with Orthophosphorous Acid. *J. Org. Chem* **1966**, *31* (5), 1603–1607. <https://doi.org/10.1021/jo01343a067>.

- (73) Zakariyya, Q. L. Synthesis and Characterization of Modified Alendronic Acid as Environmentally Friendly Oilfield Scale Inhibitors. Bachelor's thesis, University of Stavanger, Stavanger, Norway, 2019.
- (74) Mady, M. F.; Kelland, M. A. Study on Various Readily Available Proteins as New Green Scale Inhibitors for Oilfield Scale Control. *Energy Fuels* **2017**, *31* (6), 5940–5947. <https://doi.org/10.1021/acs.energyfuels.7b00508>.
- (75) Mady, M. F.; Malmin, H.; Kelland, M. A. Sulfonated Nonpolymeric Aminophosphonate Scale Inhibitors—Improving the Compatibility and Biodegradability. *Energy Fuels* **2019**, *33* (7), 6197–6204. <https://doi.org/10.1021/acs.energyfuels.9b01032>.
- (76) Cacho, J.; Lopez-Molinero, A.; Guitart, A. Performance Comparison of Five Metallochromic Indicators for Barium. **1987**, *36* (3), 339–347. [https://doi.org/10.1016/0026-265X\(87\)90176-7](https://doi.org/10.1016/0026-265X(87)90176-7).
- (77) NACE International. *Laboratory Screening Test to Determine the Ability of Scale Inhibitors to Prevent the Precipitation of Barium Sulfate and/or Strontium Sulfate from Solution (for Oil and Gas Production Systems)*; NACE International: Houston, Tex., 2002.
- (78) D19 Committee. *Test Methods for Calcium and Magnesium In Water*; ASTM International. <https://doi.org/10.1520/D0511-14>.
- (79) *Standard Methods for the Examination of Water and Wastewater*, 18th ed.; Greenberg, A. E., American Public Health Association, American Water Works Association, Water Pollution Control Federation, Eds.; American Public Health Ass: Washington, 1992.
- (80) IS 2263 (1979): Methods of Preparation of Indicator Solutions. **1980**, 17.
- (81) Mady, M. F.; Charoensumran, P.; Ajiro, H.; Kelland, M. A. Synthesis and Characterization of Modified Aliphatic Polycarbonates as Environmentally Friendly Oilfield Scale Inhibitors. *Energy Fuels* **2018**, *32* (6), 6746–6755. <https://doi.org/10.1021/acs.energyfuels.8b01168>.
- (82) Amjad, Z. Investigations on the Evaluation of Polymeric Calcium Sulfate Dihydrate (Gypsum) Scale Inhibitors in the Presence of Phosphonates. *Desalination and Water Treatment* **2012**, *37* (1–3), 268–276. <https://doi.org/10.1080/19443994.2012.661282>.
- (83) Dogan, Ö.; Akyol, E.; Baris, S.; Öner, M. Control of Crystallization Processes by Diblock Copolymers. In *Advances in Crystal Growth Inhibition Technologies*; Amjad, Z., Ed.; Kluwer Academic Publishers: Boston, 2002; pp 197–205. https://doi.org/10.1007/0-306-46924-3_14.
- (84) Adam, U. S.; Robb, I. D. Adsorption and Exchange of Polyelectrolytes on Crystal Surfaces. *J. Chem. Soc., Faraday Trans. 1* **1983**, *79* (11), 2745. <https://doi.org/10.1039/f19837902745>.
- (85) Chen, J.; Xu, L.; Han, J.; Su, M.; Wu, Q. Synthesis of Modified Polyaspartic Acid and Evaluation of Its Scale Inhibition and Dispersion Capacity. *Desalination* **2015**, *358*, 42–48. <https://doi.org/10.1016/j.desal.2014.11.010>.

- (86) G.Ternan, N.; Mc Grath, J. W.; Mc Mullan, G.; Quinn, J. P. Review: Organophosphonates: Occurrence, Synthesis and Biodegradation by Microorganisms. *World Journal of Microbiology and Biotechnology* **1998**, *14* (5), 635–647. <https://doi.org/10.1023/A:1008848401799>.
- (87) Bergogne-Bérézin, E. Fosfomycin and Derivatives. In *Antimicrobial Agents*; Bryskier, A., Ed.; ASM Press: USA, 2014; pp 972–982. <https://doi.org/10.1128/9781555815929.ch37>.
- (88) Cao, Y. The Intriguing Biology and Chemistry of Fosfomycin: The Only Marketed Phosphonate Antibiotic. *RSC Advances* **2019**, *15*. <https://doi.org/10.1039/C9RA08299A>.
- (89) Keating, G. M. Fosfomycin Trometamol: A Review of Its Use as a Single-Dose Oral Treatment for Patients with Acute Lower Urinary Tract Infections and Pregnant Women with Asymptomatic Bacteriuria. *Drugs* **2013**, *73* (17), 1951–1966. <https://doi.org/10.1007/s40265-013-0143-y>.
- (90) Patel, S. S.; Balfour, J. A.; Bryson, H. M. Fosfomycin Tromethamine: A Review of Its Antibacterial Activity, Pharmacokinetic Properties and Therapeutic Efficacy as a Single-Dose Oral Treatment for Acute Uncomplicated Lower Urinary Tract Infections. *Drugs* **1997**, *53* (4), 637–656. <https://doi.org/10.2165/00003495-199753040-00007>.
- (91) Gledhill, W. E.; Feijtel, T. C. J. Environmental Properties and Safety Assessment of Organic Phosphonates Used for Detergent and Water Treatment Applications. In *Detergents*; Oude, N. T., Ed.; Springer Berlin Heidelberg: Berlin, Heidelberg, 1992; pp 261–285. https://doi.org/10.1007/978-3-540-47108-0_8.

8. APPENDIX A – NMR SPECTRA: PROJECT 1

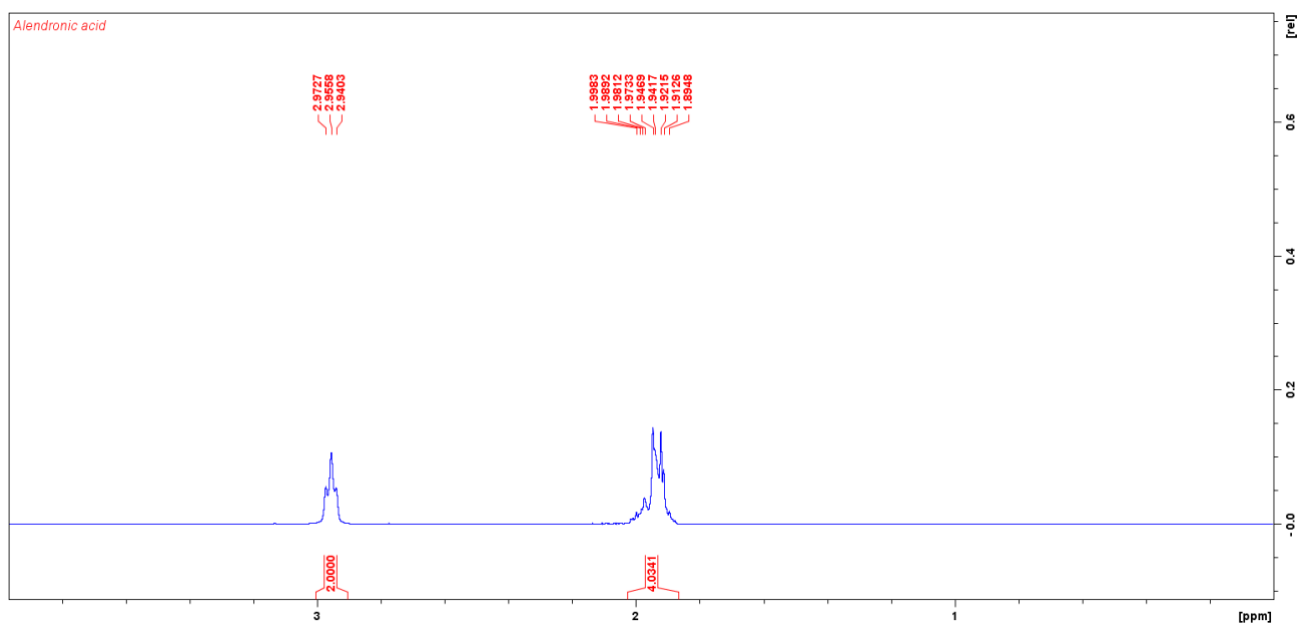


Figure 35. ^1H NMR for SI-1.

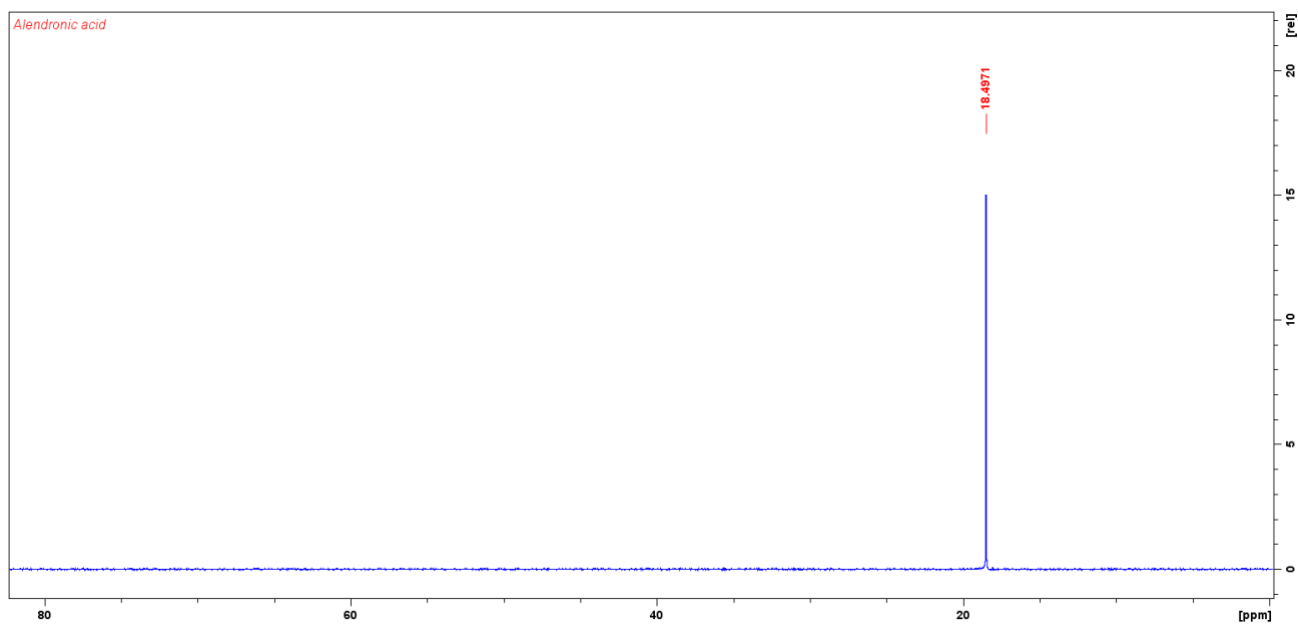


Figure 36. ^{31}P NMR for SI-1.

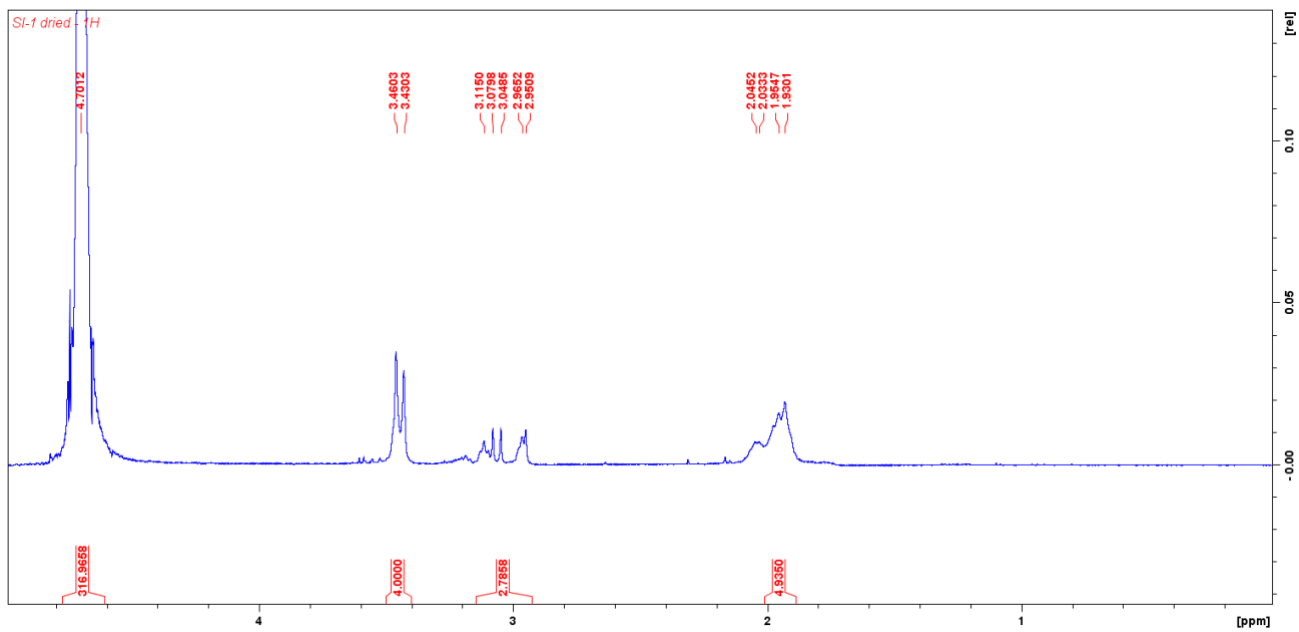


Figure 37. ^1H NMR spectra for SI-2.

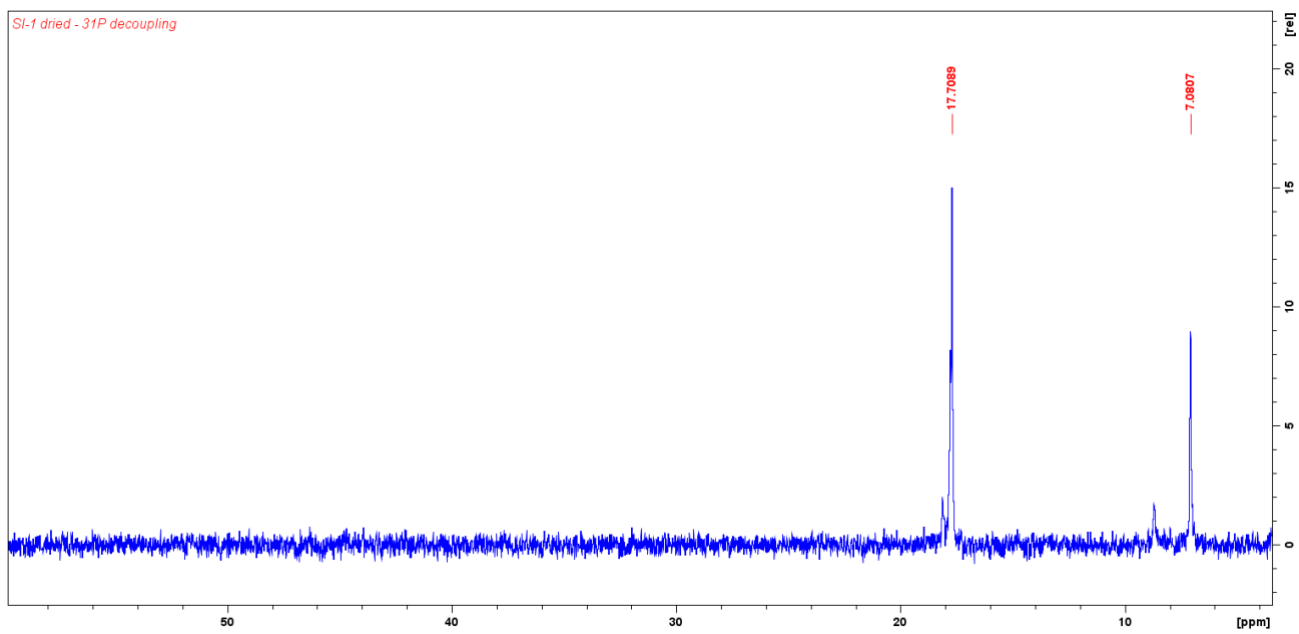


Figure 38. ^{31}P NMR spectra for SI-2.

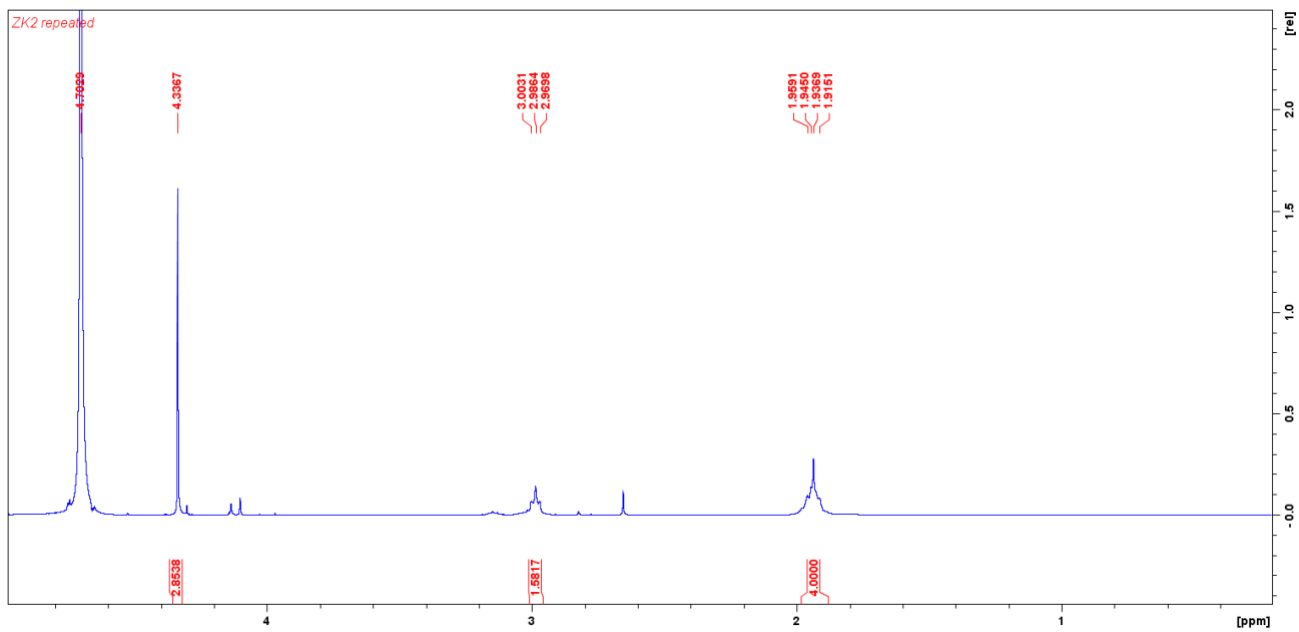


Figure 39. ^1H NMR spectra for SI-3.

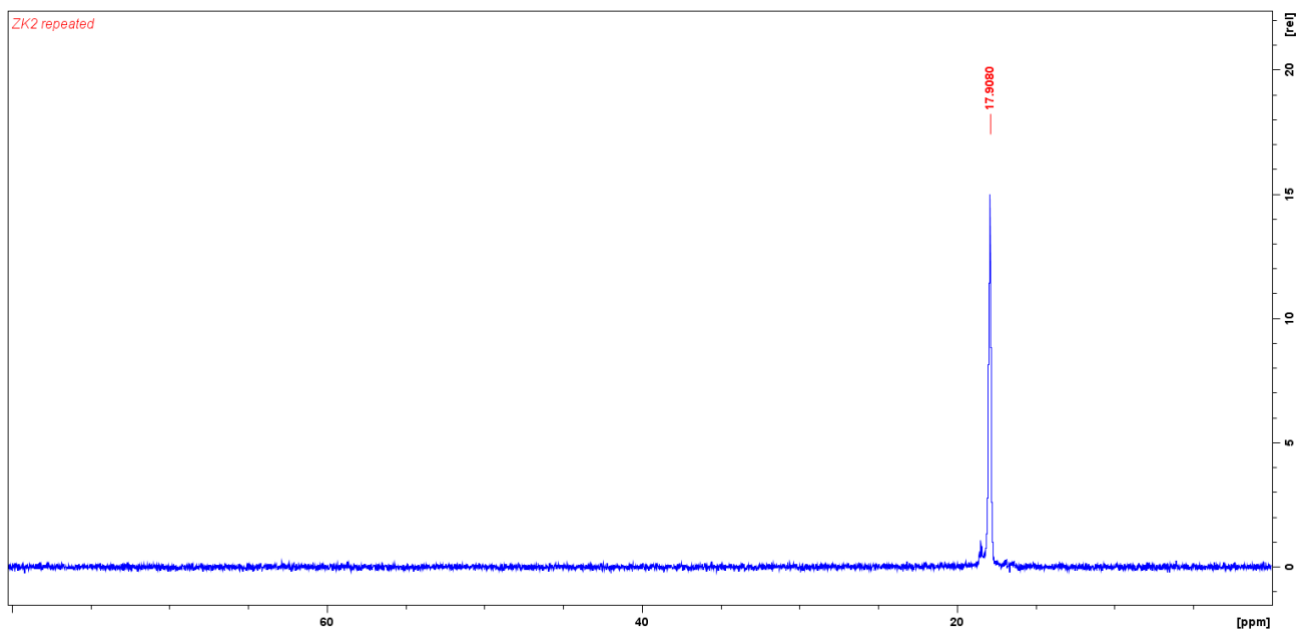


Figure 40. ^{31}P NMR spectra for SI-3.

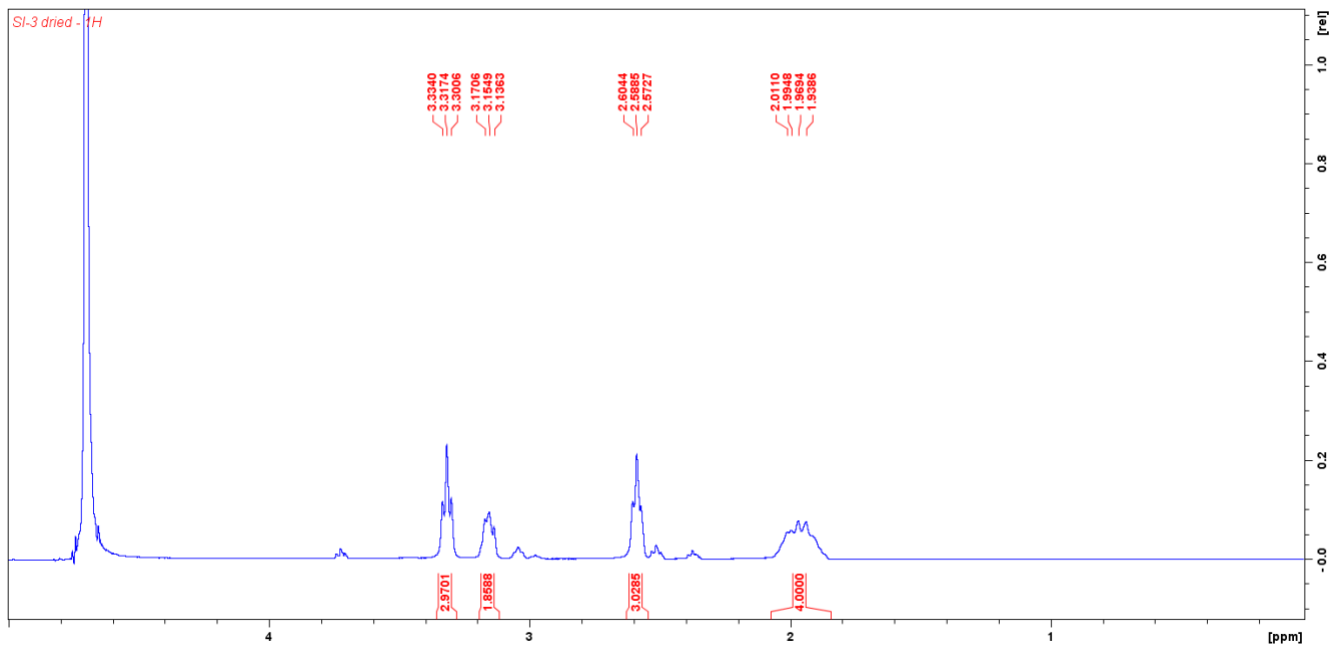


Figure 41. ^1H NMR for SI-4.

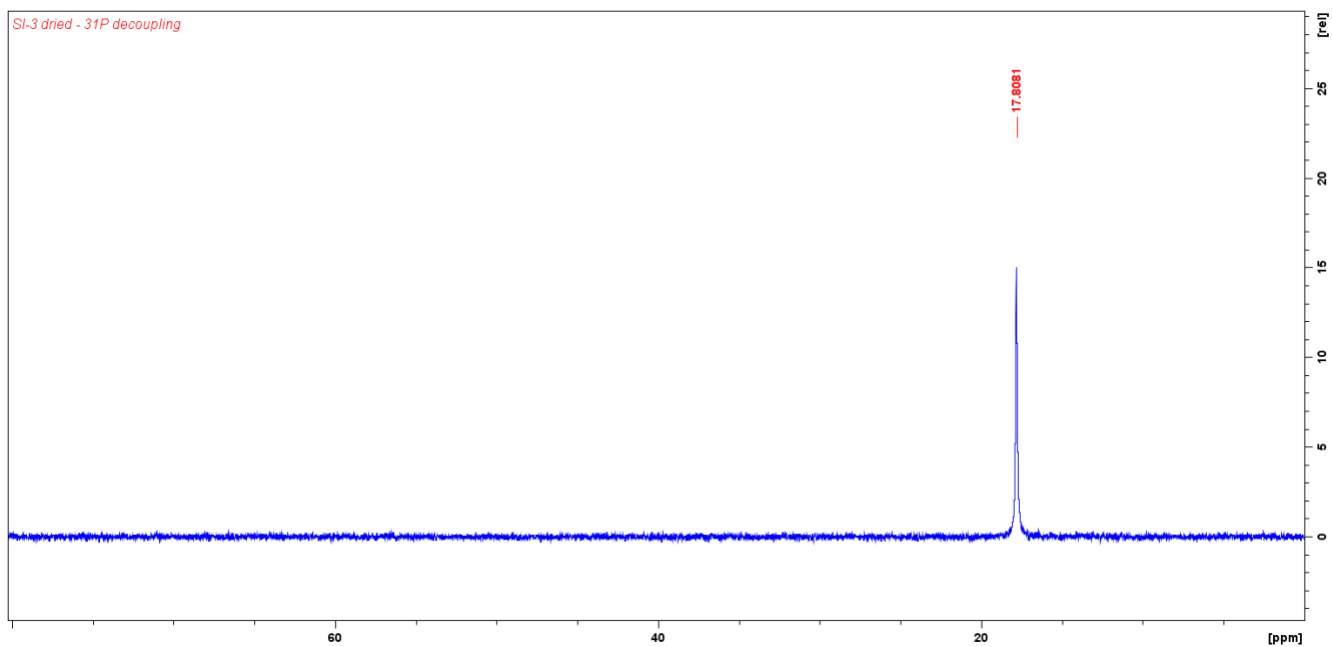


Figure 42. ^{31}P NMR for SI-4.

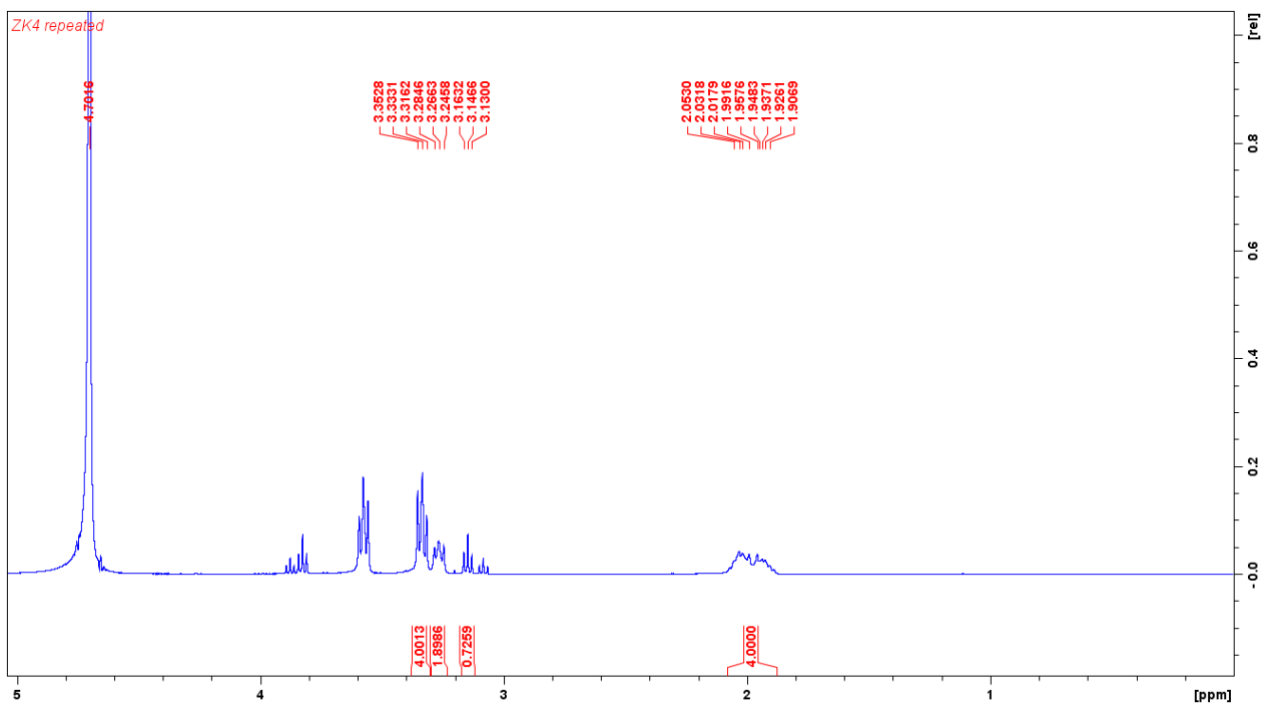


Figure 43. ^1H NMR for SI-5.

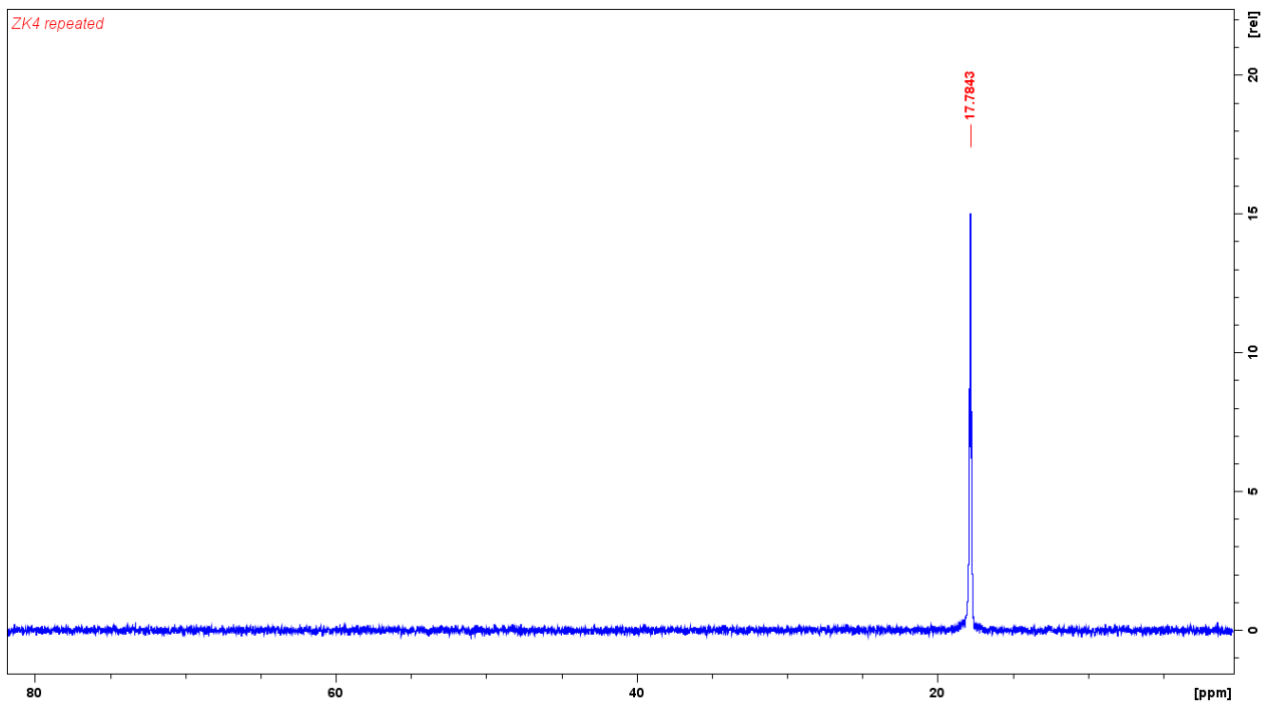


Figure 44. ^{31}P NMR for SI-5.

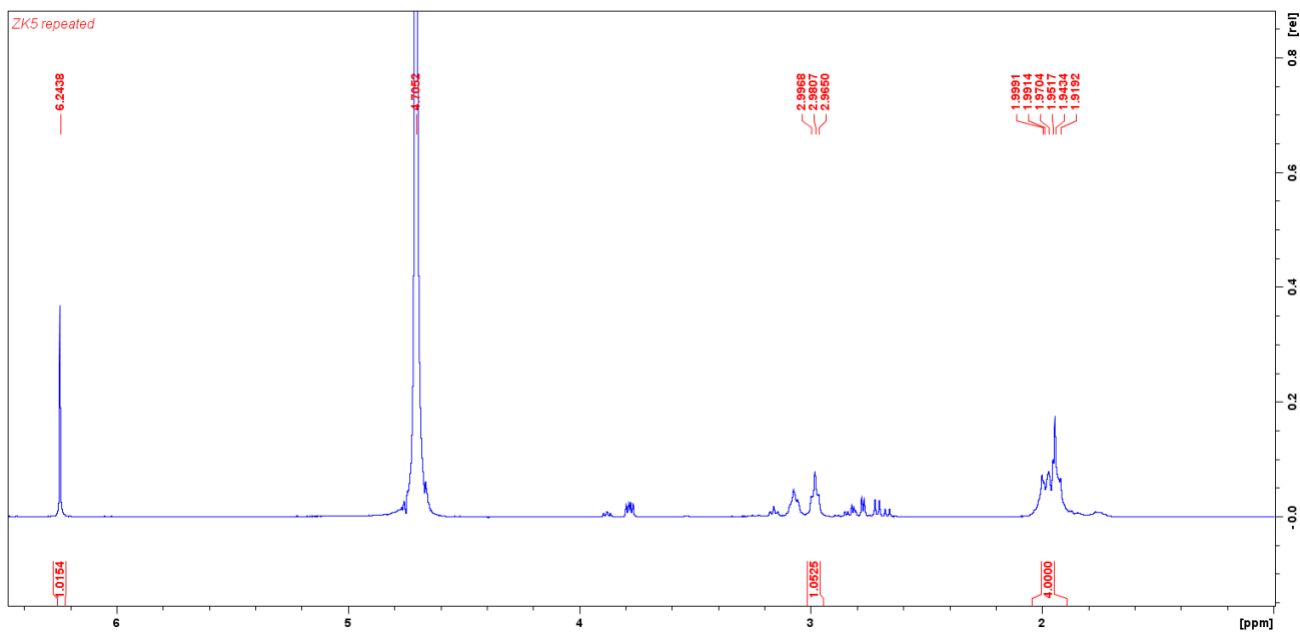


Figure 45. ^1H NMR for SI-6.

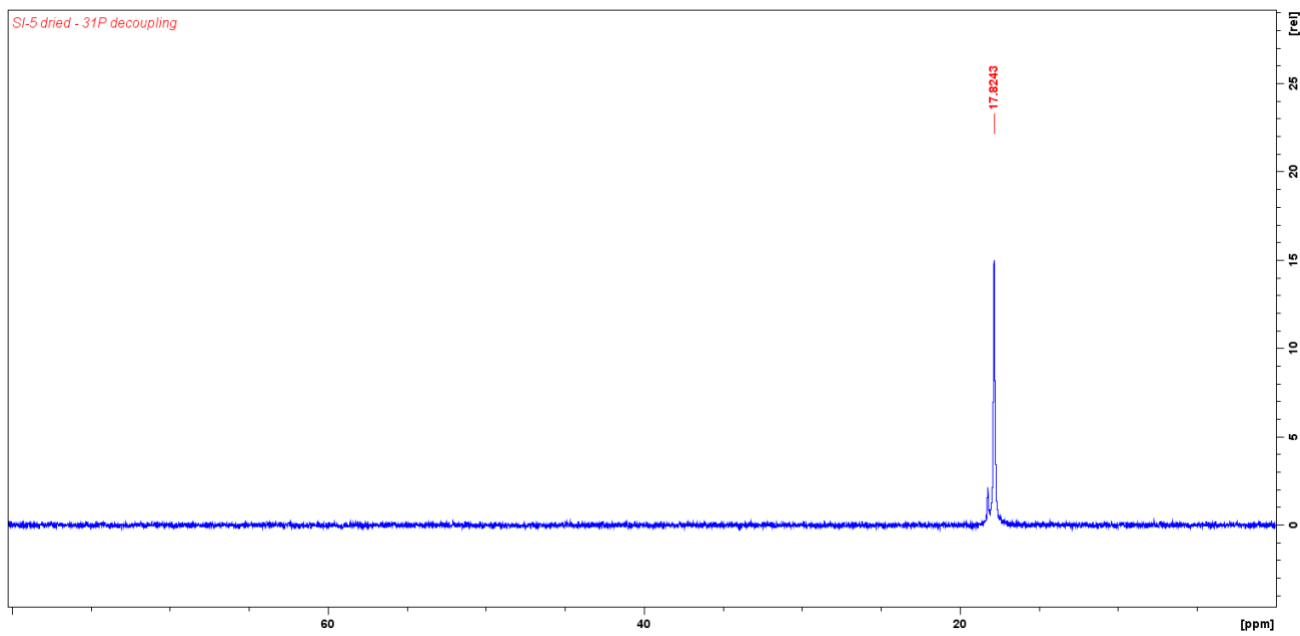


Figure 46. ^{31}P NMR for SI-6.

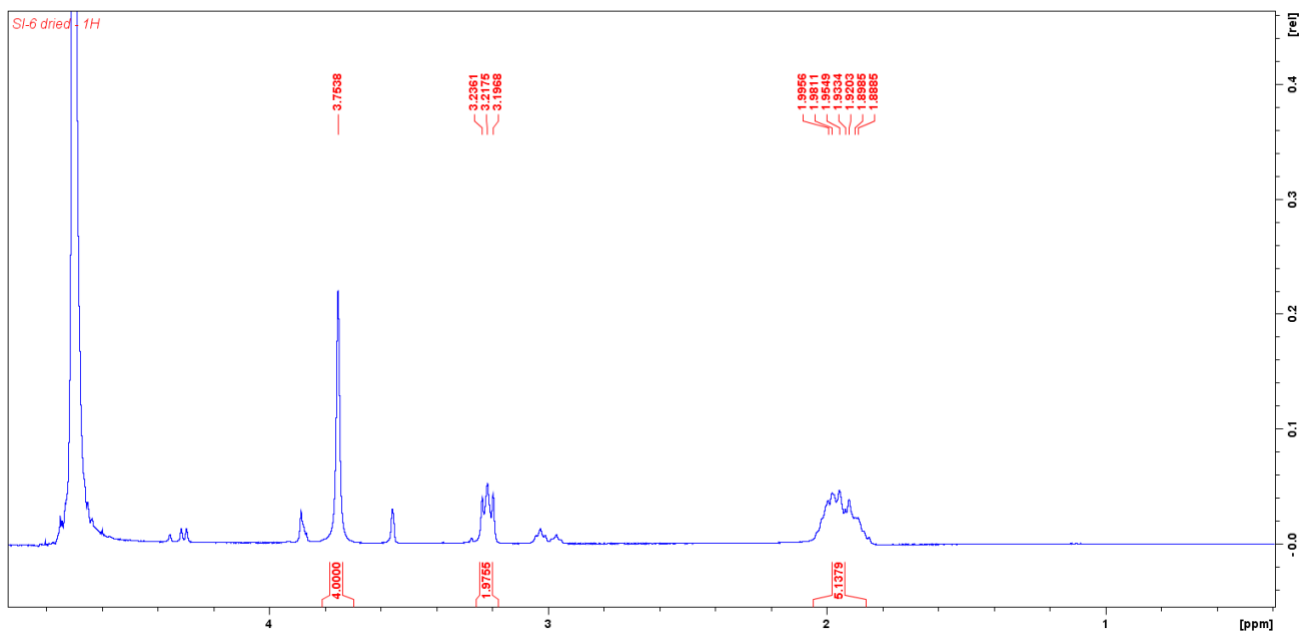


Figure 47. ^1H NMR for SI-7.

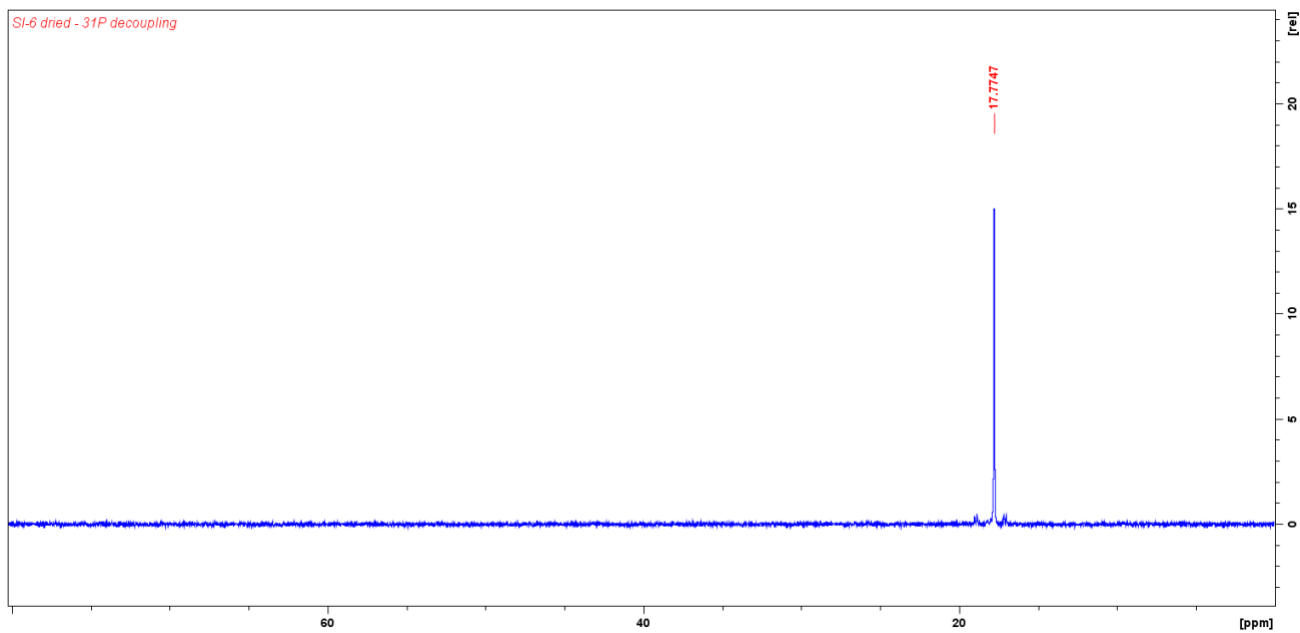


Figure 48. ^{31}P NMR for SI-7.

9. APPENDIX B – FTIR SPECTRA: PROJECT 1

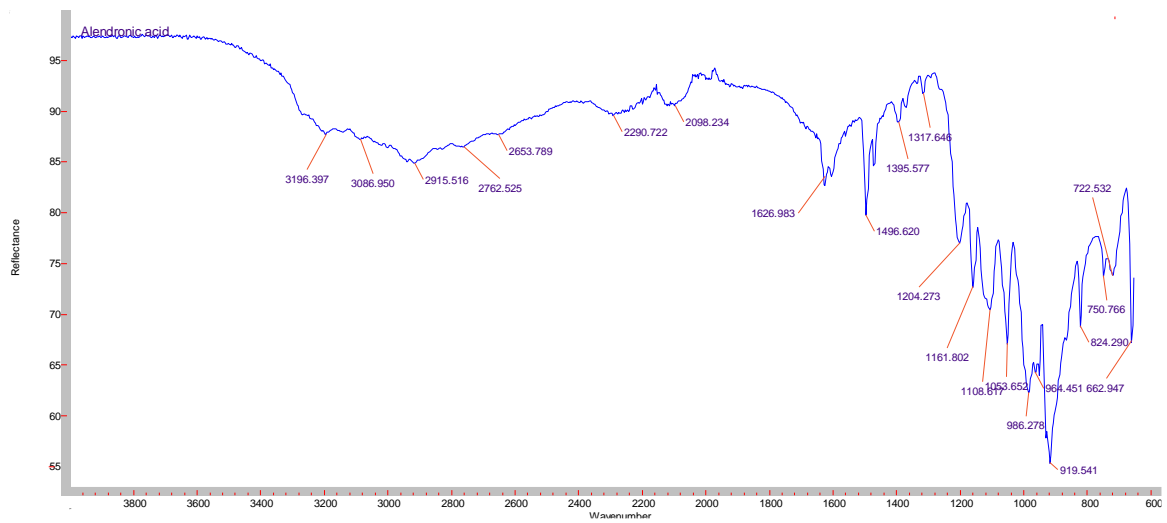


Figure 49. FTIR spectra for SI-1.

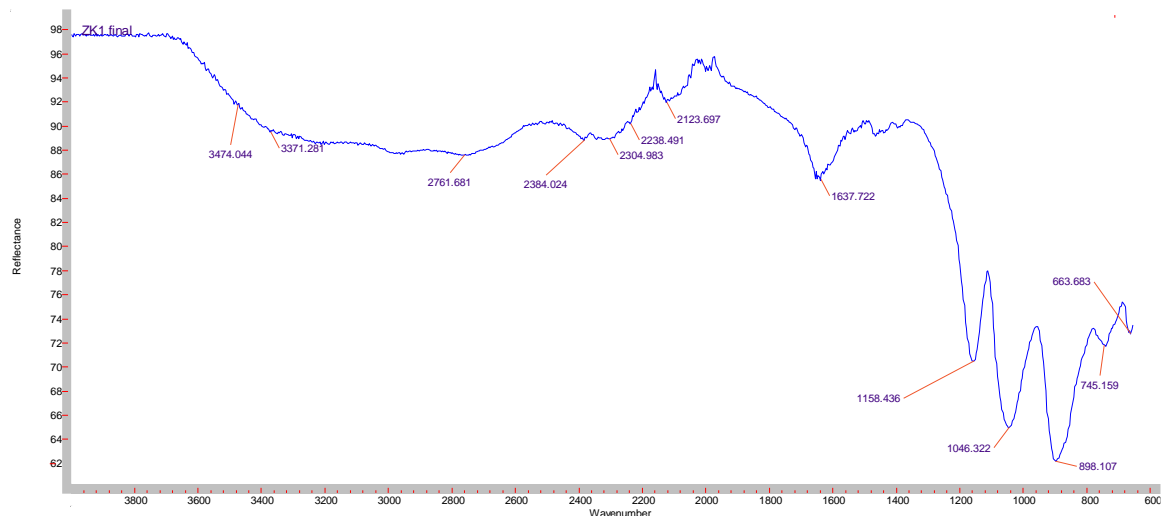


Figure 50. FTIR spectra for SI-2.

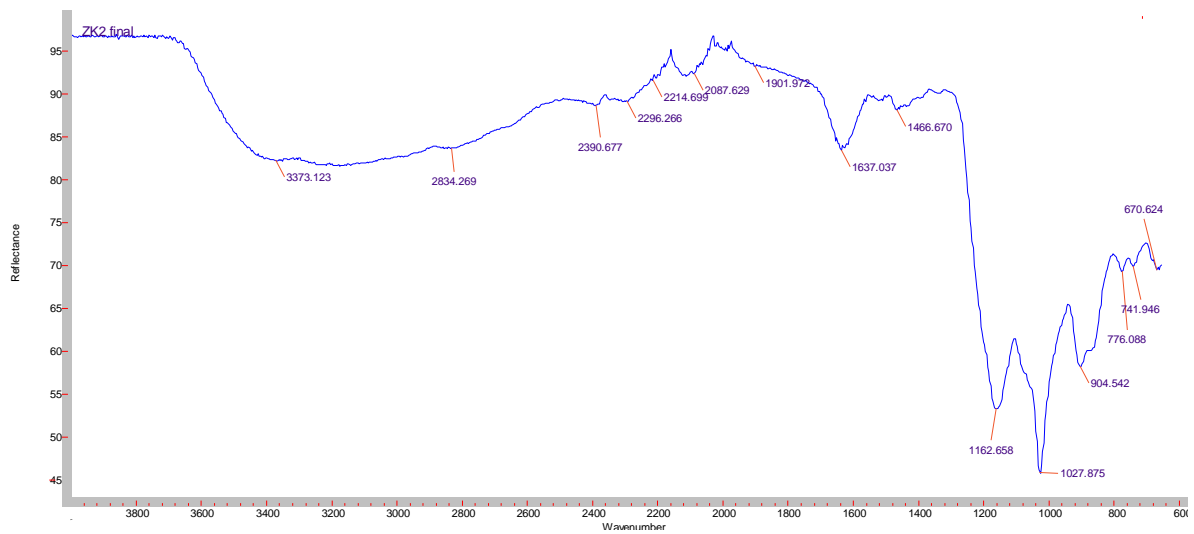


Figure 51. FTIR spectra for SI-3.

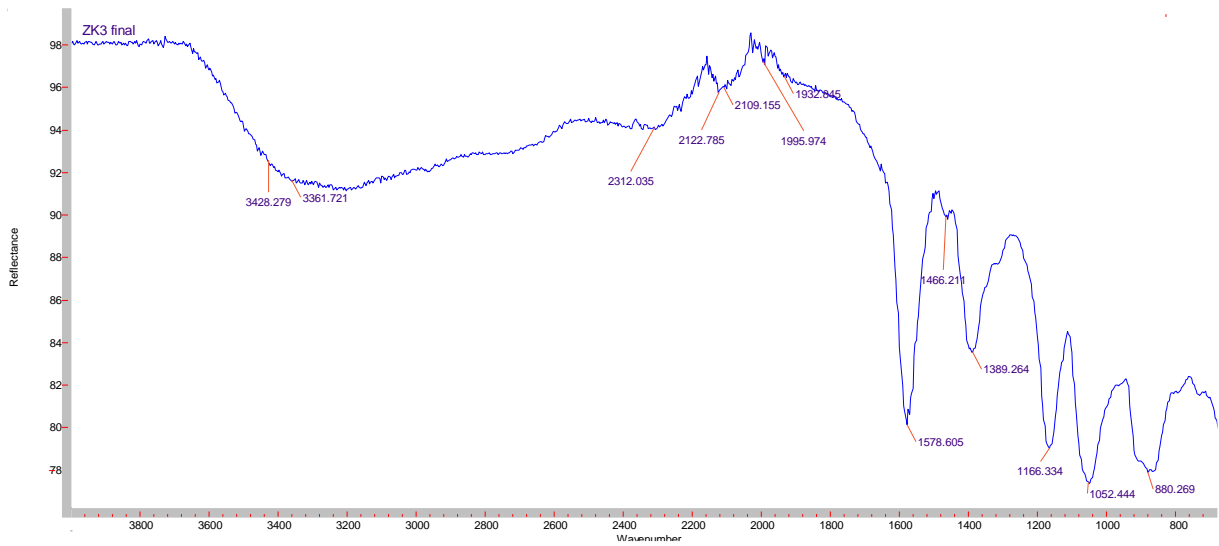


Figure 52. FTIR spectra for SI-4.

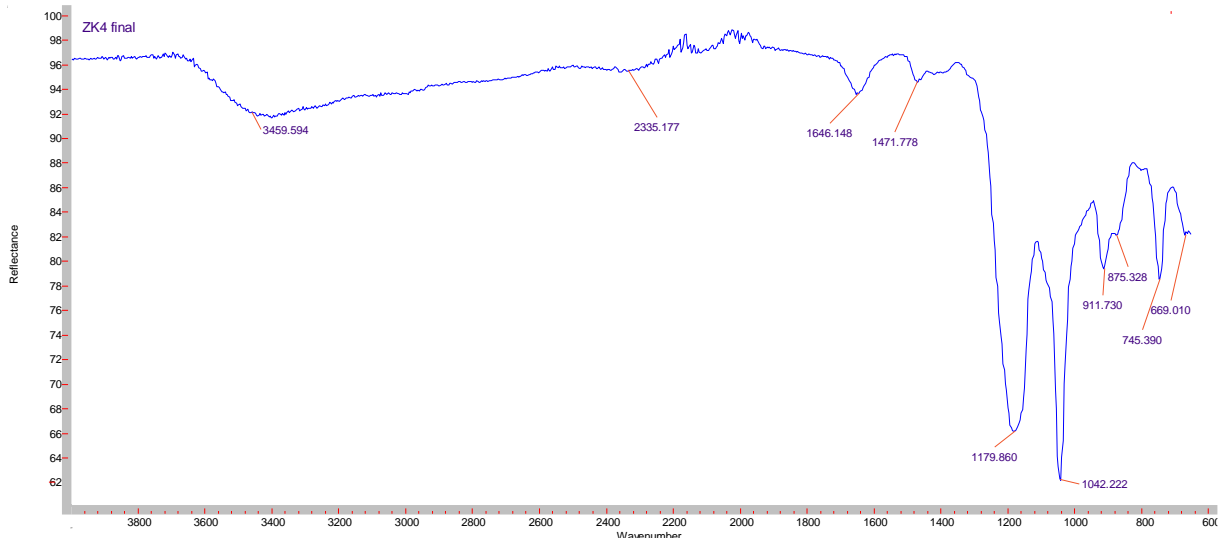


Figure 53. FTIR spectra for SI-5.

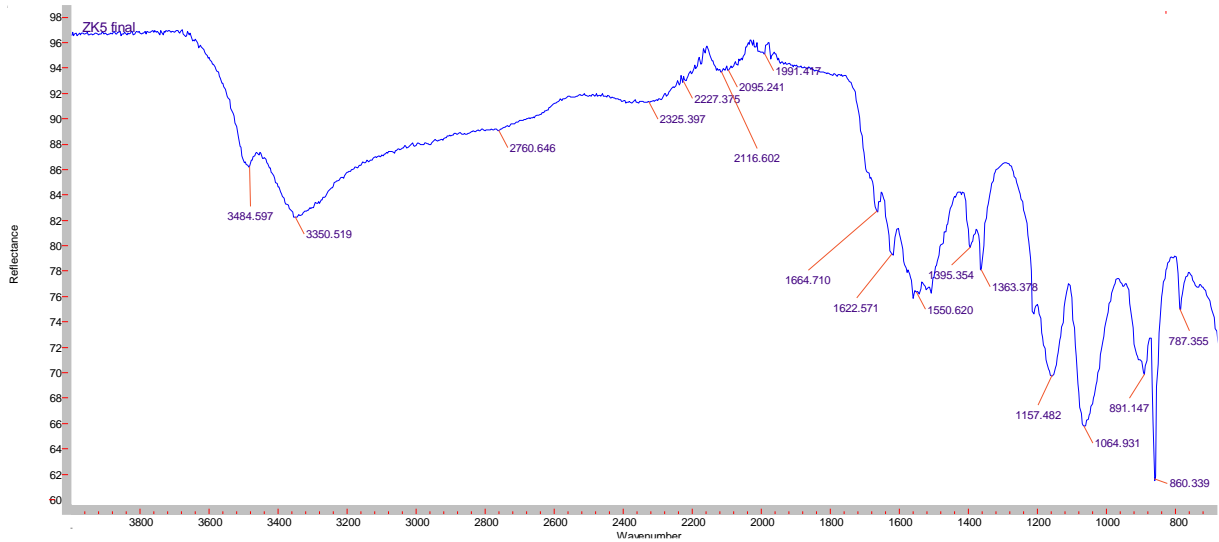


Figure 54. FTIR spectra for SI-6.

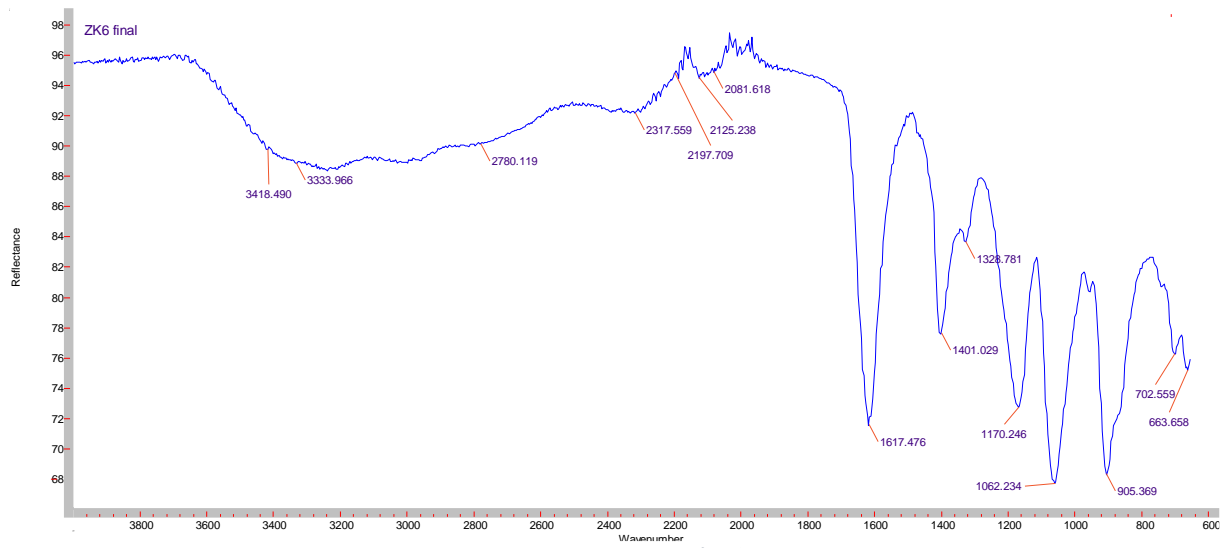


Figure 55. FTIR spectra for SI-7.

10. APPENDIX C – NUTRIENTS SOLUTIONS

a. Solution A*

Concentration (g/L)	Component
16.2	K ₂ HPO ₄
0.8	KH ₂ PO ₄

* - pH adjusted to 8.2.

b. Solution B

Concentration (g/L)	Component
25	NaNO ₃
0.6	NH ₄ Cl
0.2	EDTA
0.05	FeCl ₃

c. Solution C

Concentration (g/L)	Component
2.5	CaCl ₂
1.5	MgSO ₄

d. Solution D

Concentration (g/L)	Component
0.5	EDTA
0.5	MnSO ₄ .2H ₂ O
3	MgSO ₄ .7H ₂ O
1	NaCl
0.1	FeSO ₄ .7H ₂ O
0.1	CoCl ₂ .6H ₂ O
0.1	CaCl ₂ .6H ₂ O
0.1	ZnCl ₂
0.01	CuSO ₄ .5H ₂ O
0.02	NiCl ₂ .6H ₂ O
0.001	Na ₂ SeO ₃
0.01	AlK(SO ₄) ₂
0.01	H ₃ BO ₃
0.01	Na ₂ MoO ₄
0.01	Na ₂ WO ₄ .2H ₂ O

e. Amino Acids Solution

Amino acids are added from a commercially available solution, RPMI 1640 amino acids solution (50x). (<http://sigmaaldrich.com/catalog/product/sigma/r7131?lang=en®ion=NO>).

f. Vitamins Solution

Concentration (mg/L)	Component
20	Myoinositol
0.1	Thiamine Hydrochloride
0.1	Pyridoxine Hydrochloride
1	Nicotinic Acid
0.5	Glycine
0.01	Biotin
0.1	Folic Acid

11. APPENDIX D – STATIC BOTTLE TESTS RESULTS: PROJECT 1

Table 25. Standard gypsum static tests results - Project 1

	SI conc. (ppm)	EDTA titrated (mL)			Ca ²⁺ concentration (mg/L)			Ca ²⁺ conc. Average (mg/L)	% Inhibition			% Inhibition	
		Rep 1	Rep 2	Rep 3	Rep 1	Rep 2	Rep 3	CaCO ₃ retained in solution (mg/L)	Rep 1	Rep 2	Rep 3	Average	SD
PVS	100	3,75	3,75	3,75	1503,75	1503,75	1503,75	1504	98	98	98	98	0,10
	50	3,75	3,70	3,75	1503,75	1483,70	1503,75	1497	98	92	98	96	3,42
	20	3,70	3,75	3,70	1483,70	1503,75	1483,70	1490	93	98	93	95	2,99
	10	3,65	3,75	3,75	1463,65	1503,75	1503,75	1490	88	98	98	95	5,89
	5	3,65	3,70	3,75	1463,65	1483,70	1503,75	1484	88	92	98	93	5,14
	2	3,65	3,70	3,70	1463,65	1483,70	1483,70	1477	88	92	93	91	2,66
	1	3,65	3,70	3,65	1463,65	1483,70	1463,65	1470	88	92	87	89	2,74
	0	2,80	2,90	2,85	1122,80	1162,90	1142,85	1143	0	0	0	0	0,00
	0	3,75	3,80	3,75	1503,75	1523,80	1503,75	1510	-	-	-	-	-
ATMP	100	3,75	3,70	3,70	1503,75	1483,70	1483,70	1490	100	95	95	97	2,97
	50	3,70	3,65	3,70	1483,70	1463,65	1483,70	1477	95	89	95	93	3,26
	20	3,65	3,65	3,65	1463,65	1463,65	1463,65	1464	90	89	90	90	0,50
	10	3,65	3,60	3,60	1463,65	1443,60	1443,60	1450	90	84	85	87	3,41
	5	3,60	3,60	3,65	1443,60	1443,60	1463,65	1450	86	84	90	87	3,00
	2	3,60	3,60	3,65	1443,60	1443,60	1463,65	1450	86	84	90	87	3,00
	1	3,65	3,55	3,60	1463,65	1423,55	1443,60	1444	90	79	85	85	5,77
	0	2,70	2,80	2,75	1082,70	1122,80	1102,75	1103	0	0	0	0	0,00
	0	3,80	3,70	3,75	1523,8	1483,7	1503,75	1504	-	-	-	-	-
CMI	100	3,85	3,80	3,80	1543,85	1523,80	1523,80	1530	102	97	97	98	2,80
	50	3,75	3,80	3,75	1503,75	1523,80	1503,75	1510	92	97	92	94	2,60
	20	3,75	3,80	3,75	1503,75	1523,80	1503,75	1510	92	97	92	94	2,60
	10	3,70	3,75	3,70	1483,70	1503,75	1483,70	1490	88	92	87	89	2,40
	5	3,60	3,70	3,65	1443,60	1483,70	1463,65	1464	78	86	82	82	3,99
	2	3,55	3,60	3,60	1423,55	1443,60	1443,60	1437	74	76	77	76	1,82
	1	3,45	3,50	3,55	1383,45	1403,50	1423,55	1404	65	66	73	68	4,24
	0	2,75	2,85	2,80	1102,75	1142,85	1122,80	1123	0	0	0	0	0,00
	0	3,85	3,85	3,80	1543,85	1543,85	1523,80	1537	-	-	-	-	-
SI-1	100	4,05	4,10	4,05	1624,05	1644,10	1624,05	1631	99	103	99	100	2,44

	50	4,05	4,00	4,05	1624,05	1604,00	1624,05	1617	99	94	99	97	2,51
	20	4,00	4,00	4,05	1604,00	1604,00	1624,05	1611	95	94	99	96	2,44
	10	4,05	4,00	4,00	1624,05	1604,00	1604,00	1611	99	94	95	96	2,44
	5	3,85	3,85	3,90	1543,85	1543,85	1563,90	1551	82	81	86	83	2,62
	2	3,80	3,85	3,90	1523,80	1543,85	1563,90	1544	78	81	86	82	4,13
	1	3,75	3,80	3,75	1503,75	1523,80	1503,75	1510	74	77	74	75	1,83
	0	2,85	2,90	2,85	1142,85	1162,90	1142,85	1150	0	0	0	0	0,00
	0	4,00	4,10	4,10	1604,00	1644,10	1644,10	1630,73	-	-	-	-	-
SI-2	100	4,10	4,00	4,10	1644,10	1604,00	1644,10	1631	103	94	103	100	5,03
	50	4,00	4,10	4,05	1604,00	1644,10	1624,05	1624	95	103	99	99	4,13
	20	4,05	4,05	4,00	1624,05	1624,05	1604,00	1617	99	99	94	97	2,49
	10	4,05	4,00	4,00	1624,05	1604,00	1604,00	1611	99	94	94	96	2,62
	5	4,00	4,05	3,95	1604,00	1624,05	1583,95	1604	95	99	90	94	4,26
	2	3,95	4,00	4,00	1583,95	1604,00	1604,00	1597	91	94	94	93	1,95
	1	3,85	3,80	3,85	1543,85	1523,80	1543,85	1537	83	76	81	80	3,56
	0	2,80	2,95	2,90	1122,80	1182,95	1162,90	1156	0	0	0	0	0,00
	0	4,05	4,1	4,05	1624,05	1644,10	1624,05	1630,73	-	-	-	-	-
SI-2*	100	4,05	4,05	4,05	1624,05	1624,05	1624,05	1624	99	99	99	99	0,09
	50	4,05	4,05	4,00	1624,05	1624,05	1604,00	1617	99	99	94	97	2,49
	20	4,10	4,00	4,05	1644,10	1604,00	1624,05	1624	103	94	99	98	4,30
	10	4,10	4,05	4,00	1644,10	1624,05	1604,00	1624	103	99	94	98	4,17
	5	4,05	4,00	4,05	1624,05	1604,00	1624,05	1617	99	94	99	97	2,66
	2	4,05	4,00	4,05	1624,05	1604,00	1624,05	1617	99	94	99	97	2,66
	1	4,05	4,00	4,05	1624,05	1604,00	1624,05	1617	99	94	99	97	2,66
	0	2,80	2,95	2,90	1122,80	1182,95	1162,90	1156	0	0	0	0	0,00
	0	4,05	4,10	4,05	1624,05	1644,10	1624,05	1630,73	-	-	-	-	-
SI-3	100	3,80	3,75	3,75	1523,80	1503,75	1503,75	1510	103	99	99	100	2,41
	50	3,70	3,75	3,75	1483,70	1503,75	1503,75	1497	95	99	99	97	2,34
	20	3,55	3,60	3,60	1423,55	1443,60	1443,60	1437	82	86	86	85	2,03
	10	3,30	3,40	3,35	1323,30	1363,40	1343,35	1343	62	69	64	65	3,50
	5	3,05	3,10	3,10	1223,05	1243,10	1243,10	1236	41	43	43	42	1,02
	2	2,70	2,75	2,75	1082,70	1102,75	1102,75	1096	12	13	13	13	0,31
	1	2,70	2,75	2,75	1082,70	1102,75	1102,75	1096	12	13	13	13	0,31
	0	2,55	2,60	2,60	1022,55	1042,60	1042,60	1036	0	0	0	0	0,00

	0	3,75	3,75	3,80	1503,75	1503,75	1523,80	1510,43	-	-	-	-	-
SI-4	100	3,75	3,80	3,80	1503,75	1523,80	1523,80	1517	96	100	100	99	2,51
	50	3,75	3,80	3,80	1503,75	1523,80	1523,80	1517	96	100	100	99	2,51
	20	3,80	3,80	3,75	1523,80	1523,80	1503,75	1517	100	100	96	99	2,51
	10	3,80	3,75	3,80	1523,80	1503,75	1523,80	1517	100	96	100	99	2,41
	5	3,75	3,80	3,75	1503,75	1523,80	1503,75	1510	96	100	96	97	2,51
	2	3,80	3,80	3,70	1523,80	1523,80	1483,70	1510	100	100	91	97	5,02
	1	3,80	3,75	3,70	1523,80	1503,75	1483,70	1504	100	96	91	96	4,35
	0	2,65	2,60	2,65	1062,65	1042,60	1062,65	1056	0	0	0	0	0,00
	0	3,75	3,8	3,85	1503,75	1523,80	1543,85	1523,80	-	-	-	-	-
SI-5	100	4,10	4,15	4,20	1644,10	1664,15	1684,20	1664	91	95	99	95	3,80
	50	4,15	4,10	4,10	1664,15	1644,10	1644,10	1651	95	91	91	92	2,19
	20	4,00	4,10	4,00	1604,00	1644,10	1604,00	1617	84	91	84	86	4,38
	10	3,75	3,80	3,85	1503,75	1523,80	1543,85	1524	65	68	72	68	3,80
	5	3,25	3,35	3,35	1303,25	1343,35	1343,35	1330	27	34	34	32	4,38
	2	3,20	3,20	3,25	1283,20	1283,20	1303,25	1290	23	23	27	24	2,19
	1	3,00	3,15	3,15	1203,00	1263,15	1263,15	1243	8	19	19	15	6,58
	0	2,90	2,90	2,90	1162,90	1162,90	1162,90	1163	0	0	0	0	0,00
	0	4,20	4,25	4,20	1684,20	1704,25	1684,20	1690,88	-	-	-	-	-
SI-5*	100	4,00	4,05	4,10	1604,00	1624,05	1644,10	1624	84	88	91	88	3,35
	50	3,95	4,05	4,00	1583,95	1624,05	1604,00	1604	80	88	83	84	3,97
	20	3,65	3,60	3,65	1463,65	1443,60	1463,65	1457	59	56	55	57	1,66
	10	3,55	3,65	3,60	1423,55	1463,65	1443,60	1444	51	60	51	54	5,04
	5	3,20	3,15	3,20	1283,20	1263,15	1283,20	1277	26	25	20	23	3,16
	2	3,20	3,10	3,20	1283,20	1243,10	1283,20	1270	26	21	20	22	3,06
	1	3,15	3,15	3,15	1263,15	1263,15	1263,15	1263	22	25	16	21	4,57
	0	2,85	2,80	2,95	1142,85	1122,80	1182,95	1150	0	0	0	0	0,00
	0	4,20	4,25	4,20	1684,20	1704,25	1684,20	1690,88	-	-	-	-	-
SI-6	100	3,75	3,80	3,80	1503,75	1523,80	1523,80	1517	97	102	102	100	2,87
	50	3,80	3,75	3,80	1523,80	1503,75	1523,80	1517	102	97	102	100	2,73
	20	3,80	3,75	3,75	1523,80	1503,75	1503,75	1510	102	97	97	98	2,80
	10	3,70	3,75	3,75	1483,70	1503,75	1503,75	1497	92	97	97	95	3,07
	5	3,70	3,75	3,70	1483,70	1503,75	1483,70	1490	92	97	92	93	3,00
	2	3,65	3,70	3,70	1463,65	1483,70	1483,70	1477	86	92	92	90	3,29

	1	3,60	3,65	3,65	1443,60	1463,65	1463,65	1457	81	88	87	85	3,50
	0	2,80	2,70	2,75	1122,80	1082,70	1102,75	1103	0	0	0	0	0,00
	0	3,80	3,75	3,80	1523,80	1503,75	1523,80	1517,12	-	-	-	-	-
SI-7	100	3,80	3,80	3,75	1523,80	1523,80	1503,75	1517	100	100	95	98	2,62
	50	3,75	3,80	3,80	1503,75	1523,80	1523,80	1517	95	100	100	98	2,75
	20	3,80	3,75	3,75	1523,80	1503,75	1503,75	1510	100	96	95	97	2,52
	10	3,75	3,80	3,75	1503,75	1523,80	1503,75	1510	95	100	95	97	2,69
	5	3,80	3,75	3,75	1523,80	1503,75	1503,75	1510	100	96	95	97	2,52
	2	3,75	3,75	3,70	1503,75	1503,75	1483,70	1497	95	96	91	94	2,69
	1	3,75	3,70	3,75	1503,75	1483,70	1503,75	1497	95	92	95	94	2,13
	0	2,75	2,60	2,70	1102,75	1042,60	1082,70	1076	0	0	0	0	0,00
	0	3,75	3,80	3,85	1503,75	1523,80	1543,85	1523,80	-	-	-	-	-
SI-7*	100	4,00	4,05	4,00	1604,00	1624,05	1604,00	1611	98	103	98	100	2,82
	50	4,05	4,00	4,00	1624,05	1604,00	1604,00	1611	103	98	98	100	2,82
	20	4,00	4,05	4,00	1604,00	1624,05	1604,00	1611	98	103	98	100	2,82
	10	4,00	4,00	4,00	1604,00	1604,00	1604,00	1604	98	98	98	98	0,04
	5	4,00	4,00	4,00	1604,00	1604,00	1604,00	1604	98	98	98	98	0,04
	2	3,95	4,00	3,95	1583,95	1604,00	1583,95	1591	93	98	94	95	2,75
	1	3,85	3,90	3,80	1543,85	1563,90	1523,80	1544	84	89	80	84	4,43
	0	3,00	3,00	2,95	1203,00	1203,00	1182,95	1196	0	0	0	0	0,00
	0	4,00	4,00	4,05	1604,00	1604,00	1624,05	1610,68	-	-	-	-	-

Table 26. Standard calcite static test results - Project 1

	SI conc. (ppm)	EDTA titrated (mL)			Ca ²⁺ concentration (mg/L)			Ca ²⁺ conc. Average (mg/L)	% Inhibition			% Inhibition	
		Rep 1	Rep 2	Rep 3	Rep 1	Rep 2	Rep 3	CaCO ₃ retained in solution (mg/L)	Rep 1	Rep 2	Rep 3	Average	SD
PVS	100	4,00	4,05	4,05	1604,00	1624,05	1624,05	1617	95	98	98	97	1,54
	50	3,90	4,00	3,95	1563,90	1604,00	1583,95	1584	90	95	92	92	2,59
	20	3,75	3,70	3,75	1503,75	1483,70	1503,75	1497	81	77	80	79	2,50
	10	3,30	3,35	3,25	1323,30	1343,35	1303,25	1323	56	55	50	54	2,98
	5	3,15	3,10	3,10	1263,15	1243,10	1243,10	1250	48	40	42	43	4,12
	2	2,55	2,60	2,60	1022,55	1042,60	1042,60	1036	14	9	12	12	2,42
	1	2,40	2,50	2,50	962,40	1002,50	1002,50	989	6	3	6	5	1,58
	0	2,30	2,45	2,40	922,30	982,45	962,40	956	0	0	0	0	0,00
	0	4,00	4,10	4,15	1604,00	1644,10	1664,15	1637	-	-	-	-	-
ATMP	100	3,90	3,90	3,95	1563,90	1563,90	1583,95	1571	85	84	87	85	1,44
	50	3,65	3,60	3,65	1463,65	1443,60	1463,65	1457	72	67	70	70	2,22
	20	3,55	3,55	3,50	1423,55	1423,55	1403,50	1417	66	64	62	64	2,36
	10	3,45	3,45	3,40	1383,45	1383,45	1363,40	1377	61	59	56	59	2,50
	5	3,30	3,35	3,35	1323,30	1343,35	1343,35	1337	53	53	53	53	0,10
	2	3,30	3,30	3,25	1323,30	1323,30	1303,25	1317	53	50	48	50	2,72
	1	2,85	2,90	2,90	1142,85	1162,90	1162,90	1156	29	28	28	28	0,67
	0	2,30	2,40	2,40	922,30	962,40	962,40	949	0	0	0	0	0,00
	0	4,2	4,2	4,15	1684,2	1684,2	1664,15	1678	-	-	-	-	-
CMI	100	3,50	3,70	3,65	1403,50	1483,70	1463,65	1450	63	74	72	70	5,72
	50	3,50	3,35	3,45	1403,50	1343,35	1383,45	1377	63	53	61	59	5,14
	20	3,15	3,10	3,15	1263,15	1243,10	1263,15	1256	43	39	43	42	2,69
	10	3,10	3,05	3,05	1243,10	1223,05	1223,05	1230	40	36	38	38	2,39
	5	2,70	2,70	2,65	1082,70	1082,70	1062,65	1076	17	15	14	16	1,56
	2	2,65	2,60	2,60	1062,65	1042,60	1042,60	1049	14	9	12	12	2,76
	1	2,55	2,60	2,60	1022,55	1042,60	1042,60	1036	9	9	12	10	1,60
	0	2,40	2,45	2,40	962,40	982,45	962,40	969	0	0	0	0	0,00
	0	4,15	4,15	4,10	1664,15	1664,15	1644,10	1657	-	-	-	-	-
SI-1	100	3,75	3,80	3,75	1503,75	1523,80	1503,75	1510	76	77	74	76	1,38
	50	3,70	3,75	3,70	1483,70	1503,75	1483,70	1490	73	74	72	73	1,38
	20	3,50	3,55	3,55	1403,50	1423,55	1423,55	1417	63	63	63	63	0,40
	10	3,50	3,55	3,50	1403,50	1423,55	1403,50	1410	63	63	61	62	1,43

	5	3,20	3,20	3,20	1283,20	1283,20	1283,20	1283	47	44	44	45	1,69
	2	2,80	2,90	2,85	1122,80	1162,90	1142,85	1143	26	28	25	26	1,38
	1	2,55	2,55	2,55	1022,55	1022,55	1022,55	1023	13	8	8	10	2,76
	0	2,30	2,40	2,40	922,30	962,40	962,40	949	0	0	0	0	0,00
	0	4,20	4,25	4,20	1684,20	1704,25	1684,20	1690,88	-	-	-	-	-
SI-2	100	3,50	3,40	3,45	1403,50	1363,40	1383,45	1383	59	52	57	56	3,64
	50	3,35	3,35	3,35	1343,35	1343,35	1343,35	1343	50	49	52	50	1,39
	20	3,15	3,15	3,10	1263,15	1263,15	1243,10	1256	39	38	38	38	0,88
	10	3,05	3,05	3,05	1223,05	1223,05	1223,05	1223	34	32	35	34	1,86
	5	2,95	3,00	2,90	1182,95	1203,00	1162,90	1183	28	29	27	28	0,79
	2	2,45	2,50	2,50	982,45	1002,50	1002,50	996	0	0	5	2	3,15
	1	2,45	2,45	2,45	982,45	982,45	982,45	982	0	-3	3	0	2,81
	0	2,45	2,50	2,40	982,45	1002,50	962,40	982	0	0	0	0	0,00
	0	4,20	4,25	4,25	1684,20	1704,25	1704,25	1697,57	-	-	-	-	-
SI-2*	100	3,75	3,70	3,70	1503,75	1483,70	1483,70	1490	78	76	76	77	1,21
	50	3,50	3,50	3,50	1403,50	1403,50	1403,50	1404	63	64	65	64	1,10
	20	3,40	3,45	3,40	1363,40	1383,45	1363,40	1370	56	61	59	59	2,19
	10	3,35	3,35	3,30	1343,35	1343,35	1323,30	1337	53	55	53	54	0,88
	5	3,00	3,00	3,00	1203,00	1203,00	1203,00	1203	31	33	35	33	2,02
	2	2,75	2,75	2,70	1102,75	1102,75	1082,70	1096	16	18	18	17	1,35
	1	2,55	2,50	2,55	1022,55	1002,50	1022,55	1016	3	3	9	5	3,32
	0	2,50	2,45	2,40	1002,50	982,45	962,40	982	0	0	0	0	0,00
	0	4,05	4,10	4,15	1624,05	1644,10	1664,15	1644,10	-	-	-	-	-
SI-3	100	3,80	3,90	3,80	1523,80	1563,90	1523,80	1537	82	88	82	84	3,56
	50	3,60	3,60	3,65	1443,60	1443,60	1463,65	1450	71	71	73	71	1,23
	20	3,30	3,45	3,40	1323,30	1383,45	1363,40	1357	53	62	58	57	4,41
	10	3,05	3,10	3,10	1223,05	1243,10	1243,10	1236	38	41	39	40	1,48
	5	2,85	2,85	2,90	1142,85	1142,85	1162,90	1150	26	26	27	27	0,46
	2	2,70	2,65	2,70	1082,70	1062,65	1082,70	1076	18	15	15	16	1,59
	1	2,60	2,65	2,60	1042,60	1062,65	1042,60	1049	12	15	9	12	2,81
	0	2,40	2,40	2,45	962,40	962,40	982,45	969	0	0	0	0	0,00
	0	4,05	4,10	4,15	1624,05	1644,1	1664,15	1644,10	-	-	-	-	-
SI-4	100	3,75	3,75	3,80	1503,75	1503,75	1523,80	1510	81	81	84	82	1,45
	50	3,55	3,65	3,60	1423,55	1463,65	1443,60	1444	69	75	71	72	3,04

	20	3,40	3,50	3,45	1363,40	1403,50	1383,45	1383	60	66	62	63	3,07
	10	3,30	3,35	3,30	1323,30	1343,35	1323,30	1330	54	57	53	55	2,26
	5	3,25	3,25	3,20	1303,25	1303,25	1283,20	1297	51	51	46	49	2,66
	2	2,70	2,65	2,70	1082,70	1062,65	1082,70	1076	18	15	15	16	1,61
	1	2,40	2,45	2,45	962,40	982,45	982,45	976	0	3	0	1	1,73
	0	2,4	2,40	2,45	962,40	962,40	982,45	969	0	0	0	0	0,00
	0	4,15	4,05	4	1664,15	1624,05	1604	1630,73	-	-	-	-	-
SI-5	100	3,70	3,60	3,65	1483,70	1443,60	1463,65	1464	79	73	75	75	2,94
	50	3,60	3,60	3,65	1443,60	1443,60	1463,65	1450	73	73	75	74	1,26
	20	3,30	3,40	3,35	1323,30	1363,40	1343,35	1343	55	61	57	58	3,00
	10	2,90	2,90	2,95	1162,90	1162,90	1182,95	1170	32	32	33	32	0,55
	5	2,80	2,75	2,80	1122,80	1102,75	1122,80	1116	26	23	24	25	1,52
	2	2,55	2,55	2,50	1022,55	1022,55	1002,50	1016	12	12	6	10	3,26
	1	2,40	2,45	2,45	962,40	982,45	982,45	976	3	6	3	4	1,66
	0	2,35	2,35	2,40	942,35	942,35	962,40	949	0	0	0	0	0,00
0	4,15	4,00	4,05	1664,15	1604,00	1624,05	1630,73	-	-	-	-	-	
SI-5*	100	3,85	3,80	3,85	1543,85	1523,80	1543,85	1537	84	81	84	83	1,81
	50	3,75	3,70	3,75	1503,75	1483,70	1503,75	1497	79	75	78	77	1,87
	20	3,40	3,35	3,40	1363,40	1343,35	1363,40	1357	59	55	58	57	2,09
	10	3,00	3,05	2,95	1203,00	1223,05	1182,95	1203	36	38	32	35	3,07
	5	2,75	2,80	2,75	1102,75	1122,80	1102,75	1109	22	23	20	22	1,51
	2	2,40	2,45	2,45	962,40	982,45	982,45	976	3	3	3	3	0,05
	1	2,40	2,40	2,45	962,40	962,40	982,45	969	3	0	3	2	1,64
	0	2,35	2,40	2,40	942,35	962,40	962,40	956	0	0	0	0	0,00
0	4,10	4,15	4,15	1644,1	1664,15	1664,15	1657,47	-	-	-	-	-	
SI-6	100	3,65	3,65	3,70	1463,65	1463,65	1483,70	1470	74	74	76	75	1,53
	50	3,55	3,50	3,55	1423,55	1403,50	1423,55	1417	68	66	68	67	1,12
	20	3,35	3,40	3,35	1343,35	1363,40	1343,35	1350	56	60	56	57	2,38
	10	3,30	3,25	3,30	1323,30	1303,25	1323,30	1317	53	51	53	52	0,87
	5	3,10	3,10	3,05	1243,10	1243,10	1223,05	1236	41	43	38	41	2,34
	2	2,70	2,65	2,60	1082,70	1062,65	1042,60	1063	18	17	12	16	3,26
	1	2,45	2,50	2,50	982,45	1002,50	1002,50	996	3	9	6	6	2,82
	0	2,40	2,35	2,40	962,40	942,35	962,40	956	0	0	0	0	0,00
0	4,05	4,15	4,10	1624,05	1664,15	1644,1	1644,10	-	-	-	-	-	

SI-7	100	3,80	3,75	3,75	1523,80	1503,75	1503,75	1510	82	78	79	80	1,97
	50	3,65	3,65	3,65	1463,65	1463,65	1463,65	1464	73	72	73	72	0,49
	20	3,50	3,55	3,50	1403,50	1423,55	1403,50	1410	64	66	64	64	1,15
	10	3,45	3,50	3,45	1383,45	1403,50	1383,45	1390	61	63	61	61	1,09
	5	3,20	3,25	3,20	1283,20	1303,25	1283,20	1290	45	47	45	46	0,82
	2	2,75	2,80	2,80	1102,75	1122,80	1122,80	1116	18	19	21	19	1,61
	1	2,50	2,55	2,50	1002,50	1022,55	1002,50	1009	3	3	3	3	0,05
	0	2,45	2,50	2,45	982,45	1002,50	982,45	989	0	0	0	0	0,00
	0	4,05	4,15	4,1	1624,05	1664,15	1644,10	1644,10	-	-	-	-	-
SI-7*	100	3,50	3,55	3,50	1403,50	1423,55	1403,50	1410	68	70	68	69	1,21
	50	3,45	3,45	3,40	1383,45	1383,45	1363,40	1377	65	64	62	64	1,51
	20	3,40	3,40	3,35	1363,40	1363,40	1343,35	1357	62	61	59	61	1,50
	10	3,40	3,35	3,35	1363,40	1343,35	1343,35	1350	62	58	59	60	2,16
	5	3,25	3,35	3,30	1303,25	1343,35	1323,30	1323	53	58	56	56	2,38
	2	3,15	3,15	3,20	1263,15	1263,15	1283,20	1270	48	46	50	48	2,32
	1	3,15	3,10	3,10	1263,15	1243,10	1243,10	1250	48	43	45	45	2,36
	0	2,35	2,40	2,35	942,35	962,40	942,35	949	0	0	0	0	0,00
	0	4,00	4,10	4,00	1604,00	1644,10	1604	1617,37	-	-	-	-	-

Table 27. Heidrun calcite static test results - Project 1

	SI conc. (ppm)	EDTA titrated (mL)			Ca ²⁺ concentration (mg/L)			Ca ²⁺ conc. Average (mg/L)	% Inhibition			% Inhibition	
		Rep 1	Rep 2	Rep 3	Rep 1	Rep 2	Rep 3	CaCO ₃ retained in solution (mg/L)	Rep 1	Rep 2	Rep 3	Average	SD
PVS	100	5,15	5,15	5,15	1032,58	1032,58	1032,58	1033	99	99	98	99	0,12
	50	5,10	5,15	5,15	1022,55	1032,58	1032,58	1029	94	99	98	97	2,91
	20	5,15	5,10	5,15	1032,58	1022,55	1032,58	1029	99	93	98	97	3,14
	10	5,10	5,05	5,15	1022,55	1012,53	1032,58	1023	94	88	98	93	5,40
	5	5,05	5,10	5,15	1012,53	1022,55	1032,58	1023	88	93	98	93	5,08
	2	4,60	4,75	4,70	922,30	952,38	942,35	939	42	55	43	46	7,24
	1	4,40	4,55	4,40	882,20	912,28	882,20	892	21	33	6	20	13,38
	0	4,20	4,25	4,35	842,10	852,13	872,18	855	0	0	0	0	0,00
	0	5,15	5,25	5,10	1032,58	1052,63	1022,55	1035,92	-	-	-	-	-
ATMP	100	5,15	5,20	5,15	1032,58	1042,60	1032,58	1036	89	93	88	90	2,64
	50	5,10	5,20	5,10	1022,55	1042,60	1022,55	1029	84	93	83	87	5,57
	20	5,25	5,25	5,20	1052,63	1052,63	1042,60	1049	99	99	94	97	3,00
	10	5,30	5,25	5,20	1062,65	1052,63	1042,60	1053	104	99	94	99	5,10
	5	5,20	5,30	5,25	1042,60	1062,65	1052,63	1053	94	104	99	99	5,14
	2	5,10	5,15	5,10	1022,55	1032,58	1022,55	1026	84	88	83	85	2,42
	1	4,80	4,70	4,80	962,40	942,35	962,40	956	54	38	52	48	8,61
	0	4,25	4,35	4,30	852,13	872,18	862,15	862	0	0	0	0	0,00
	0	5,25	5,35	5,25	1052,63	1072,68	1052,63	1055,13	-	-	-	-	-
CMI	100	5,15	5,20	5,15	1032,58	1042,60	1032,58	1036	99	104	99	100	3,02
	50	5,10	5,15	5,10	1022,55	1032,58	1022,55	1026	93	99	94	95	3,11
	20	5,05	5,05	5,05	1012,53	1012,53	1012,53	1013	88	88	88	88	0,37
	10	4,90	5,05	4,95	982,45	1012,53	992,48	996	71	88	78	79	8,61
	5	5,15	5,15	5,10	1032,58	1032,58	1022,55	1029	99	99	94	97	2,98
	2	5,10	5,00	5,10	1022,55	1002,50	1022,55	1016	93	83	94	90	5,90
	1	4,40	4,60	4,45	882,20	922,30	892,23	899	16	42	26	28	12,68
	0	4,25	4,20	4,20	852,13	842,10	842,10	845	0	0	0	0	0,00
	0	5,15	5,25	5,10	1032,58	1052,63	1022,55	1035	-	-	-	-	-
SI-1	100	5,15	5,15	5,10	1032,58	1032,58	1022,55	1029	100	100	95	98	2,89
	50	5,10	5,10	5,15	1022,55	1022,55	1032,58	1026	95	95	100	97	2,82
	20	5,10	5,10	5,15	1022,55	1022,55	1032,58	1026	95	95	100	97	2,82
	10	5,05	5,10	5,10	1012,53	1022,55	1022,55	1019	90	95	95	93	2,96

	5	5,10	5,05	5,05	1022,55	1012,53	1012,53	1016	95	90	90	92	2,76
	2	5,00	5,05	5,00	1002,50	1012,53	1002,50	1006	85	90	85	87	3,16
	1	4,95	5,00	4,95	992,48	1002,50	992,48	996	80	86	80	82	3,30
	0	4,15	4,10	4,15	832,08	822,05	832,08	829	0	0	0	0	0,00
	0	5,10	5,15	5,20	1022,55	1032,58	1042,60	1032,58	-	-	-	-	-
SI-2	100	5,05	5,00	5,00	1012,53	1002,50	1002,50	1006	93	87	86	88	3,83
	50	4,95	4,95	5,00	992,48	992,48	1002,50	996	82	81	86	83	2,61
	20	4,85	4,80	4,90	972,43	962,40	982,45	972	71	63	73	69	5,20
	10	4,80	4,85	4,80	962,40	972,43	962,40	966	65	69	61	65	4,01
	5	4,85	4,75	4,80	972,43	952,38	962,40	962	71	58	61	63	6,84
	2	4,70	4,75	4,70	942,35	952,38	942,35	946	55	58	49	54	4,41
	1	4,50	4,60	4,55	902,25	922,30	912,28	912	33	40	31	35	5,14
	0	4,20	4,25	4,30	842,10	852,13	862,15	852	0	0	0	0	0,00
	0	5,10	5,15	5,10	1022,55	1032,58	1022,55	1025,89	-	-	-	-	-
SI-2*	100	2,70	2,65	2,65	1082,70	1062,65	1062,65	1069	87	77	79	81	5,11
	50	2,65	2,60	2,60	1062,65	1042,60	1042,60	1049	77	68	71	72	4,97
	20	2,60	2,60	2,65	1042,60	1042,60	1062,65	1049	68	68	79	72	6,74
	10	2,60	2,60	2,55	1042,60	1042,60	1022,55	1036	68	68	62	66	3,45
	5	2,55	2,60	2,55	1022,55	1042,60	1022,55	1029	58	68	62	63	4,88
	2	2,50	2,50	2,50	1002,50	1002,50	1002,50	1003	48	48	53	50	2,63
	1	2,50	2,45	2,45	1002,50	982,45	982,45	989	48	39	44	44	4,85
	0	2,25	2,25	2,20	902,25	902,25	882,20	896	0	0	0	0	0,00
	0	2,75	2,80	2,75	1102,75	1122,80	1102,75	1109,43	-	-	-	-	-
SI-3	100	5,15	5,10	5,20	1032,58	1022,55	1042,60	1033	100	95	105	100	5,13
	50	5,10	5,15	5,15	1022,55	1032,58	1032,58	1029	95	100	100	98	2,75
	20	5,15	5,10	5,15	1032,58	1022,55	1032,58	1029	100	95	100	98	2,89
	10	5,00	5,15	5,20	1002,50	1032,58	1042,60	1026	86	100	105	97	10,12
	5	4,80	4,95	4,85	962,40	992,48	972,43	976	67	80	68	72	7,24
	2	4,75	4,80	4,60	952,38	962,40	922,30	946	62	65	42	56	12,42
	1	4,25	4,15	4,20	852,13	832,08	842,10	842	14	0	0	5	8,25
	0	4,10	4,15	4,20	822,05	832,08	842,10	832	0	0	0	0	0,00
			5,20	5,10	5,15	1042,60	1022,55	1032,58	1032,58	-	-	-	-
SI-4	100	5,25	5,15	5,15	1052,63	1032,58	1032,58	1039	100	90	90	94	5,50
	50	5,15	5,15	5,20	1032,58	1032,58	1042,60	1036	90	90	95	92	2,90

	20	5,15	5,15	5,15	1032,58	1032,58	1032,58	1033	90	90	90	90	0,27
	10	5,15	5,10	5,15	1032,58	1022,55	1032,58	1029	90	86	90	89	2,62
	5	4,90	5,10	5,05	982,45	1022,55	1012,53	1006	65	86	81	77	10,85
	2	4,65	4,60	4,55	932,33	922,30	912,28	922	40	38	33	37	3,43
	1	4,50	4,60	4,65	902,25	922,30	932,33	919	25	38	43	35	9,25
	0	4,25	4,20	4,20	852,13	842,10	842,10	845	0	0	0	0	0,00
	0	5,20	5,25	5,30	1042,60	1052,63	1062,65	1052,63	-	-	-	-	-
SI-5	100	5,05	5,15	5,15	1012,53	1032,58	1032,58	1026	93	103	103	100	5,73
	50	5,15	5,10	5,10	1032,58	1022,55	1022,55	1026	103	98	98	100	2,86
	20	5,05	5,15	5,10	1012,53	1032,58	1022,55	1023	93	103	98	98	4,92
	10	5,10	5,15	5,05	1022,55	1032,58	1012,53	1023	98	103	93	98	5,09
	5	4,65	4,70	4,60	932,33	942,35	922,30	932	54	59	47	53	6,28
	2	4,40	4,35	4,50	882,20	872,18	902,25	886	30	25	36	30	5,83
	1	4,35	4,30	4,35	872,18	862,15	872,18	869	25	20	21	22	2,60
	0	4,10	4,10	4,15	822,05	822,05	832,08	825	0	0	0	0	0,00
	0	5,10	5,05	5,20	1022,55	1012,53	1042,60	1025,89	-	-	-	-	-
SI-5*	100	2,75	2,70	2,75	1102,75	1082,70	1102,75	1096	100	91	100	97	5,25
	50	2,75	2,70	2,75	1102,75	1082,70	1102,75	1096	100	91	100	97	5,25
	20	2,75	2,70	2,75	1102,75	1082,70	1102,75	1096	100	91	100	97	5,25
	10	2,70	2,70	2,75	1082,70	1082,70	1102,75	1089	92	91	100	94	5,04
	5	2,45	2,55	2,50	982,45	1022,55	1002,50	1003	50	64	55	56	6,94
	2	2,35	2,45	2,40	942,35	982,45	962,40	962	33	45	36	38	6,31
	1	2,35	2,40	2,35	942,35	962,40	942,35	949	33	36	27	32	4,63
	0	2,15	2,20	2,20	862,15	882,20	882,20	876	0	0	0	0	0,00
	0	2,75	2,80	2,70	1102,75	1122,80	1082,70	1102,75	-	-	-	-	-
SI-6	100	5,15	5,10	5,10	1032,58	1022,55	1022,55	1026	103	98	98	100	2,86
	50	5,10	5,10	5,15	1022,55	1022,55	1032,58	1026	98	98	103	100	2,94
	20	5,10	5,10	5,10	1022,55	1022,55	1022,55	1023	98	98	98	98	0,05
	10	5,05	5,05	5,10	1012,53	1012,53	1022,55	1016	93	93	98	95	2,79
	5	5,05	5,10	5,00	1012,53	1022,55	1002,50	1013	93	98	88	93	5,22
	2	4,60	4,60	4,55	922,30	922,30	912,28	919	49	49	41	47	4,50
	1	4,55	4,45	4,55	912,28	892,23	912,28	906	44	34	41	40	5,06
	0	4,10	4,10	4,15	822,05	822,05	832,08	825	0	0	0	0	0,00
	0	5,10	5,05	5,20	1022,55	1012,53	1042,60	1025,89	-	-	-	-	-

SI-7	100	5,20	5,15	5,20	1042,60	1032,58	1042,60	1039	102	97	102	100	2,75
	50	5,15	5,15	5,15	1032,58	1032,58	1032,58	1033	97	97	97	97	0,09
	20	5,15	5,15	5,10	1032,58	1032,58	1022,55	1029	97	97	92	95	2,62
	10	5,10	5,20	5,10	1022,55	1042,60	1022,55	1029	92	102	92	95	5,37
	5	5,05	5,15	5,05	1012,53	1032,58	1012,53	1019	88	97	88	91	5,24
	2	4,90	4,85	4,90	982,45	972,43	982,45	979	74	68	74	72	3,52
	1	4,55	4,55	4,50	912,28	912,28	902,25	909	42	39	37	39	2,33
	0	4,10	4,15	4,10	822,05	832,08	822,05	825	0	0	0	0	0,00
	0	5,20	5,15	5,20	1042,60	1032,58	1042,60	1039,26	-	-	-	-	-
SI-7*	100	2,80	2,75	2,85	1122,80	1102,75	1142,85	1123	100	91	109	100	9,09
	50	2,75	2,80	2,85	1102,75	1122,80	1142,85	1123	92	100	109	100	8,40
	20	2,75	2,80	2,80	1102,75	1122,80	1122,80	1116	92	100	100	97	4,44
	10	2,75	2,80	2,75	1102,75	1122,80	1102,75	1109	92	100	91	94	4,90
	5	2,80	2,75	2,75	1122,80	1102,75	1102,75	1109	100	91	91	94	5,25
	2	2,55	2,65	2,60	1022,55	1062,65	1042,60	1043	62	73	64	66	5,95
	1	2,55	2,55	2,50	1022,55	1022,55	1002,50	1016	62	55	45	54	8,06
	0	2,15	2,25	2,25	862,15	902,25	902,25	889	0	0	0	0	0,00
	0	2,85	2,75	2,80	1142,85	1102,75	1122,80	1122,80	-	-	-	-	-

12. APPENDIX E – CALCIUM COMPATIBILITY RESULTS – PROJECT 1

Table 28. Ca^{2+} tolerance tests at 30000 ppm (3 wt%) NaCl for SI-2, SI-3 and SI-6.

SI	Ca ²⁺ dose (ppm)	SI dose (ppm)	pH	Appearance				
				after mixing	30 minutes	1 hour	4 hours	24 hours
SI-2	100	100	4.52	clear	clear	clear	clear	clear
		1000	4.11	clear	clear	clear	clear	clear
		10000	4.55	hazy	hazy	hazy	hazy	hazy
		50000	5.01	clear	clear	clear	clear	clear
	1000	100	4.43	hazy	hazy	hazy	hazy	precipitate
		1000	4.26	hazy	hazy	hazy	hazy	precipitate
		10000	4.39	hazy	hazy	hazy	hazy	precipitate
		50000	4.35	hazy	hazy	hazy	precipitate	precipitate
SI-3	100	100	4.31	clear	clear	clear	clear	clear
		1000	3.78	clear	clear	clear	clear	clear
		10000	4.01	clear	clear	clear	clear	clear
		50000	4.81	clear	clear	clear	clear	clear
	1000	100	5.04	clear	clear	clear	clear	clear
		1000	5.05	clear	clear	clear	clear	clear
		10000	4.71	hazy	hazy	hazy	precipitate	precipitate
		50000	4.84	hazy	hazy	precipitate	precipitate	precipitate
SI-6	100	100	4.74	clear	clear	clear	clear	clear
		1000	4.46	clear	clear	clear	clear	clear
		10000	4.26	clear	hazy	hazy	hazy	hazy
		50000	4.18	clear	clear	clear	clear	clear
	1000	100	4.50	clear	clear	clear	clear	clear
		1000	4.20	hazy	hazy	hazy	hazy	hazy
		10000	4.40	hazy	hazy	precipitate	precipitate	precipitate
		50000	5.01	hazy	precipitate	precipitate	precipitate	precipitate

13. APPENDIX F – NMR SPECTRA: PROJECT 2

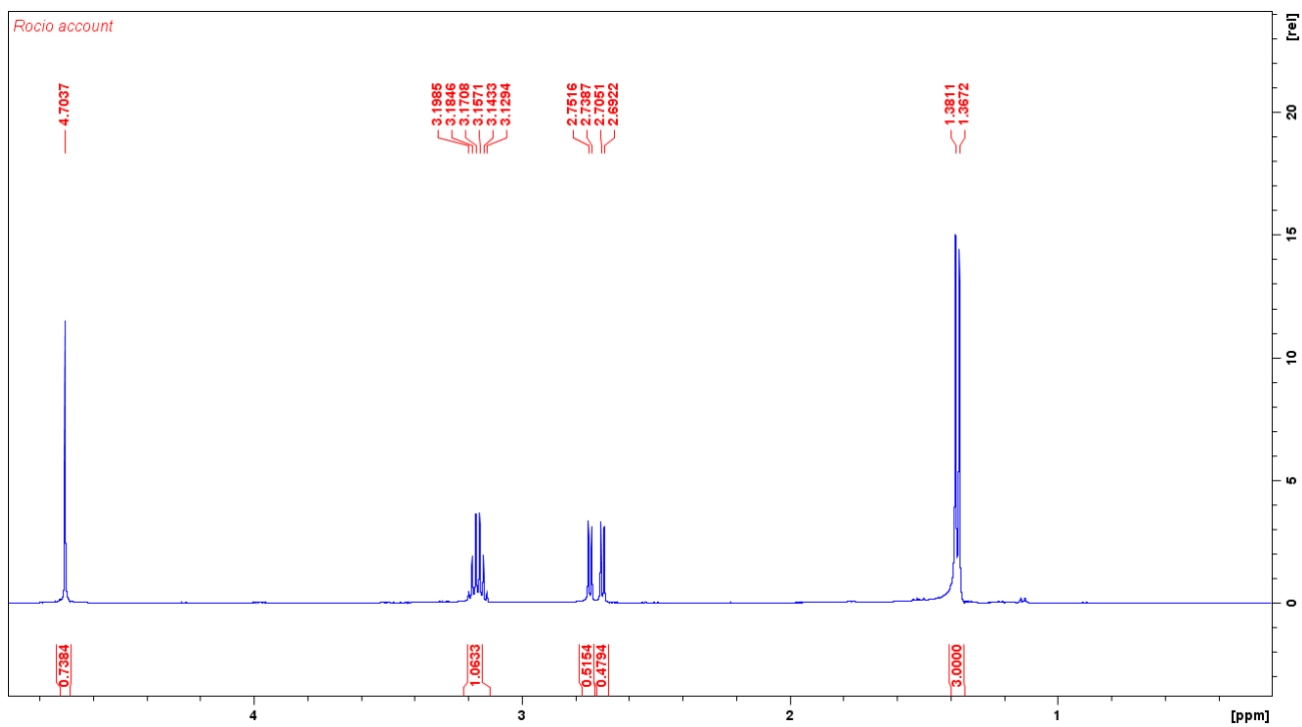


Figure 56. ¹H NMR spectra for SI-8.

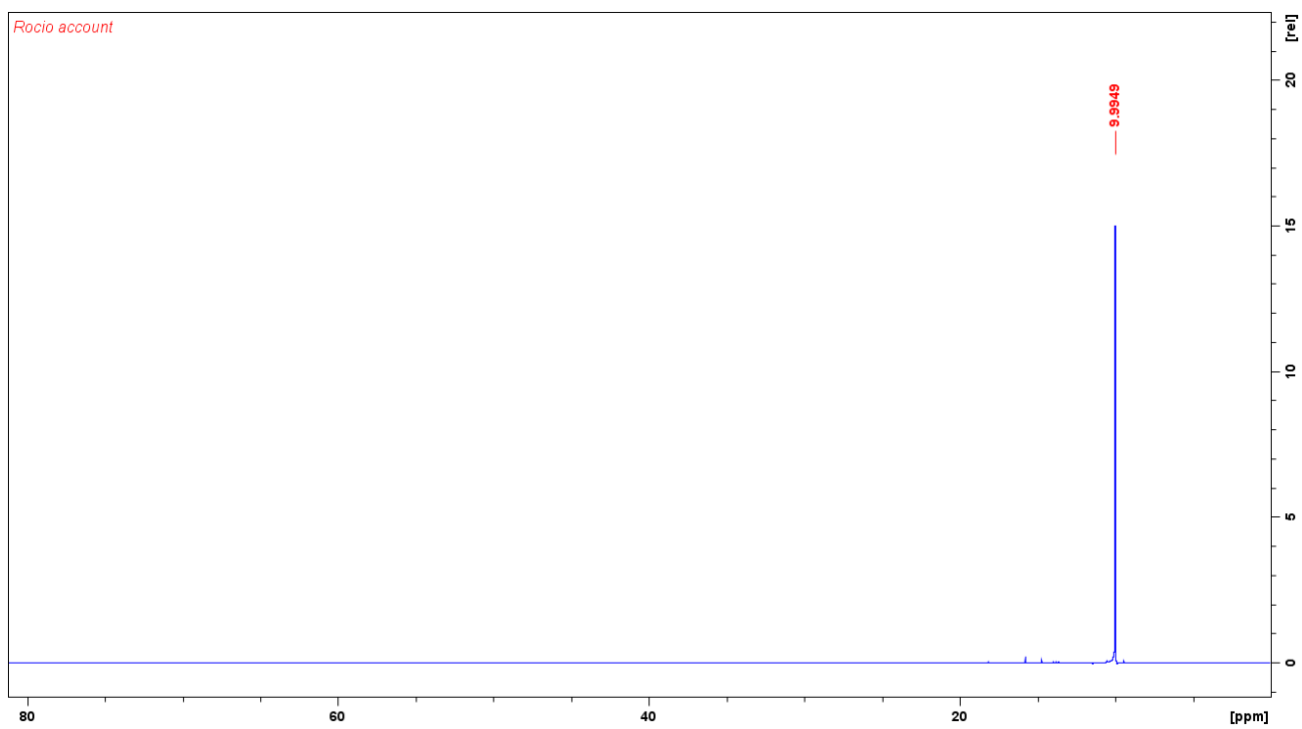


Figure 57. ³¹P NMR for SI-8.

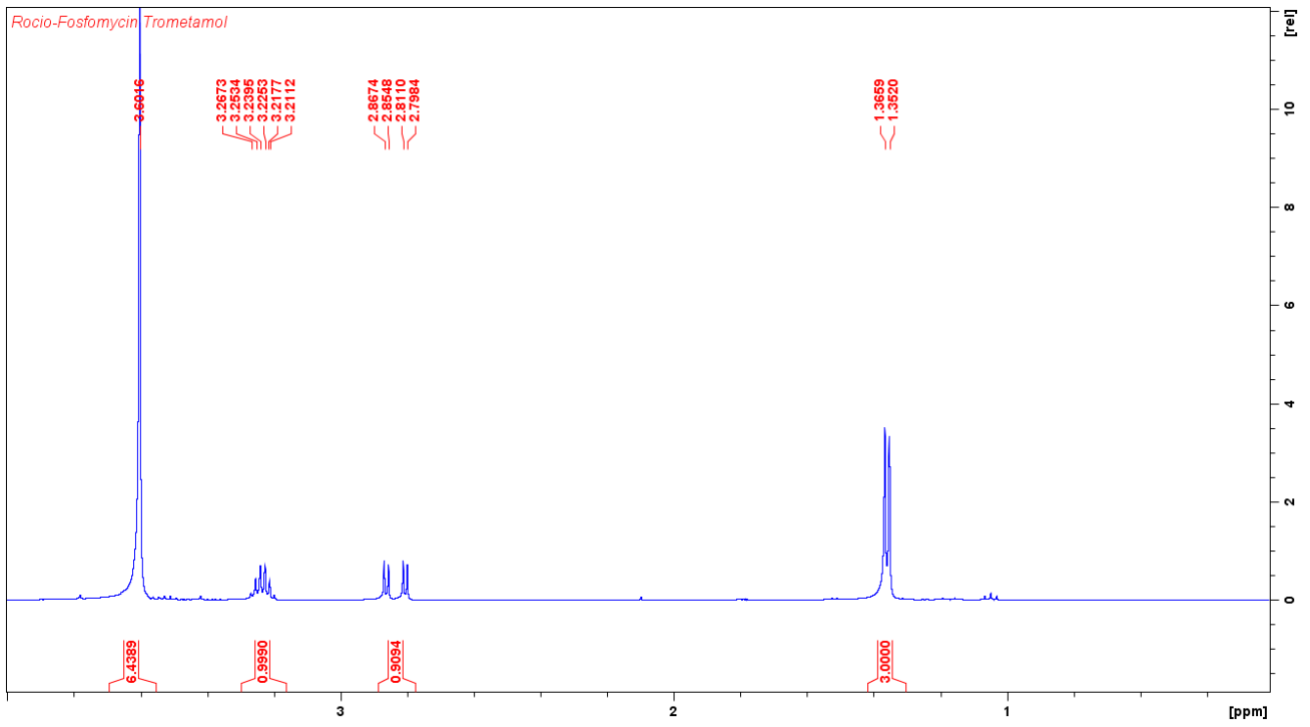


Figure 58. ^1H NMR for SI-9.

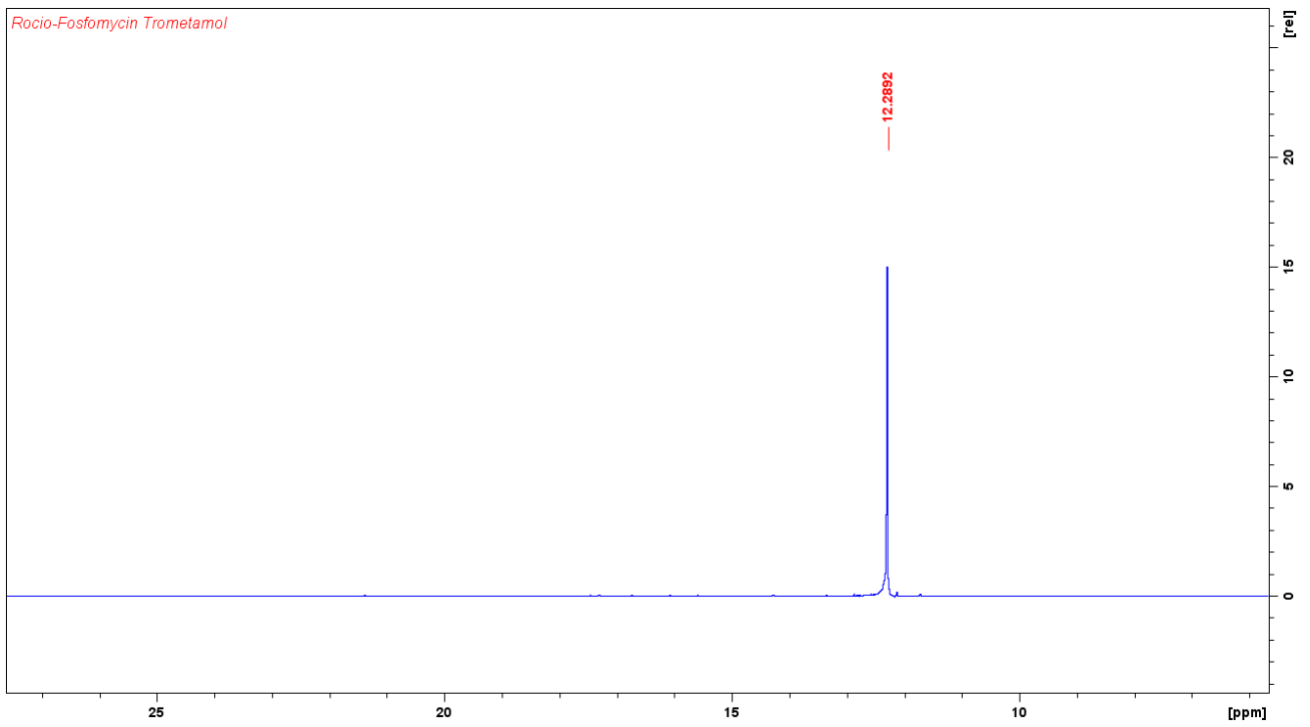


Figure 59. ^{31}P NMR for SI-9.

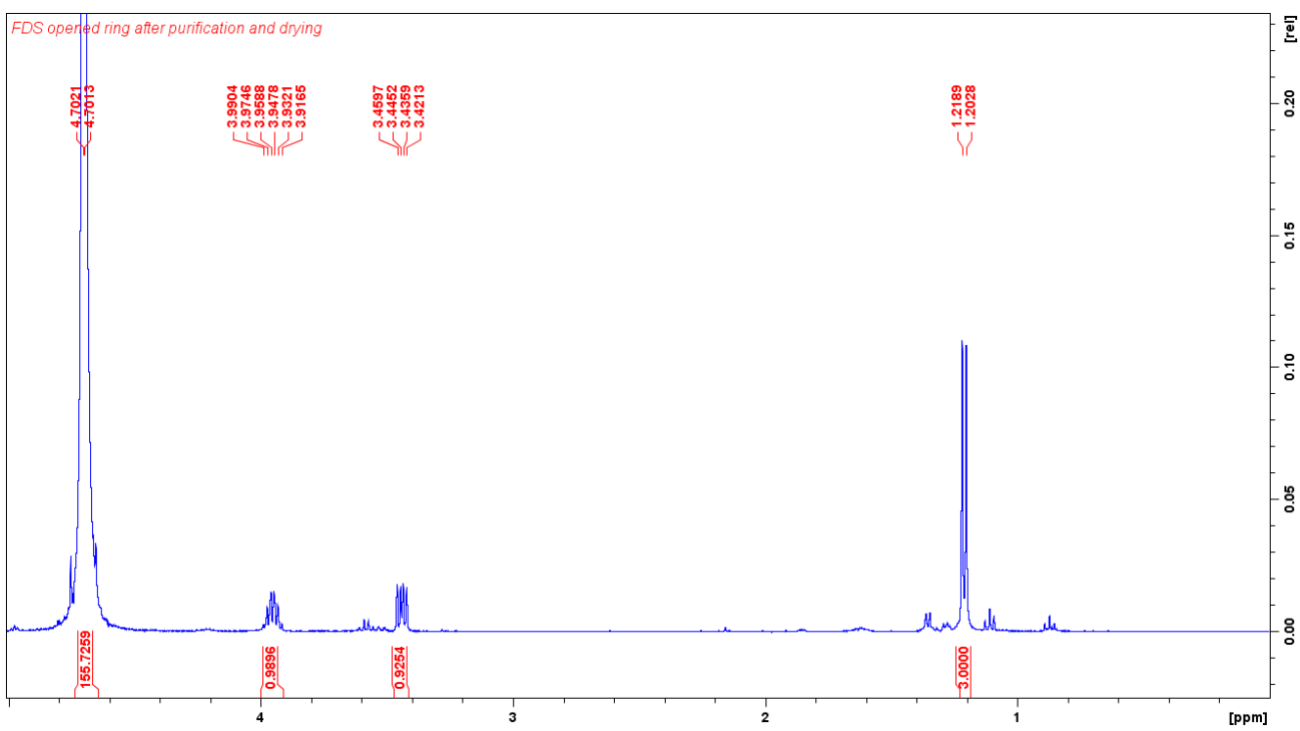


Figure 60. ^1H NMR for SI-10.

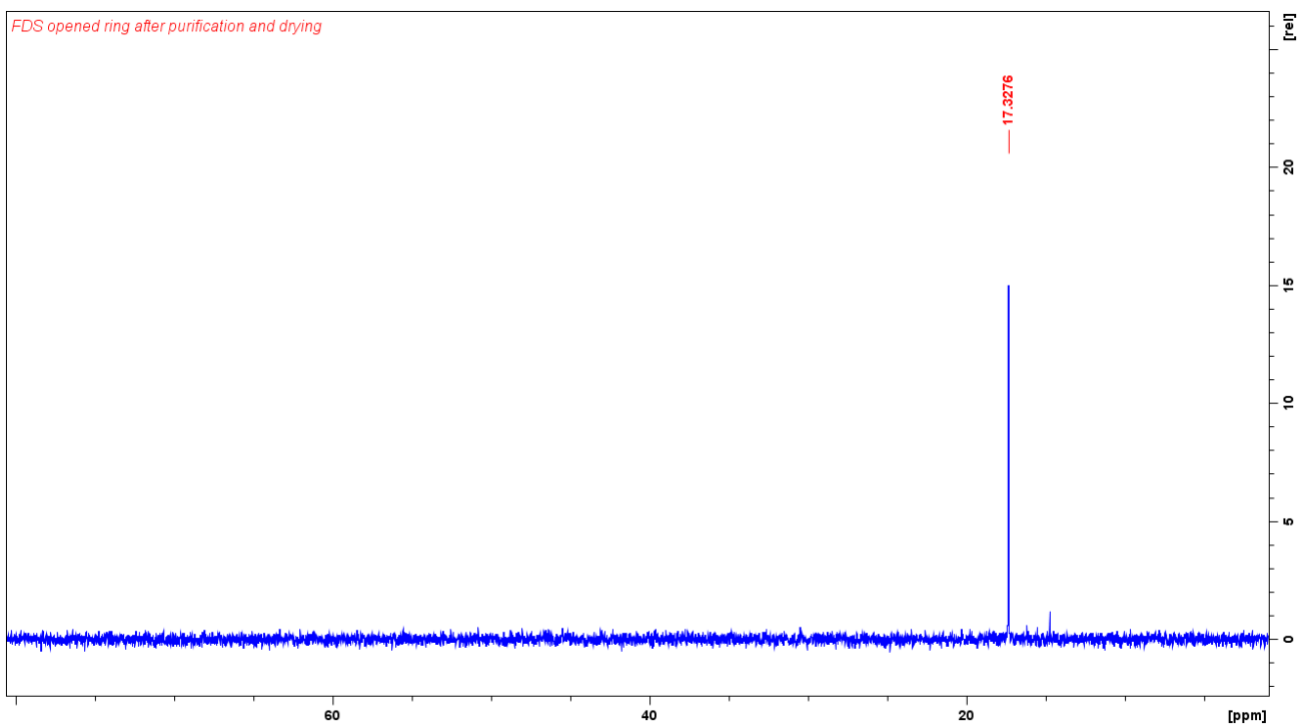


Figure 61. ^{31}P NMR for SI-10.

14. APPENDIX G – FTIR SPECTRA: PROJECT 2

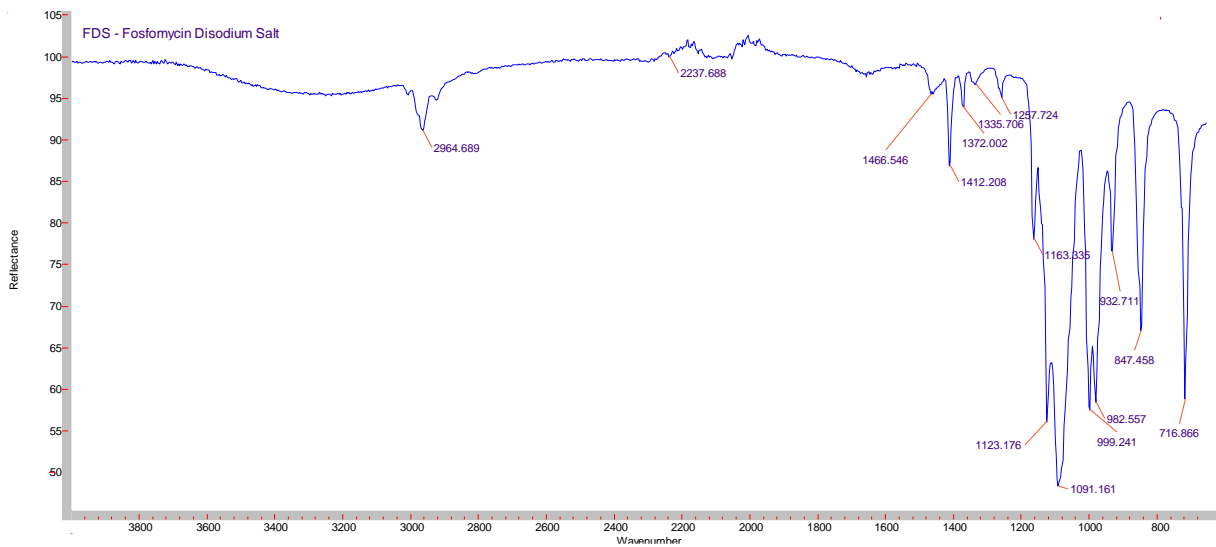


Figure 62. FTIR spectra for SI-8.

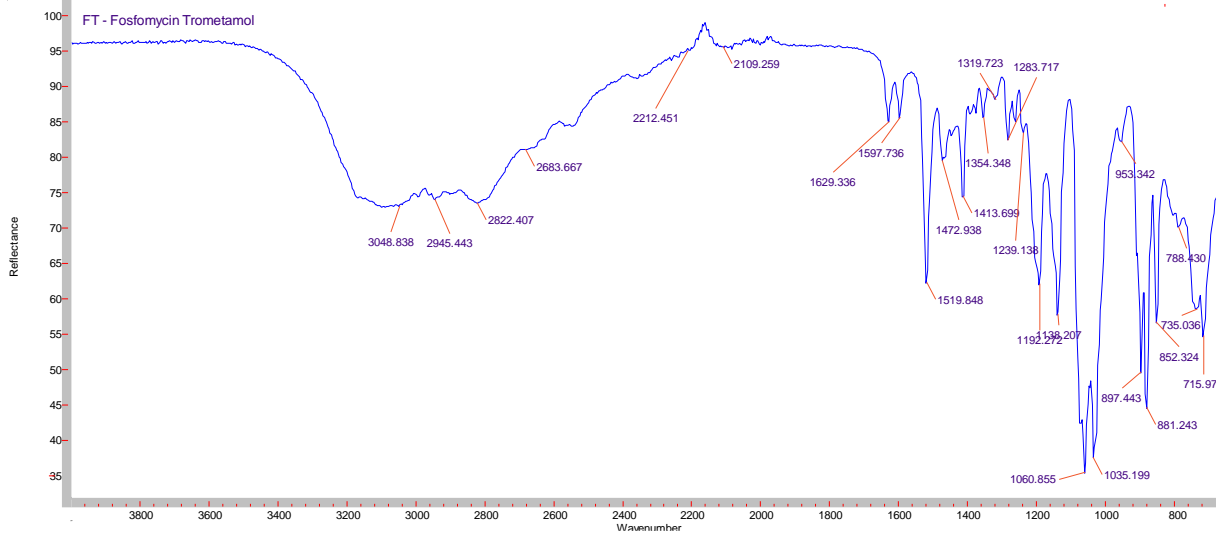


Figure 63. FTIR spectra for SI-9.

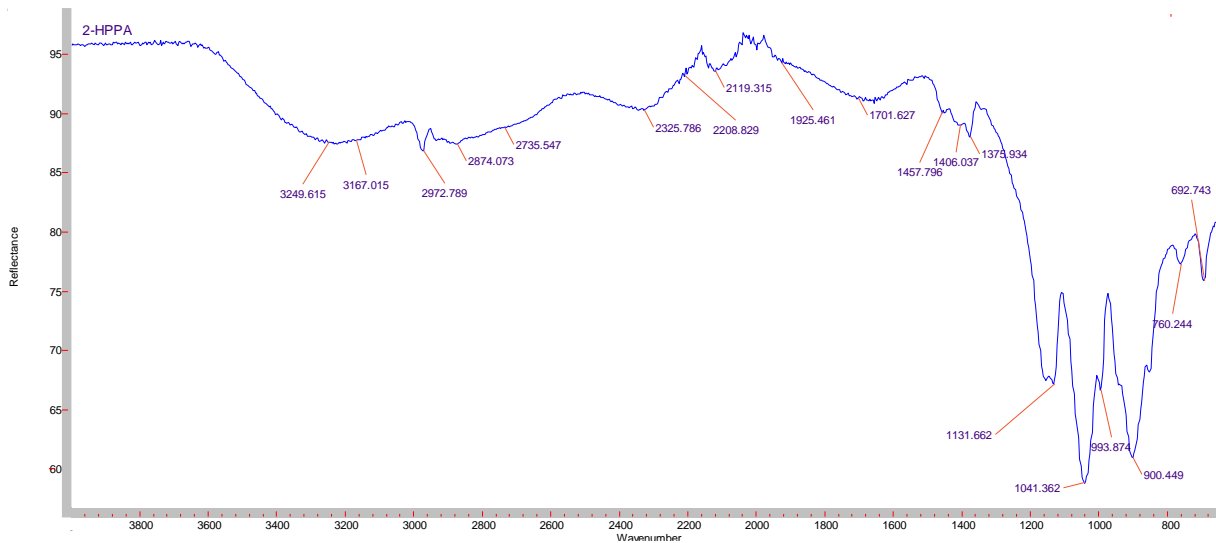


Figure 64. FTIR spectra for SI-10.

15. APPENDIX H – STATIC BOTTLE TESTS RESULTS: PROJECT 2

Table 29. Standard gypsum static test results - Project 2

	SI conc. (ppm)	EDTA titrated (mL)			Ca ²⁺ concentration (mg/L)			Ca ²⁺ conc. Average (mg/L)	% Inhibition			% Inhibition	
		Rep 1	Rep 2	Rep 3	Rep 1	Rep 2	Rep 3	CaCO ₃ retained in solution (mg/L)	Rep 1	Rep 2	Rep 3	Average	SD
HPAA	100	3,70	3,75	3,70	1483,70	1503,75	1483,70	1490	95	100	95	97	2,89
	50	3,70	3,65	3,70	1483,70	1463,65	1483,70	1477	95	89	95	93	3,19
	20	3,65	3,65	3,70	1463,65	1463,65	1483,70	1470	90	89	95	91	3,05
	10	3,55	3,55	3,60	1423,55	1423,55	1443,60	1430	80	79	85	81	3,23
	5	3,40	3,35	3,40	1363,40	1343,35	1363,40	1357	65	58	65	63	4,10
	2	3,10	3,15	3,15	1243,10	1263,15	1263,15	1256	35	37	40	37	2,53
	1	3,10	3,10	3,05	1243,10	1243,10	1223,05	1236	35	32	30	32	2,56
	0	2,75	2,80	2,75	1102,75	1122,80	1102,75	1109	0	0	0	0	0,00
	0	3,80	3,70	3,75	1523,80	1483,70	1503,75	1504	-	-	-	-	-
HPAA*	100	3,70	3,80	3,75	1483,70	1523,80	1503,75	1504	86	98	92	92	6,13
	50	3,80	3,70	3,70	1523,80	1483,70	1483,70	1497	98	86	87	90	6,84
	20	3,65	3,70	3,65	1463,65	1483,70	1463,65	1470	80	86	81	82	3,25
	10	3,65	3,60	3,70	1463,65	1443,60	1483,70	1464	80	73	87	80	6,54
	5	3,60	3,55	3,55	1443,60	1423,55	1423,55	1430	73	67	69	70	3,14
	2	3,55	3,55	3,50	1423,55	1423,55	1403,50	1417	67	67	63	66	2,24
	1	3,50	3,45	3,50	1403,50	1383,45	1403,50	1397	61	55	63	60	4,33
	0	3,00	3,00	2,95	1203,00	1203,00	1182,95	1196	0	0	0	0	0,00
	0	3,85	3,80	3,80	1543,85	1523,80	1523,80	1530	-	-	-	-	-
SI-8	100	3,75	3,70	3,70	1503,75	1483,70	1483,70	1490	102	96	96	98	3,61
	50	3,70	3,65	3,70	1483,70	1463,65	1483,70	1477	96	89	96	94	3,76
	20	3,60	3,60	3,65	1443,60	1443,60	1463,65	1450	84	83	89	85	3,43
	10	3,15	3,20	3,20	1263,15	1283,20	1283,20	1277	30	32	32	31	1,11
	5	3,10	3,05	3,10	1243,10	1223,05	1243,10	1236	24	13	19	19	5,63
	2	2,95	2,95	3,00	1182,95	1182,95	1203,00	1190	6	0	6	4	3,58
	1	2,95	2,95	3,00	1182,95	1182,95	1203,00	1190	6	0	6	4	3,58
	0	2,90	2,95	2,95	1162,90	1182,95	1182,95	1176	0	0	0	0	0,00
	0	3,75	3,70	3,75	1503,75	1483,70	1503,75	1497	-	-	-	-	-
SI-8*	100	3,50	3,50	3,50	1403,50	1403,50	1403,50	1404	81	81	82	81	0,43

	50	3,00	3,05	3,00	1203,00	1223,05	1203,00	1210	41	45	43	43	2,03
	20	2,65	2,70	2,70	1062,65	1082,70	1082,70	1076	12	16	19	16	3,67
	10	2,65	2,60	2,65	1062,65	1042,60	1062,65	1056	12	8	16	12	3,74
	5	2,55	2,60	2,60	1022,55	1042,60	1042,60	1036	4	8	12	8	3,82
	2	2,60	2,55	2,55	1042,60	1022,55	1022,55	1029	8	4	8	7	2,25
	1	2,55	2,50	2,55	1022,55	1002,50	1022,55	1016	4	0	8	4	3,90
	0	2,50	2,50	2,45	1002,50	1002,50	982,45	996	0	0	0	0	0,00
	0	3,75	3,70	3,75	1503,75	1483,7	1503,75	1497	-	-	-	-	-
SI-9	100	3,70	3,65	3,70	1483,70	1463,65	1483,70	1477	92	87	92	91	3,01
	50	3,40	3,45	3,45	1363,40	1383,45	1383,45	1377	65	68	69	67	2,36
	20	3,20	3,20	3,25	1283,20	1283,20	1303,25	1290	46	44	51	47	3,66
	10	2,90	2,95	2,90	1162,90	1182,95	1162,90	1170	18	19	18	19	0,52
	5	2,80	2,85	2,85	1122,80	1142,85	1142,85	1136	9	10	14	11	2,55
	2	2,75	2,80	2,75	1102,75	1122,80	1102,75	1109	5	5	5	5	0,13
	1	2,70	2,75	2,70	1082,70	1102,75	1082,70	1089	0	0	0	0	0,00
	0	2,70	2,75	2,70	1082,70	1102,75	1082,70	1089	0	0	0	0	0,00
0	3,75	3,80	3,80	1503,75	1523,80	1523,80	1517	-	-	-	-	-	
SI-9*	100	3,60	3,65	3,65	1443,60	1463,65	1463,65	1457	95	100	100	98	2,75
	50	3,50	3,50	3,45	1403,50	1403,50	1383,45	1397	86	86	82	84	2,25
	20	2,95	2,95	3,00	1182,95	1182,95	1203,00	1190	33	33	41	36	4,37
	10	2,95	2,95	2,90	1182,95	1182,95	1162,90	1176	33	33	32	33	0,87
	5	2,80	2,85	2,85	1122,80	1142,85	1142,85	1136	19	24	27	23	4,13
	2	2,80	2,75	2,75	1122,80	1102,75	1102,75	1109	19	14	18	17	2,54
	1	2,70	2,75	2,70	1082,70	1102,75	1082,70	1089	10	14	14	12	2,58
	0	2,60	2,60	2,55	1042,60	1042,60	1022,55	1036	0	0	0	0	0,00
0	3,65	3,65	3,65	1463,65	1463,65	1463,65	1464	-	-	-	-	-	
SI-10	100	3,70	3,75	3,70	1483,70	1503,75	1483,70	1490	94	98	93	95	2,80
	50	3,65	3,70	3,70	1463,65	1483,70	1483,70	1477	89	94	93	92	2,62
	20	3,60	3,60	3,65	1443,60	1443,60	1463,65	1450	84	84	89	86	2,40
	10	3,50	3,55	3,55	1403,50	1423,55	1423,55	1417	75	80	79	78	2,47
	5	3,40	3,35	3,40	1363,40	1343,35	1363,40	1357	66	61	64	63	2,37
	2	3,15	3,10	3,15	1263,15	1243,10	1263,15	1256	42	38	39	40	2,36
	1	2,95	3,00	3,00	1182,95	1203,00	1203,00	1196	23	28	25	25	2,44
	0	2,70	2,70	2,75	1082,70	1082,70	1102,75	1089	0	0	0	0	0,00

	0	3,75	3,75	3,8	1503,75	1503,75	1523,8	1510	-	-	-	-	-
	100	3,75	3,65	3,70	1463,65	1423,55	1443,60	1444	104	92	98	98	5,89
	50	3,70	3,65	3,70	1443,60	1423,55	1443,60	1437	98	92	98	96	3,33
	20	3,65	3,60	3,60	1423,55	1403,50	1403,50	1410	92	87	87	89	2,87
	10	3,50	3,50	3,45	1363,40	1363,40	1343,35	1357	73	75	71	73	2,07
SI-10*	5	3,45	3,45	3,45	1343,35	1343,35	1343,35	1343	67	69	71	69	1,78
	2	3,35	3,40	3,45	1303,25	1323,30	1343,35	1323	55	63	71	63	7,91
	1	3,15	3,20	3,20	1223,05	1243,10	1243,10	1236	31	40	44	38	6,78
	0	2,90	2,85	2,80	1122,80	1102,75	1082,70	1103	0	0	0	0	0,00
	0	3,65	3,75	3,75	1423,55	1463,65	1463,65	1450	-	-	-	-	-

Table 30. Standard calcite static test results - Project 2

	SI conc. (ppm)	EDTA titrated (mL)			Ca ²⁺ concentration (mg/L)			Ca ²⁺ conc. Average (mg/L)	% Inhibition			% Inhibition	
		Rep 1	Rep 2	Rep 3	Rep 1	Rep 2	Rep 3	CaCO ₃ retained in solution (mg/L)	Rep 1	Rep 2	Rep 3	Average	SD
HPAA	100	3,65	3,70	3,65	1463,65	1483,70	1463,65	1470	69	73	70	71	1,92
	50	3,40	3,40	3,45	1363,40	1363,40	1383,45	1370	55	56	59	57	2,08
	20	3,05	3,00	3,00	1223,05	1203,00	1203,00	1210	35	34	34	34	0,56
	10	2,90	2,95	2,95	1162,90	1182,95	1182,95	1176	26	31	31	29	2,82
	5	2,75	2,70	2,75	1102,75	1082,70	1102,75	1096	17	17	20	18	1,50
	2	2,45	2,50	2,45	982,45	1002,50	982,45	989	0	6	3	3	2,80
	1	2,45	2,40	2,45	982,45	962,40	982,45	976	0	0	3	1	1,62
	0	2,45	2,40	2,40	982,45	962,40	962,40	969	0	0	0	0	0,00
	0	4,20	4,20	4,15	1684,2	1684,2	1664,15	1678	-	-	-	-	-
HPAA*	100	3,85	3,80	3,90	1483,70	1463,65	1503,75	1484	76	72	79	75	3,20
	50	3,60	3,65	3,70	1383,45	1403,50	1423,55	1404	62	63	67	64	2,87
	20	3,30	3,35	3,35	1263,15	1283,20	1283,20	1277	45	46	48	46	1,40
	10	2,95	2,90	2,90	1122,80	1102,75	1102,75	1109	25	20	22	23	2,53
	5	2,75	2,85	2,80	1042,60	1082,70	1062,65	1063	14	17	17	16	1,78
	2	2,55	2,60	2,55	962,40	982,45	962,40	969	3	3	3	3	0,05
	1	2,55	2,55	2,50	962,40	962,40	942,35	956	3	0	0	1	1,62
	0	2,50	2,55	2,50	942,35	962,40	942,35	949	0	0	0	0	0,00
	0	4,35	4,30	4,20	1684,20	1664,15	1624,05	1657	-	-	-	-	-
SI-8	100	3,15	3,15	3,15	1263,15	1263,15	1263,15	1263	43	44	43	43	0,92
	50	2,75	2,80	2,75	1102,75	1122,80	1102,75	1109	20	25	20	22	2,89
	20	2,65	2,70	2,70	1062,65	1082,70	1082,70	1076	14	19	17	17	2,58
	10	2,50	2,55	2,50	1002,50	1022,55	1002,50	1009	6	11	6	8	3,12
	5	2,50	2,55	2,50	1002,50	1022,55	1002,50	1009	6	11	6	8	3,12
	2	2,45	2,45	2,45	982,45	982,45	982,45	982	3	6	3	4	1,56
	1	2,40	2,40	2,40	962,40	962,40	962,40	962	0	3	0	1	1,60
	0	2,40	2,35	2,40	962,40	942,35	962,40	956	0	0	0	0	0,00
	0	4,15	4,20	4,10	1664,15	1684,2	1644,10	1664	-	-	-	-	-
SI-8*	100	3,40	3,45	3,45	1363,40	1383,45	1383,45	1377	57	61	60	59	2,05
	50	3,20	3,20	3,20	1283,20	1283,20	1283,20	1283	46	47	46	46	0,87
	20	2,75	2,80	2,75	1102,75	1122,80	1102,75	1109	20	25	20	22	2,89
	10	2,60	2,65	2,65	1042,60	1062,65	1062,65	1056	11	17	14	14	2,62

	5	2,60	2,60	2,60	1042,60	1042,60	1042,60		1043	11	14	11	12	1,42
	2	2,60	2,55	2,60	1042,60	1022,55	1042,60		1036	11	11	11	11	0,18
	1	2,55	2,50	2,50	1022,55	1002,50	1002,50		1009	9	8	6	8	1,59
	0	2,40	2,35	2,40	962,40	942,35	962,40		956	0	0	0	0	0,00
	0	4,15	4,20	4,10	1664,15	1684,2	1644,10		1664	-	-	-	-	-
SI-9	100	3,25	3,25	3,20	1303,25	1303,25	1283,20		1297	50	48	47	48	1,46
	50	2,75	2,70	2,70	1102,75	1082,70	1082,70		1089	20	15	17	18	2,70
	20	2,50	2,55	2,50	1002,50	1022,55	1002,50		1009	6	6	6	6	0,10
	10	2,40	2,45	2,45	962,40	982,45	982,45		976	0	0	3	1	1,68
	5	2,40	2,45	2,40	962,40	982,45	962,40		969	0	0	0	0	0,00
	2	2,40	2,45	2,40	962,40	982,45	962,40		969	0	0	0	0	0,00
	1	2,40	2,45	2,40	962,40	982,45	962,40		969	0	0	0	0	0,00
	0	2,40	2,45	2,40	962,40	982,45	962,40		969	0	0	0	0	0,00
	0	4,05	4,15	4,15	1624,05	1664,15	1664,15		1651	-	-	-	-	-
SI-9*	100	3,45	3,45	3,40	1383,45	1383,45	1363,40		1377	61	61	57	60	2,40
	50	3,00	3,00	2,95	1203,00	1203,00	1182,95		1196	35	35	30	33	2,86
	20	2,55	2,60	2,55	1022,55	1042,60	1022,55		1029	9	12	6	9	2,83
	10	2,45	2,50	2,45	982,45	1002,50	982,45		989	3	6	0	3	2,91
	5	2,50	2,45	2,45	1002,50	982,45	982,45		989	6	3	0	3	2,91
	2	2,40	2,45	2,45	962,40	982,45	982,45		976	0	3	0	1	1,68
	1	2,45	2,45	2,45	982,45	982,45	982,45		982	3	3	0	2	1,68
	0	2,40	2,40	2,45	962,40	962,40	982,45		969	0	0	0	0	0,00
	0	4,05	4,15	4,15	1624,05	1664,15	1664,15		1651	-	-	-	-	-
SI-10	100	3,45	3,50	3,50	1383,45	1403,50	1403,50		1397	59	63	63	62	2,34
	50	3,15	3,15	3,10	1263,15	1263,15	1243,10		1256	42	43	40	42	1,45
	20	2,75	2,70	2,70	1102,75	1082,70	1082,70		1089	18	17	17	17	0,30
	10	2,60	2,65	2,60	1042,60	1062,65	1042,60		1049	9	14	12	12	2,76
	5	2,55	2,55	2,60	1022,55	1022,55	1042,60		1029	6	9	12	9	2,80
	2	2,50	2,55	2,50	1002,50	1022,55	1002,50		1009	3	9	6	6	2,84
	1	2,45	2,40	2,45	982,45	962,40	982,45		976	0	0	3	1	1,67
	0	2,45	2,40	2,40	982,45	962,40	962,40		969	0	0	0	0	0,00
	0	4,15	4,15	4,10	1664,15	1664,15	1644,10		1657	-	-	-	-	-
	100	3,55	3,45	3,50	1383,45	1343,35	1363,40		1363	60	53	58	57	3,88
	50	2,90	3,05	2,95	1122,80	1182,95	1142,85		1150	21	28	26	25	3,57

	20	2,65	2,70	2,70	1022,55	1042,60	1042,60	1036	6	6	12	8	3,21
	10	2,70	2,60	2,60	1042,60	1002,50	1002,50	1016	9	0	6	5	4,56
SI-10*	5	2,55	2,60	2,55	982,45	1002,50	982,45	989	0	0	3	1	1,68
	2	2,55	2,60	2,55	982,45	1002,50	982,45	989	0	0	3	1	1,68
	1	2,55	2,60	2,50	982,45	1002,50	962,40	982	0	0	0	0	0,00
	0	2,55	2,60	2,50	982,45	1002,50	962,40	982	0	0	0	0	0,00
	0	4,20	4,25	4,20	1644,10	1664,15	1644,10	1651	-	-	-	-	-

Table 31. Heidrun calcite static test results - Project 2

	SI conc. (ppm)	EDTA titrated (mL)			Ca ²⁺ concentration (mg/L)			Ca ²⁺ conc. Average (mg/L)	% Inhibition			% Inhibition	
		Rep 1	Rep 2	Rep 3	Rep 1	Rep 2	Rep 3	CaCO ₃ retained in solution (mg/L)	Rep 1	Rep 2	Rep 3	Average	SD
HPAA	100	5,35	5,35	5,40	1072,68	1072,68	1082,70	1076	98	98	103	100	2,78
	50	5,30	5,35	5,40	1062,65	1072,68	1082,70	1073	93	98	103	98	5,21
	20	5,30	5,35	5,35	1062,65	1072,68	1072,68	1069	93	98	98	97	3,30
	10	5,30	5,35	5,30	1062,65	1072,68	1062,65	1066	93	98	94	95	3,04
	5	5,30	5,30	5,35	1062,65	1062,65	1072,68	1066	93	94	98	95	3,04
	2	4,75	4,70	4,70	952,38	942,35	942,35	946	33	38	38	36	2,76
	1	4,50	4,45	4,50	902,25	892,23	902,25	899	5	14	19	13	6,74
	0	4,45	4,30	4,30	892,23	862,15	862,15	872	0	0	0	0	0,00
	0	5,40	5,35	5,35	1082,70	1072,68	1072,68	1076	-	-	-	-	-
HPAA*	100	2,80	2,75	2,70	1122,80	1102,75	1082,70	1103	94	81	72	82	10,75
	50	2,70	2,70	2,70	1082,70	1082,70	1082,70	1083	75	69	72	72	2,89
	20	2,85	2,80	2,75	1142,85	1122,80	1102,75	1123	103	92	83	93	10,19
	10	2,75	2,70	2,75	1102,75	1082,70	1102,75	1096	84	69	83	79	8,32
	5	2,60	2,55	2,60	1042,60	1022,55	1042,60	1036	56	35	52	48	11,41
	2	2,50	2,50	2,55	1002,50	1002,50	1022,55	1009	37	23	41	34	9,64
	1	2,35	2,45	2,35	942,35	982,45	942,35	956	9	12	0	7	6,13
	0	2,30	2,40	2,35	922,30	962,40	942,35	942	0	0	0	0	0,00
	0	2,80	2,85	2,85	1122,80	1142,85	1142,85	1136	-	-	-	-	-
SI-8	100	5,10	5,20	5,15	1022,55	1042,60	1032,58	1033	88	97	92	92	4,27
	50	4,90	4,95	4,90	982,45	992,48	982,45	986	71	73	69	71	1,68
	20	4,70	4,65	4,70	942,35	932,33	942,35	939	53	44	51	49	4,92
	10	4,60	4,55	4,55	922,30	912,28	912,28	916	44	34	37	38	5,26
	5	4,50	4,50	4,50	902,25	902,25	902,25	902	35	29	32	32	3,13
	2	4,45	4,40	4,40	892,23	882,20	882,20	886	31	19	23	24	5,88
	1	4,45	4,40	4,40	892,23	882,20	882,20	886	31	19	23	24	5,88
	0	4,10	4,20	4,15	822,05	842,10	832,08	832	0	0	0	0	0,00
	0	5,20	5,20	5,30	1042,60	1042,60	1062,65	1049	-	-	-	-	-
SI-8*	100	5,10	5,05	5,05	1022,55	1012,53	1012,53	1016	95	90	90	92	2,76
	50	5,00	5,05	4,95	1002,50	1012,53	992,48	1003	85	90	81	85	4,53
	20	4,95	4,95	4,85	992,48	992,48	972,43	986	80	80	71	77	4,95
	10	4,60	4,65	4,65	922,30	932,33	932,33	929	45	50	52	49	3,77

	5	4,35	4,35	4,30	872,18	872,18	862,15	869	20	20	19	20	0,55
	2	4,30	4,35	4,25	862,15	872,18	852,13	862	15	20	14	16	3,11
	1	4,15	4,20	4,15	832,08	842,10	832,08	835	0	5	5	3	2,82
	0	4,15	4,15	4,10	832,08	832,08	822,05	829	0	0	0	0	0,00
	0	5,15	5,20	5,10	1032,58	1042,60	1022,55	1033	-	-	-	-	-
SI-9	100	5,05	5,20	5,15	1012,53	1042,60	1032,58	1029	59	74	70	68	7,72
	50	5,05	5,00	4,95	1012,53	1002,50	992,48	1003	59	54	52	55	3,79
	20	4,80	4,80	4,75	962,40	962,40	952,38	959	34	34	33	34	0,93
	10	4,70	4,65	4,70	942,35	932,33	942,35	939	25	20	28	24	4,25
	5	4,60	4,65	4,60	922,30	932,33	922,30	926	15	20	19	18	2,61
	2	4,60	4,60	4,55	922,30	922,30	912,28	919	15	15	14	15	0,40
	1	4,55	4,55	4,60	912,28	912,28	922,30	916	10	10	19	13	5,15
	0	4,45	4,45	4,40	892,23	892,23	882,20	889	0	0	0	0	0,00
	0	5,50	5,45	5,45	1102,75	1092,73	1092,73	1096	-	-	-	-	-
SI-9*	100	5,05	5,10	5,05	1012,53	1022,55	1012,53	1016	93	98	93	95	2,94
	50	5,00	5,05	5,00	1002,50	1012,53	1002,50	1006	88	93	89	90	3,03
	20	4,95	4,95	4,90	992,48	992,48	982,45	989	83	84	79	82	2,63
	10	4,10	4,25	4,20	822,05	852,13	842,10	839	-5	15	10	6	10,38
	5	4,15	4,10	4,10	832,08	822,05	822,05	825	0	0	0	0	0,00
	2	4,15	4,10	4,10	832,08	822,05	822,05	825	0	0	0	0	0,00
	1	4,15	4,10	4,10	832,08	822,05	822,05	825	0	0	0	0	0,00
	0	4,15	4,10	4,10	832,08	822,05	822,05	825	0	0	0	0	0,00
	0	5,10	5,10	5,15	1022,55	1022,55	1032,58	1026	-	-	-	-	-
SI-10	100	2,70	2,70	2,75	1082,70	1082,70	1102,75	1089	94	94	103	97	5,26
	50	2,60	2,55	2,60	1042,60	1022,55	1042,60	1036	75	66	77	73	6,13
	20	2,55	2,50	2,50	1022,55	1002,50	1002,50	1009	66	56	60	61	4,72
	10	2,40	2,45	2,40	962,40	982,45	962,40	969	38	47	43	42	4,70
	5	2,25	2,30	2,25	902,25	922,30	902,25	909	9	19	17	15	5,01
	2	2,20	2,20	2,15	882,20	882,20	862,15	876	0	0	0	0	0,00
	1	2,20	2,20	2,15	882,20	882,20	862,15	876	0	0	0	0	0,00
	0	2,20	2,20	2,15	882,20	882,20	862,15	876	0	0	0	0	0,00
	0	2,75	2,70	2,75	1102,75	1082,70	1102,75	1096	-	-	-	-	-
	100	2,75	2,80	2,75	1062,65	1082,70	1062,65	1069	87	96	86	90	5,58
	50	2,70	2,80	2,75	1042,60	1082,70	1062,65	1063	77	96	86	86	9,31

SI-10*	20	2,65	2,65	2,60	1022,55	1022,55	1002,50	1016	68	60	54	60	7,10
	10	2,60	2,55	2,60	1002,50	982,45	1002,50	996	58	36	54	49	11,66
	5	2,50	2,50	2,45	962,40	962,40	942,35	956	39	24	21	28	9,32
	2	2,40	2,50	2,45	922,30	962,40	942,35	942	19	24	21	22	2,33
	1	2,35	2,45	2,40	902,25	942,35	922,30	922	10	12	11	11	1,16
	0	2,30	2,40	2,35	882,20	922,30	902,25	902	0	0	0	0	0,00
	0	2,80	2,85	2,80	1082,70	1102,75	1082,70	1089	-	-	-	-	-

16. APPENDIX I - SEAWATER BIODEGRADABILITY RESULTS

Table 32. Seawater biodegradability results - Project 1 and Project 2.

Compound	Final BOD in mg/L				N into NH ₄ (No nitrification)		N into NO ₂ (Partial nitrification)		N into NO ₃ (Complete nitrification)	
	flask #1	flask #2	flask #3	Average	ThBOD (mgCOD/L)	BOD ₂₈ %degradation	ThBOD (mgCOD/L)	BOD ₂₈ %degradation	ThBOD (mgCOD/L)	BOD ₂₈ %degradation
Positive Control	126,7	114,7	115,7	119,03	166,54	71%	166,54	71%	166,54	71%
SI-1	0	0,6	4,5	2,55	42,39	6%	53,95	5%	57,81	4%
SI-2	0	2,6	5,4	4,00	37,34	11%	43,92	9%	46,12	9%
SI-3	3,5	2,6	4,5	3,53	37,32	9%	43,91	8%	46,10	8%
SI-4	0	0	1,6	1,60	56,15	3%	63,48	3%	65,92	2%
SI-5	0,6	0	0	0,60	47,45	1%	53,64	1%	55,70	1%
SI-6	4,5	4,5	3,5	4,17	47,01	9%	55,31	8%	58,07	7%
SI-7	0	3,5	2,6	3,05	44,69	7%	52,58	6%	55,21	6%
SI-8	0	0	0,6	0,60	55,63	1%	55,63	1%	55,63	1%
SI-9	0	0	0,6	0,60	62,97	1%	74,08	1%	77,78	1%